THE
PHYSICAL REVIEW
A Journal of Experimental and Theoretical Physics Established by E. L. Nichols in 1893
VOL. 60, NO. 6 SEPTEMBER 15, 1941 SECOND SERIES

Energy and Multipole Order of Nuclear Gamma-Rays

A. C. HELMHOLZ
Department of Physics, Radiation Laboratory, University of California, Berkeley, California
(Received June 17, 1941)

The energies of some nuclear gamma-rays emitted in deuteron-induced radioactivities have been measured with a magnetic β-ray spectrograph with photographic film as detector. The energies measured were those of the conversion electrons, and in some cases also those of the photoelectrons ejected from a heavy element. Independent measurements of the multipole order have been obtained where possible from the internal conversion coefficient, the K/L conversion ratio, and the lifetime of the γ-ray transition. In the case of eight out of the fourteen γ-rays measured, a fairly definite assignment of the multipole order has been made. In the nuclei Zn^{69}, Kr^{83}, Sr^{87}, and $Ag^{107\text{ or }109}$ the probable nuclear spins of the states involved are given.

TWO of the most important characteristics of a nuclear gamma-ray are its energy and its multipole order. When several gamma-rays are present or there is a branching of some sort, a knowledge of the intensity, that is the number of quanta per disintegration, is also valuable. Knowing these three quantities, one can construct a nuclear level scheme with some certainty, particularly for the lighter nuclei in which the level density is not so great as to introduce great complexity. The object of this work has been to make as definite a determination as possible of these characteristics of γ-rays from some artificially radioactive nuclei.

The measurements of the energy have been accomplished with a magnetic β-ray spectrograph according to the well-established methods. There are three independent experimental results which provide information on the multipole order of γ-rays, and where possible all three have been used to check one another. First, the internal conversion coefficient, that is, the ratio of the probability of the emission of a conversion electron to the probability of the emission of a quantum, is for low energy γ-rays very sensitive to the multipole order. For example, Dancoff and Morrison[1] derived the formula:

$$\alpha_k = Z^3\left(\frac{e^2}{hc}\right)^4 \frac{l}{l+1}\left(\frac{2}{E}\right)^{l+5/2} \qquad (1)$$

for the conversion coefficient in the K shell, where E is the gamma-ray energy in units of mc^2 and l is the multipole order. It is apparent that for high energy γ-rays, 300 kev or more, the change of α with l is not rapid; and since the experimental measurement of α is difficult, the method ceases to be of much value. If the transition takes place between two states of angular momentum $\mathbf{J}$ and $\mathbf{J}'$, the value of l will be the lowest value of $\mathbf{J}-\mathbf{J}'$ allowed by the parity and arguments of symmetry.* The transition may be either electric or magnetic. If the transition with $l=|J-J'|$, is allowed, electric 2^l-pole radiation only is important. On the other hand, if this transition is

[1] S. M. Dancoff and P. Morrison, Phys. Rev. **55**, 122 (1939).
* For a full discussion of this question see reference 1.

forbidden by the parity, either magnetic 2^l-pole radiation, electric 2^{l+1}-pole radiation, or both may be important. As an example, consider the case of a nucleus with $J=9/2$, $J'=1/2$, values which might be determined spectroscopically from hyperfine structure data. The most probable transition will be by electric $2^{9/2-1/2}$- or 2^4-pole radiation. However, if the parity of the two states is opposite, this type of radiation is forbidden, and magnetic 2^4-pole radiation might occur. Alternatively, since the vector difference of $9/2$ and $1/2$ could be 5, electric 2^5-pole radiation could occur. Formula (1) is for electric radiation. Nelson and Hebb[2] have calculated the conversion coefficients for magnetic radiation for both the K and the L shell. To decide, for example, between magnetic 2^4-pole and electric 2^5-pole radiation in the case mentioned above, is, however, very difficult on the basis of only values of α (see case of Zn^{69} below). Therefore, it is very valuable to have a second method of getting the multipole order which depends on the ratio of the K conversion to the L conversion. Hebb and Nelson[2] showed that this ratio is sensitive to the multipole order, and also that magnetic and electric radiations can be distinguished in this way. Since the ratio is easier to measure than the conversion coefficient, this method is especially noteworthy. Thirdly, if the difference in angular momentum of two states is large enough (4 units for energy differences of about 150 kev and allowed electric multipole radiations), the transition will be sufficiently forbidden so as to proceed with a measurable lifetime. This phenomenon, known as isomerism, was explained in detail by Weizsäcker.[3] Pontecorvo, and Hebb and Uhlenbeck[4] showed that the process of internal conversion tends to speed up the transition, so that the lifetime of the transition calculated from the purely electromagnetic considerations must be divided by $1+\alpha$, where α is the total conversion coefficient. The theoretical expression for the decay constant of an electric transition of energy $\hbar\omega$ in ergs and change in angular momentum $l=\mathbf{J}-\mathbf{J}'$ is:†

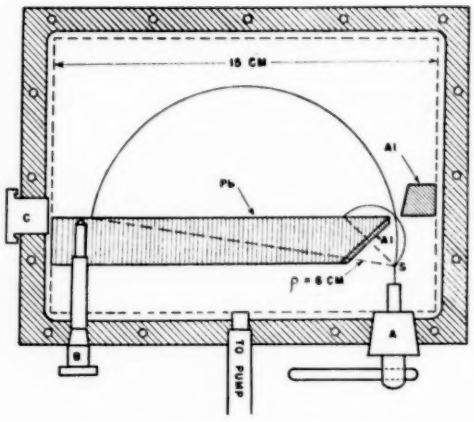

FIG. 1. The magnetic spectrograph.

$$\lambda=\left(\frac{\omega}{c}\right)^{2l+1}\frac{e^2}{\hbar}\eta^2\frac{x^{2l}}{[1\cdot3\cdot5\cdot\cdots(2l-1)]^2}\ \text{sec}^{-1}. \quad (2)$$

η is a factor of the order of unity and x is the dimension of the radiating multipole, for which the best approximation is the nuclear radius or $A^{\frac{1}{3}}\times1.4\times10^{-13}$ cm. For simplicity in calculation this can be put in the form:

$$\log_{10}\lambda=20.3-2\log_{10}[1\cdot3\cdot5\cdot\cdots(2l-1)]-[2l+1][1.30-\log_{10}E]-2l[0.84-\tfrac{1}{3}\log A], \quad (3)$$

where now E is the energy of the γ-ray in Mev, A is the atomic number, and l is the change in angular momentum. If, as discussed above, the transition with the lowest possible value of $\mathbf{J}-\mathbf{J}'$ is allowed, the radiation will be electric $2^{|J-J'|}$-pole, and the theoretical half-life will be given by $0.693/\lambda(l)$. On the other hand, if the transition proceeds by magnetic 2^l-pole or electric 2^{l+1}-pole radiation, the value of l to be used in the formula is $l+1$. Consequently, including the effect of internal conversion, we may calculate the expected half-lives τ from the following formulae:

$\tau=.693(\alpha+1)^{-1}\lambda(l)^{-1}$ for electric 2^l-pole radiation.

$\tau=.693(\alpha+1)^{-1}\lambda(l+1)^{-1}$ for magnetic 2^l-pole radiation.

As can be seen from Eq. (3), for γ-rays of the

[2] M. H. Hebb and E. Nelson, Phys. Rev. **58**, 486 (1940).
[3] C. F. v. Weizsäcker, Naturwiss. **24**, 813 (1936).
[4] B. Pontecorvo, *Travaux du Congrès du Palais de la Découverte* (Paris, 1937); M. H. Hebb and G. E. Uhlenbeck, Physica **5**, 605 (1938).

† I am indebted to Dr. E. Segrè for the correct form of this equation.

order of 100 kev in energy, λ may change by as much as a factor of 10^5 due to a change of 1 in l. Hence, disagreement with an experimental result by as much as a factor of 50 does not obviate an assignment to a certain value of l.

Although none of the above-mentioned methods of determining the multipole order is definitive, an agreement of all three can be considered convincing evidence of the correctness of the interpretation.

Experimental Technique

Figure 1 is a diagram of the β-ray spectrograph‡ used in these experiments. Except where marked, the spectrograph was made of brass. The interior was lined with white Bakelite to reduce scattering. The source was usually placed in a small Al boat 1.5 cm long and of the order of 1 mm wide and held in position by the ends of a wire U, the base of which was clamped in the tapered brass plug, *A*. This allowed a variation of the perpendicular distance from the source to photographic film. The distance was usually 1.5–2 cm and was measured with calipers to about 0.2 mm. In case a foil was used as source it was mounted on a thin piece of brass which, in turn, was clamped in the plug *A*, the arrangement being similar to that of Valley and McCreary.[5] The photographic film, introduced at *C*, fitted into a grooved track attached to the Pb block. The brass plug *C* was fitted with a gasket and held in place by two screws. Removing the plug *B* allowed light to produce a fiducial mark on the film 12 cm from the center of the slit. Thus radii of curvature up to about 6 cm could be used. The film used was Agfa x-ray film. It was developed in standard x-ray developer for 8 minutes. The distance from the fiducial mark to the lines or edges on the film was usually measured with calipers, although several checks were made by measurement with a microphotometer. The lid to the spectrograph was fitted with a gasket and screwed down to be vacuum tight. A small Hg diffusion pump backed by a Cenco Hyvac pumped out the spectrograph to a vacuum of the order of 10^{-4} mm of Hg. In many instances, the use of the Hg pump was unnecessary.

‡ Except for a few small changes it was designed by Professor S. W. Barnes.

[5] G. E. Valley and R. L. McCreary, Phys. Rev. **56**, 863 (1939).

The magnetic field was supplied by an electromagnet run on storage batteries. By checking the strength of the field about twice a day, it was kept constant within 1 percent. The measurement of the fields was performed with a flip coil and ballistic galvanometer. The sensitivity of the galvanometer was determined both with a 50-mh mutual inductance in the usual way, and with a Hibbert magnetic standard which reproduced a point on a sensitivity curve previously taken with a standard solenoid. The two methods of calibration agreed within 1 percent. No natural radioactive standard was available to check the values of the magnetic field, but the energies of the electrons from the 6.7-hr. Cd and Ga^{67} agree well with those of Valley and McCreary.[5] For high energies, the value of the energy of Pb photoelectrons from annihilation radiation is a good check.

In most cases the element of which the source consisted was separated chemically from the target bombarded in the cyclotron. When the element bombarded is different from the element used as a source, this method provides a means of obtaining a concentrated activity, which is essential for this type of work. The active material was then placed in the Al boat. In the case of Kr and Se formed by Se+D, Se was distilled in vacuum onto a 1-mil Al foil, which was then bombarded in the cyclotron and placed in the spectrograph. When the energy of the gamma-ray quanta, rather than that of the electrons, was measured, the source was placed in an inverted boat made of Pb or whatever material was desired as the source of photoelectrons. Alternatively, the source would be made up as above, and the Pb placed directly on top of the boat.

Absorption and half-life measurements were taken with a Lauritsen electroscope fitted with a 0.2-mil Al window, or with an ionization chamber filled with Freon or air and attached to an FP-54 d.c. amplifier. For half-life measurements extending over long periods of time, the sensitivity of the detectors were determined with a uranium standard each time. The measurement of the internal conversion coefficient is a measurement of the ratio of the number of electrons to the number of quanta. What one measures with electroscope or ionization chamber is the ioniza-

tion due to electrons or quanta. The ionization is proportional to the energy lost in chamber, or to the number multiplied by the energy and the percentage absorbed. The ionization of electrons is much greater than that of quanta, and the fraction of the energy lost in an ionization chamber by either electrons or γ-rays is not an easily measurable quantity, so the comparison is a very uncertain one. Nevertheless, in certain cases in which the effect of the conversion electron and of the γ-ray can be separated by absorption measurements, the method is feasible. If the electrons have a range r, an energy E_e, the γ-rays an energy E_γ, the chamber a depth d (assumed less than r), filled with a gas of absorption coefficient μ and density ρ, the ratio of the ionization due to electrons to that due to quanta is:

$$R=\frac{N_e E_e d/r^*}{N_\gamma E_\gamma(1-e^{-(\mu/\rho)d\rho})}. \tag{4}$$

If the γ-rays lose an appreciable amount of energy in the ionization chamber window by the ejection of electrons, a term $N_\gamma E_\gamma K(1-e^{-\mu x})_w$ must be added to the denominator. Here KE_γ represents the average energy which the electrons ejected from the window lose in the chamber. N_e/N_γ is, of course, α which is to be determined. As an example, experiments on Sr^{87} gave the following data:

$E_\gamma=386$ kev, $E_e=370$ kev, $d=10$ cm, $r=100$ cm

$$\mu/\rho\cdot\rho d=0.092\cdot 10\cdot 0.0012=0.0011,$$

$$(\mu/\rho\cdot\rho x)_{\text{window}}=0.095\cdot 0.007=0.00067,$$

$$R=23.6/1.1,\quad K=10/100,$$

$$\frac{23.6}{1.1}=\alpha\frac{370\,{}^{10}/_{100}}{386[(1-e^{-0.0011})+0.1(1-e^{-0.00067})]}=82\alpha,$$

$$\alpha=0.26.$$

Obviously, it is easier to compare the numbers in two groups of electrons having about the same energy. This is possible when the absorption of a γ-ray in a material of roughly the same atomic number as that of the source is mostly by photoelectric effect, for the photoelectrons then have the same energy as the conversion electrons. In addition, the two sources of electrons should have the same thickness, that of the "source" of photoelectrons being necessarily r, their range. Under these conditions the ratio of the ionization from conversion electrons to that from the photoelectrons of the transition effect is the ratio of the numbers in the two groups. If the same source is used, first bare, to get the ionization from the conversion electrons, then covered with absorber of photoelectric absorption coefficient μ for the γ-ray, the ratio of the ionizations is:

$$R=N_e/N_\gamma(1-e^{-(\mu/\rho)\rho r}). \tag{5}$$

The uncertainties are the distribution in angle of the ejected photoelectrons which can be roughly estimated from the geometry, and the part played by the Compton electrons. If the γ-ray energy is high compared with the K binding energy, a heavy material like Pb may be used as absorber without changing the energy distribution of the electrons absorbed in the chamber too much. As an example of this type of measurement, for Ga^{67}, Cu was used as a source of photoelectrons from the 93-kev γ-ray. Absorption curves showed the curves for conversion and photoelectrons to be very similar. $r\rho$ is 10 mg/cm^2; μ/ρ is 0.47 cm^2/g;

$$R=9.5/0.064=\alpha/(0.010\cdot 0.47)\quad \alpha=0.7.$$

If a K-electron capture is followed by internal conversion, absorption measurements can separate the effect of the electrons from that of the x-rays, and the numbers can be compared.[6] In cases of low atomic number the disparity in ionization is often not so great. Likewise, the number of γ-rays can be compared with the number of x-rays. To take the first case, if f is the fluorescent yield, there will be f x-rays per disintegration and $\alpha/(1+\alpha)$ conversion electrons. If the electrons all come from the K shell, there will be $f\alpha/1+\alpha$ additional x-rays. With the same symbols as in Eq. (4):

$$R=\frac{N_e E_e d/r}{f(1+(\alpha/1+\alpha))NE_x(1-e^{-(\mu/\rho)_x\rho d})},$$

* This assumes that the energy loss per unit length of path is constant over the whole path length. The assumption is erroneous since the range is not a linear function of the energy, but it is simple and accurate enough for this purpose.

[6] This is the method used by L. W. Alvarez, Phys. Rev. **54**, 486 (1938).

where N is the number of disintegrations. $N_e/N=\alpha/1+\alpha$ so that:

$$R=\frac{\alpha}{1+2\alpha}\frac{E_e d/r}{(1-e^{-(\mu/\rho)_x\rho d})}. \tag{6}$$

Similar considerations apply to the comparison of x-rays and γ-rays. The formula is

$$R=\frac{1}{(1+2\alpha)f}\frac{E_\gamma(1-e^{-(\mu/\rho)_\gamma\rho d})}{E_x(1-e^{-(\mu/\rho)_x\rho d})} \tag{7}$$

in the case that the absorption in the ionization chamber window is unimportant. The correction term mentioned for Eq. (4) must be added if it is not. As an example, for the case of the 6.7 hr. Cd, the data were:

$E_\gamma=92$ kev, $E_x=22$ kev, $d=10$ cm.
Gas in ionization chamber CCl_2F_2 at 1.67 atmospheres. $\frac{1}{2}$ conversion electrons come from K shell.

$$(\mu/\rho)_x d\rho=0.33,\quad (\mu/\rho)_\gamma d\rho=0.017,$$

$$f=0.75,\quad R=3/1000,$$

$$\frac{3}{1000}=\frac{92(1-e^{-0.017})}{22(1-e^{-0.33})}\frac{1}{0.75}\frac{2}{(2+3\alpha)},$$

$$\alpha=75.$$

The uncertainty in the above types of measurement may be as great as 3× the value found, but since the values of α for values of l differing by one may differ by a factor of 10, the method is useful. Ellis and Aston[7] determined α by comparing, in a β-ray spectrograph, the intensity of conversion electrons with that of photoelectrons ejected by quanta. This method is useful if α is small; but it requires a considerable amount of not too certain calculation concerning the distribution in energy and direction of the photoelectrons. An accurate method is to compare, by means of a β-ray spectrograph equipped with counter, the number of disintegration electrons with conversion electrons. This has been used, for example, by Flammersfeld.[8]

The ratio of the K to the L conversion has, in most cases, been measured photometrically on films from the spectrograph, using as a standard a film exposed to Ga^{67} electrons for various lengths of time. If the ratio is large or the background large, the difficulty is obvious. Another method attempted in some cases is to obtain equal blackenings at the same point on two films by exposing the L line at the required higher field for longer times. This has the disadvantage that the background will be higher for the longer exposure. In the case of Ga^{67}, both methods have been used to give a K/L ratio of 8, which is in agreement with that determined by Valley and McCreary.[5]

As has been noted before, a transition may consist of both electric and magnetic radiation. From the formulae of Hebb and Nelson[2] one can calculate the K/L ratio for both kinds of radiation. Then if the observed ratio N_K/N_L lies between the two, the percentage of the transitions occurring by electric radiation is:*

$$\frac{E}{M+E}=\frac{1+\alpha_K+\alpha_L}{1+\alpha_K+\alpha_L+[(\alpha_K-N_K\alpha_L/N_L)/(\beta_L-N_K\beta_K/N_L)](1+\beta_K+\beta_L)}, \tag{8}$$

where α_K and α_L are the electric conversion coefficients, β_K and β_L the magnetic, and E and M the number of the transitions per sec. proceeding by electric and magnetic radiation, respectively.

Experimental Results

The experimental results are summarized in Table I. These take precedence over previously reported results.[9–13] For the cases in which the data are insufficient to decide the type of

[7] C. D. Ellis and G. H. Aston, Proc. Roy. Soc. **A129**, 180 (1930).

[8] A. Flammersfeld, Zeits. f. Physik **114**, 227 (1939).

* I wish to thank Mr. E. Nelson for information on this point.

[9] A. C. Helmholz, Phys. Rev. **57**, 248 (1940).

[10] H. Walke, Phys. Rev. **57**, 163 (1940).

[11] A. Langsdorf, Jr., and E. Segrè, Phys. Rev. **57**, 105 (1940).

[12] L. W. Alvarez, A. C. Helmholz, and E. Nelson, Phys. Rev. **57**, 660 (1940).

[13] G. T. Seaborg, J. J. Livingood, and J. W. Kennedy, Phys. Rev. **57**, 363 (1940).

TABLE I. *Gamma-ray energies and multipole orders.*

NUCLEUS*	GAMMA-RAY ENERGY IN KEV	HALF-LIFE OF TRANSITION	MULTIPOLE ORDER AND TYPE OF RADIATION†
Sc^{44}	268 ±5	52 hours	$E\,2^4$ or $E\,2^5$ (?)
Zn^{69}	439 ±5	13.8 hours	$E\,2^5$ or $M\,2^4$
Zn^{67}	92.5±1		$E\,2^2$
	180 ±2		$E\,2^1$ (?)
	297 ±3		$E\,2^1$ (?)
$Sc^{79\text{ or }81}$	99 ±1	1 hour	$E\,2^4$ and $M\,2^3$
Kr^{83}	46 ±1	110 min.	$E\,2^4$ and $M\,2^3$
	29 ±1		$E\,2^1$ (?)
Sr^{87}	386 ±5	2.8 hours	$E\,2^5$
43	97 ±1	90 days	$E\,2^5$ and $M\,2^4$ or $E\,2^4$ and $M\,2^3$
$Ag^{107\text{ or }109}$	92.5±1	40 sec.	$E\,2^4$
Te^{127}	86 ±1.5	90 days	$E\,2^5$ and $M\,2^4$
Te^{129}	102 ±1.5	32 days	$E\,2^5$ and $M\,2^4$
Te^{131}	177 ±3	1.2 days	$E\,2^5$ and $M\,2^4$ or $E\,2^4$ and $M\,2^3$

* Nucleus in which γ-ray transition takes place.
† E denotes electric, M magnetic radiation.

radiation, the most likely possibilities are given. For the sake of convenience in the discussion of individual cases below, the values of l usually refer to those appropriate in the half-life calculation. Hence, for example, if $l=5$, it must be remembered that the radiation may be magnetic 2^4-pole.

Sc^{44}

The activity of Sc^{44} was discovered by Walke.[10] It is produced by the $K^{41}(\alpha, n)Sc^{44}$ and $Ca^{43}(d, n)Sc^{44}$ reactions. Walke found both a 52-hour period and a 4.1-hour period belonging to this isotope. The 52-hour period showed, besides the positrons characteristic of the 4.1-hour activity, a group of electrons of energy about 250 kev. To see whether these were really conversion electrons from the γ-ray in an isomeric transition, a sample of Sc prepared by deuteron bombardment of Ca was placed in the spectrograph and showed a line of electrons at 260 kev. Recently Smith[14] has measured more accurately the energy of this γ-ray and found 268 kev. The good agreement of this result with Walke's absorption data seems proof that these are the conversion electrons from the γ-ray responsible for the isomerism. The conversion coefficient was estimated by comparing the number of conversion electrons with the number of photoelectrons from Pb. The x-rays from Sc are not energetic enough to be measured. The result for α was 0.5. The conversion coefficient calculated from the formula of Morrison and Dancoff is 0.60 for $l=5$, 0.15 for $l=4$, both within the error of the measured value. The calculated half-life for $l=5$ is 2.5×10^5 hours, for $l=4$, 13 min. On this basis the value of $l=4$ seems preferable. The L conversion could not be observed, nor is much variation of the K/L ratio with l expected at this energy and value of Z. An accurate value of α could probably decide the correct value of l.

[14] G. P. Smith, Phys. Rev. **59**, 937A (1941).

Zn^{69}†

The isomerism in Zn was investigated by Kennedy, Seaborg, and Segrè,[15] who found that the 13.8-hour period consisted of a γ-ray transition to the ground state of Zn, which then decayed to Ga^{69} with a half-life of 57 min. They observed no conversion electrons in absorption measurements, but estimated the γ-ray energy as 470 kev and set an upper limit of 0.1 for the value of α. Valley and McCreary[5] also failed to find evidence of conversion. The conversion electrons would be few in number for such a high energy γ-ray and might be masked by the disintegration electrons. However, Zn was bombarded with 8-Mev deuterons and placed in the spectrograph. A 24-hour exposure showed a line at $H\rho$ 2640. Another spectrogram with the Zn source covered with Pb showed K and L edges due to photoelectrons ejected by the same γ-ray. The energy deduced from the single line which must be the K conversion and from the Pb photoelectrons is 439 kev. The value of the magnetic field was checked in these cases by obtaining the K and L photoelectron edges from Pb for the 511-kev annihilation radiation.

It was estimated from the strengths of the samples used that the conversion coefficient was

TABLE II. *Comparison of observed and theoretical values α and α_K/α_L for* Ga^{67}.

	CALCULATED FOR ELECTRIC RADIATION			
	$l=1$	$l=2$	$l=3$	OBSERVED
α_K/α_L	10.5	8	4.5	8
Internal conversion coeff.	0.07	0.83	7.9	0.75

† The writer was aided in the work on this element by Dr. B. D. Nag.

[15] J. W. Kennedy, G. T. Seaborg, and E. Segrè, Phys. Rev. **56**, 1095 (1939).

of the order of 0.1–0.01. From Dancoff and Morrison's formula and $l=5$, we obtain $\alpha=0.036$. The calculated half-life with $l=5$ is 272 hours, with $l=4$, 2 sec. Therefore the value of 5 seems quite definite. No L conversion could be observed so the K/L ratio could not be determined. Surprisingly enough, the calculated magnetic conversion coefficient is 0.039, so it is not possible to tell whether this is electric 2^5-pole or magnetic 2^4-pole radiation.

Zn^{69} can be made by neutron bombardment of Zn^{68} which has a spin 0. Ga^{69} has a spin of $\frac{3}{2}$,[16] so it is natural to assume that the ground state of Zn^{69} has a spin of $\frac{1}{2}$. Then the isomeric state would have a spin of $1\frac{1}{2}$, or at least $\frac{9}{2}$ if the electric transition with $l=4$ was forbidden.

Ga^{67}

Alvarez[6] first found an internally converted γ-ray in Ga^{67} formed in the reaction $Zn^{66}(d, n)Ga^{67}$, which decays by K-electron capture to Zn^{67}. Alvarez estimated the conversion coefficient as 2.* Beta-ray spectrograms showed two lines at $H\rho$ 1007 and 1065, the K and L conversion lines in Zn of a 92.5-kev gamma-ray. This result is in agreement with that of Valley and McCreary.[5] The source was obtained by dissolving Zn in 6N HCl, shaking with ether to extract $GaCl_3$, evaporating the ether to a small volume, and then putting it in the source boat drop by drop. To verify Alvarez' conclusion that the γ-ray is only partially converted a source was covered with Sn. The resulting film showed an edge at 64 kev due to the K photoelectrons ejected from Sn (K binding energy 29 kev) by the 92.5-kev gamma-ray. This picture also showed an edge at 151 kev. To prove that this came from a gamma-ray of 180 kev, another source was covered with a thin sheet of gold about 0.5 mg/cm² thick. The resulting picture then showed lines at 100 and 167 kev, the K and L photoelectrons from the 180-kev gamma-ray, and another at 216 kev resulting from a 297-kev gamma-ray. Although these gamma-rays are probably dipole radiations and the internal conversion coefficients only of the order of 0.01, sufficiently strong samples were obtainable so that exposures of several days

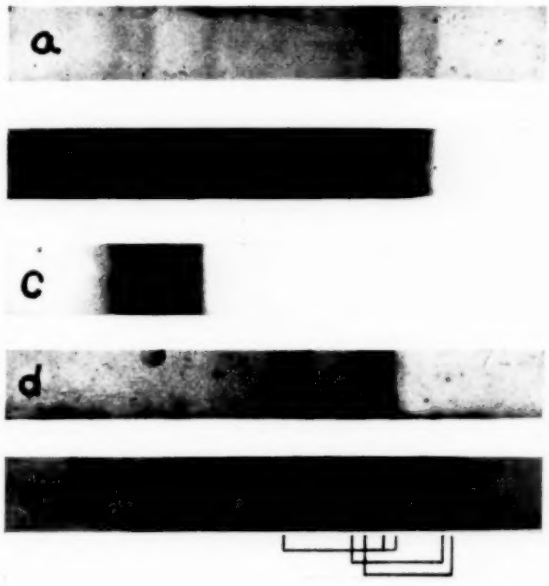

FIG. 2. Examples of β-ray spectrograph films. $H\rho$ increases to the right. (*a*) Lines from Se and Kr. (*b*) K and L lines from Sr^{87}, differing by only 2 percent in $H\rho$. (*c*) K and L lines from element 43. (*d*) K, L, and M lines from 6.7-hr. Cd. (*e*) Film from radioactive Te isotopes. K, L, and M lines of 86-kev γ-ray, K and L lines from 102 and 107-kev γ-rays.

showed conversion lines at 170 kev and 288 kev. It might be thought that these were photoelectrons from the source, but the photoelectric absorption coefficient is very low in Ga for these γ-rays, and, since the source is separated without carrier, there would not be enough material to produce the effect. Since thé source boat is made of Al, photoelectrons from it would differ in energy. The L conversion of these two gamma-rays is probably very small and was not observed. The K/L ratio of the 92.5-kev gamma-ray is 8 to 1, as measured from single films and by exposing one film to eight times as much radiation as another.

Several different measurements of the internal conversion coefficient were made. The experiment of Alvarez comparing the numbers of electrons and x-rays was repeated. The ionization of the photoelectrons ejected from a sheet of copper was compared with that of the conversion electrons as mentioned above. In addition, the ionization of the x-rays was compared with that of the unconverted gamma-ray. The gamma-ray absorption curve is difficult to resolve so that this method is not so satisfactory. Besides the three

[16] N. A. Renzetti, Phys. Rev. **57**, 753 (1940).

* His value of $\frac{3}{4}$ refers to the ratio of conversion electrons to conversion electrons plus gamma-rays.

gamma-rays mentioned, there may be even a fourth of higher energy. The results of all these determinations were quite consistent, and the value of α ranged for the most part from 0.5 to 1. From Table II one can see that this definitely establishes the gamma-ray as electric quadrupole. The conversion electrons of the 180-kev gamma-ray were not observable on an absorption curve, so that no estimate of the coefficient could be made. For the 297-kev gamma-ray, only a slight indication of the electrons was discernible, and from this and the gamma-ray intensity one deduces a coefficient appropriate to $l=1$.

Of the three gamma-rays, the 93 kev is the most intense, the 180 kev is least intense. This suggests that most of the processes proceed from Ga^{67} through the state in Zn^{67} 93 kev above ground. However, sometimes the disintegration goes through a state 93+297 kev above ground, and least often through a state 93+297+180 kev above ground, each then cascading down. The fact that the most energy is available in the first process would explain the preponderance of that type of disintegration.

Se^{79} or Se^{81}

Langsdorf and Segrè[11] found a case of isomerism in Se with a half-life of 1 hour and electrons of about 100-kev energy. To measure the energy of this converted γ-ray, a Se source was prepared as described above, and placed in the spectrograph. Two lines at $H\rho$ 1035 and 1095 were found. (See Fig. 2a). To be sure that these were due to the isomerism in Se, successive exposures were made and showed that the intensity of the lines decreased appropriately for a substance with a 1-hr. half-life. The energies of the lines are 86.8 and 96.4 kev. On addition of the K and L binding energies of Se, the γ-ray energy turns out to be 99 kev as has been reported. The K/L conversion ratio is 4. Because of the many activities produced by Se+d, it was not possible to separate out this activity for a test of the conversion coefficient. The fact that the daughter activity is β-active, going to Br, would also hinder the determination. Assuming $l=4$ for the transition, we calculate a half-life of 9 hours. The observed K/L ratio points then to a mixture of 50 percent electric and 50 percent magnetic radiations. Assuming $l=3$ or $l=5$ would make the calculated half-lives in error by large factors. In addition, an electric 2^3-pole γ-ray would not have a K/L ratio as low as 4. Therefore, the assignment to part electric 2^4-pole, part magnetic 2^3-pole radiation seems quite conclusive.

Kr^{83}

Langsdorf and Segrè[11] found that the decay of Br^{83} produces a 110-min. activity in Kr^{83}. Since Kr^{83} is stable, this activity must be due to isomerism. They found very soft electrons indicating a γ-ray of about 30 kev. Br^{83} can be produced by the Se(d, n)Br reaction, so the same pictures obtained for Se were examined for the Kr lines. In the low energy region three lines at $H\rho$ 725, 620, and 572 were found. (See Fig. 2a.) Successive exposures seemed to indicate that all three came from the same activity and that this activity was probably Kr. The Kr activity should at first grow and then decay. Actually, the first two exposures of $1\frac{1}{2}$ hr. each showed equal intensities. Thereafter the intensities fell off corresponding to a 2-hr. half-life. This evidence in conjunction with Langsdorf and Segrè's absorption measurements indicates that these lines come from Kr^{83}. One exposure showed evidence of a fourth line at about 15 kev. Therefore, the three lines seem to be the L conversion of a 29-kev γ-ray, and the K and L of a 46-kev γ-ray. The question then arises as to which transition has the life of 110 min. A similar case of two low energy γ-rays, one probably with $l=4$, the other $l=1$ has been investigated in the 4.4-hr. isomerism of Br^{80}.[17] The K/L ratio of the 46-kev γ-ray is 1. If $l=4$ for this transition, the calculated half-life is 50 hr., in good agreement with the observed value, and the radiation would be 60 percent electric, 40 percent magnetic.* The observed K/L ratio cannot be fitted by $l=1$, 2, or 3, so it seems probable that this transition has $l=4$. The failure to observe the K line of the 29-kev γ-ray would then be due not to the low K/L ratio but to the rapid decrease with energy of the sensitivity

[17] A. P. Grinberg and L. J. Roussinow, Phys. Rev. **58**, 181 (1940).

* It must be remembered that the calculation of the magnetic conversion coefficient is uncertain for γ-ray energies not much greater than the K binding energy, as in this case. Also, in the case of high atomic numbers such as Te, the electric conversion coefficient calculations are uncertain.

of the film.[18] If this γ-ray is a dipole ray, the conversion coefficient would be 3.5, which might be observable and would provide a check of this scheme. Kr^{83} has a spin of $9/2$.[19] If there were a level 75 kev above ground with spin $1/2$, another 29 kev above ground with spin $7/2$, and the transition $1/2$ to $7/2$ with electric 2^3-pole radiation was forbidden, one could explain the observations. However, the explanation seems somewhat artificial.

Sr^{87}

The isomerism in Sr^{87} was discovered by DuBridge and Marshall,[20] who found a converted γ-ray associated with a 2.75-hr. period. This Sr activity grows from the 80-hr. Y^{87}. This latter activity was produced here in great quantities in the production of Sr^{89} for biological use. Several strong samples were separated from Y and the half-life measured as 2.8 hours. The β-ray spectrograph showed the line found by DuBridge and Marshall. The K and L lines differ in $H\rho$ by only 2 percent; but by using a radius of curvature of 6 cm it was possible to separate the two lines. (See Fig. 2b.) The $H\rho$ values were 2395 and 2447, the energies 370 and 383 kev. Adding the K and L binding energies of Sr gives 386 kev as the γ-ray energy. The K/L ratio as determined from microphotometer measurements and different length exposures is 6–7. Finally, the conversion coefficient was determined as mentioned above. The average of the measured values was 0.15, in agreement with the measurements of DuBridge and Marshall.[20] For $l=5$, the calculated half-life is 520 hours, for $l=4$, 4 sec. The K/L ratio for electric 2^5-pole radiation is 6, and the conversion coefficient is 0.06, which is within the experimental error. From the half-life, $l=5$ seems preferable, and from the other data quite certain. Magnetic 2^4-pole radiation would give a K/L ratio of 10. Consequently, this is probably electric radiation.

The spin of the ground state of Sr is $9/2$.[21] If we omit from consideration, as unlikely, spins of $^1 7/2$ or $^1 9/2$, the spin of this excited state must then be $1/2$, and the transition with $l=4$ must be forbidden.

[18] For example, B. v. Borries and M. Knoll, Physik. Zeits. **35**, 279 (1934).
[19] H. Korsching, Zeits. f. Physik **109**, 349 (1938).
[20] L. A. DuBridge and J. Marshall, Phys. Rev. **56**, 706 (1939); **58**, 1 (1940).
[21] M. Heyden and H. Kopferman, Zeits. f. Physik **108**, 232 (1938).

Element 43

Kalbfell[22] reported two internally converted γ-rays from long-lived element 43. He was at the time unable to assign them to the 90- or 62-day periods measured by Cacciapuoti.[23] The same sample used by him, and another kindly supplied by Dr. E. Segrè both gave a pair of lines at $H\rho$ 960 and 1080. (See Fig. 2c). These indicate a γ-ray energy of 97 kev. A part of one of these samples was followed for 200 days with an electroscope, and decayed with a half-life of 91 ± 2 days. Absorption curves showed that almost all the ionization was due to electrons of energy about 90 kev. Therefore, the assignment of this γ-ray to the 90-day period is certain. Seaborg and Segrè[24] reported that the x-rays from a sample of the two long-lived activities were Mo K x-rays. However, several absorption measurements on the same sample using their technique of critical absorption, showed that most of the x-rays belonged to element 43. Since the sample had aged considerably since their experiments, the conclusion is that the x-rays due to the 62-day period are Mo x-rays arising from K capture, those from the 90-day period are element 43 x-rays, arising from the internally converted γ-ray of the isomeric transition. This interpretation encounters the objection that no isotopes of 43 are supposed to be stable,[25] and no activity of half-life less than 15 years growing from the 90-day period has been observed.

On the assumption that this is an isomeric transition, l must be 4 or 5. The observed K/L ratio is 2. With $l=5$, this would mean 70 percent magnetic 2^4-pole, 30 percent electric 2^5-pole radiation, a conversion coefficient of 470, and a half-life of 10^5 days. On the other hand, $l=4$ gives 50 percent electric, 50 percent magnetic radiation, $\alpha=61$, and a half-life of 0.1 day. No unconverted γ-rays were observed, but the samples used were not strong enough even were α equal to 61. Since the calculated half-lives are both in error by a factor of 10^3, there seems no adequate way of determining the multipole order unless by determining α.

[22] D. C. Kalbfell, Phys. Rev. **55**, 422 (1939).
[23] B. N. Cacciapuoti, Phys. Rev. **55**, 110 (1939).
[24] G. T. Seaborg and E. Segrè, Phys. Rev. **55**, 808 (1939).
[25] H. Jensen, Naturwiss. **26**, 381 (1938).

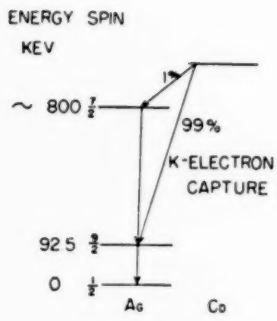

FIG. 3. Possible level scheme for 6.7-hr. Cd.

$Ag^{107 \text{ or } 109}$

The observation of the 40-sec. Ag activity growing from the 6.7-hr. Cd has been described previously.[12] The β-ray spectrograph showed the same lines observed by Valley and McCreary.[8] (See Fig. 2d.) The source in this case was prepared by dissolving the bombarded Ag in HNO_3, precipitating AgCl, adding 1 mg of Cd as carrier, and precipitating CdS. An absorption curve of the x-rays and γ-rays showed, besides the Ag K x-rays, the unconverted γ-rays of about 90 kev and a hard γ-ray of about 700 kev. The conversion coefficient calculation was given as an example above. The average observed value of 100 agrees well with 110 calculated for electric 2^4-pole radiation; and the observed K/L ratio of 1 also agrees well with the calculated value of 1. The calculation of the lifetime given in the original note[12] was done with the formula given by Bethe.[26] Using the correct formula (2), the calculated half-life is 5000 sec., which is poor agreement but somewhat better than for $l=3$, which gives 0.01 sec.

Over 5 half-lives, the 700-kev γ-ray decayed with a half-life of 6.7 hours, so it certainly belongs to this activity. It occurs in only about 1/100 of the disintegrations and must come from an excited state in Ag, through which the disintegration proceeds less often because of the reduced energy available.

The spin of the ground state of Ag is $\frac{1}{2}$,[27] so that the spin of the excited state must be at least $\frac{7}{2}$ or perhaps $\frac{9}{2}$. A possible level scheme showing the mode of disintegration is given in Fig. 3.

Te^{127}, Te^{129}, Te^{131}

Seaborg, Livingood and Kennedy[13] found three cases of isomerism in Te from the reaction Te(d, p)Te. The half-lives of the upper isomeric states and the isotopes responsible are 1.2-day Te^{131}, 32-day Te^{129}, and 90-day Te^{127}. In each case they have been able to make fairly complete isomer separations by the chemical method, suggesting that the γ-rays are fairly highly converted. The sources observed in the spectrograph at the time of the report by Seaborg, Livingood and Kennedy were weak, and since then much stronger sources have been available. Te was scraped from the target bombarded with 16-Mev deuterons and separated chemically.* It was then placed in the spectrograph and an exposure of two days made. Two lines at $H\rho$ 1375 and 1515 appeared. In longer exposures at later times these lines were absent; hence we may ascribe a γ-ray of energy 177 kev of which these are the K and L conversion lines, to the 1.2-day period. Kalbfell has observed these lines also but with weaker sources. The K/L ratio is 2. The half-life calculated with $l=5$ is 3.4×10^4 hr., with $l=4$, 4.5 min. The K/L ratio could be explained on either basis by assuming part electric and part magnetic radiation. The conversion coefficient could not be measured because of the other Te activities. It would be 20 for $l=5$, 4 for $l=4$. A good determination of the conversion coefficient would seem, at present, to be the only method of deciding the l value.

Because the source element is the same as the bombarded one, it is difficult to get high specific activity. However, exposures of 4–6 days after the 1.2-day period had died away showed five lines at $H\rho$ 807, 997, 1020, 925, and 1105. These correspond to the K, L, and M conversion in Te of an 86-kev γ-ray, the K and L of a 102-kev γ-ray (see Fig. 2e. The other pair of lines observed seem to come from a 107-kev γ-ray, whose assignment is uncertain). The L line of the former seems more intense than the K, while for the latter they seem about equal. The lines are faint and the background large, so that an accurate determination of the intensity ratio has not been possible. To determine which γ-ray

[26] H. A. Bethe, Rev. Mod. Phys. **9**, 226 (1937).
[27] D. A. Jackson and H. Kuhn, Proc. Roy. Soc. **A158**, 372 (1937).

* I wish to thank Mr. G. Friedlander for doing the chemical work.

belongs to which period, pictures were taken after 30 and 60 days. After 60 days the 86-kev γ-ray was relatively more intense than at the beginning so that it must be the γ-ray of the 90-day isomeric transition, the 102 kev that of the 32-day transition.

A γ-ray in Te with $l=5$ and an energy of 102 kev corresponds to a calculated half-life of 2400 days, too large by a factor of 75. On the other hand, the assumption of $l=4$ gives a half-life only 1/5000 the observed. The value of 5, therefore, seems quite probable. Using this value, one then calculates that a K/L ratio of 1 is consistently explained by 45 percent electric 2^5-pole radiation, 55 percent magnetic 2^4-pole radiation. Similarly, a γ-ray with $l=5$ and an energy of 86 kev in Te, gives a calculated half-life of 40,000 days, 400× longer than the observed 90 days. However, $l=4$ gives only 10 minutes as the calculated half-life, and since this is only 1/13,000 the observed value, $l=5$ seems much to be preferred. The estimated K/L ratio of 0.75, which is probably not wrong by more than 30 percent, then gives for this case also a mixture of 50 percent electric, 50 percent magnetic radiation. The calculated conversion coefficients are large, 2000 and 10,000, respectively; and no unconverted γ-rays could be observed.

Conclusion

The results discussed above indicate that in many cases of nuclear γ-rays, it is feasible to determine the type of the radiation, electric, magnetic, or both, and the multipole order. Although present formulae for the lifetimes of γ-ray transitions usually indicate a preferable value of the multipole order, in only two or three out of ten cases is the agreement of theory and experiment satisfactory. Therefore, an improvement of the theory on this point would be valuable.

In conclusion, I wish to thank Professor E. O. Lawrence, Professor L. W. Alvarez, and Dr. E. Segrè for their interest and assistance in this work; and Mr. E. Nelson for helpful discussions of the theory. This work has been aided by the financial assistance of the Research Corporation.

SEPTEMBER 15, 1941 PHYSICAL REVIEW VOLUME 60

Artificial Radioactivity of Ti^{45}

J. S. V. Allen,* M. L. Pool, J. D. Kurbatov, and L. L. Quill
The Ohio State University, Columbus, Ohio

(Received July 24, 1941)

A radioactive isotope possessing a half-life of 3.08 ± 0.06 hours has been produced by four different types of bombardment. Evidence is presented which indicates that the activity should be assigned to Ti^{45}. The four nuclear reactions are:

$$Ca^{42}+He^4\rightarrow Ti^{45}+n^1 \qquad Sc^{45}+H^2\rightarrow Ti^{45}+2n^1$$
$$Sc^{45}+H^1\rightarrow Ti^{45}+n^1 \qquad Ti^{46}+n^1\rightarrow Ti^{45}+2n^1.$$

Nuclear spin considerations indicate that a fifth reaction, $Ti^{46}(\gamma,n)Ti^{45}$, is improbable, as was verified experimentally. Analysis of cloud-chamber pictures reveals the maximum positron energy to be 1.2 Mev. On a Sargent diagram, the reaction $Ti^{45}\rightarrow Sc^{45}+e^+$, is a permitted one. The half-life of $3.08\pm.06$ hours for Ti^{45} is the weighted average of 3.17, 3.10, and 3.02 hours from $Sc(p,n)$; 3.04 hours from $Sc(d,2n)$; 3.17 hours from $Ca(\alpha,n)$; 3.0 hours from $Ti(n,2n)$.

Introduction

THE elements in the titanium region, shown in Fig. 1, have been quite thoroughly examined for radioactive isotopes by Walke and others. Walke[1] has reported many new radioactive isotopes in potassium, calcium, scandium, titanium, and vanadium, of which the two in scandium, Sc^{43} (4 hours) and Sc^{44} (4.1 hours) have

* On sabbatical leave from Bethany College, Bethany, West Virginia.

[1] H. Walke and others, Phys. Rev. **51**, 143A, 439, 1011A, 1033 (1937); **52**, 669, 777 (1937); **57**, 163, 171, 177 (1940); Proc. Roy. Soc. **A171**, 360 (1939).

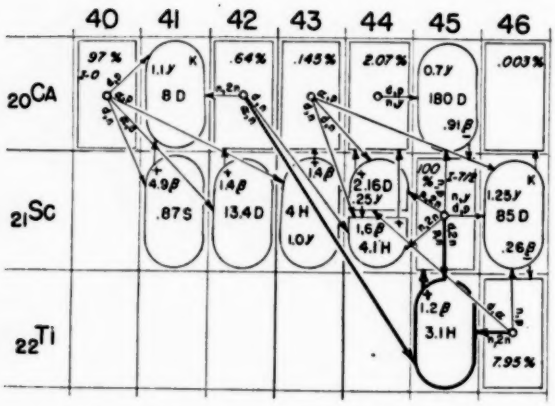

FIG. 1. Nuclear transmutation chart of the titanium region.

periods close to Ti^{45} and are of some interest in connection with the present work. The only activities in titanium that have been reported are the isomers of Ti^{51} (2.8 minutes and 72 days).[2] Calcium, scandium, and titanium have been subjected to the various bombardments but no reference has been found to the Sc+p reaction which may produce Ti^{45}. The reactions, Sc+d, Ca+α and Ti+n (fast) have been reported in the literature. However, the presence of the active isotope Ti^{45} has not been reported. In the present work, the first bombardment of scandium oxide with protons, which was followed by a chemical separation of the titanium, showed a three-hour period in the titanium fraction. The observation of this new period aroused our interest not only in assigning this period but in finding the experimental conditions which had prevented previous investigators from detecting this strong activity.

The present work was done on the 42-inch cyclotron at The Ohio State University. Radioactive measurements were made on a Wulf electrometer with an ionization chamber filled with two atmospheres of Freon. A submersive type Geiger-Müller tube was used throughout the chemical procedure to follow the extent of chemical separation.

ACTIVATION OF SCANDIUM WITH PROTONS

When scandium oxide was bombarded with 5-Mev protons for several hours, an isotope exhibiting a very strong half-life of approximately three hours was produced. The first determination of the activity showed it to have an intensity nearly 1000 times the background. The decay has been followed for more than eleven half-lives to an intensity of one-fourth background (Fig. 2). The period obtained from this curve is 3.02 hours. Values determined for other samples bombarded under similar conditions are 3.17 and 3.10 hours.

Nearly all of the activity is due to positron emission. There are a few electrons and some gamma-radiation, as measured on the electrometer, probably due to annihilation radiation. However, the quantity of gamma-radiation associated with this period is very small.

Since scandium has but a single stable isotope, the reaction $Sc^{45}(p,n)Ti^{45}$ should be the first considered. The formation of Ti^{45} was later confirmed by other nuclear reactions and other supplementary data.

It has been found[3,4] that certain radioactive elements, even in minute concentrations, may be separated in a very pure form in the absence of a carrier. The basic principle involved in this major distinction from accepted radio-chemical procedure has been extended by one of us (J.D.K.) to work given here on the separation of scandium and titanium and will be described in detail.

The precipitation of Ti^{45} in the pure state, without the addition of inactivated titanium from scandium has the advantage that the absence of a large quantity of titanium permits fast separation. This procedure reduces the amount of titanium in the precipitated state which impedes filtration and augments contamination of the titanium through adsorption of active elements. Moreover, the chemical procedures for the separation of scandium and titanium were arranged in such a way that other possible activities which might appear after bombardment could be removed and identified. During chemical separations and purifications, the volume of each fraction was estimated and the activity of ten milliliters measured with the Geiger-Müller counter.

The following elements were considered as

[2] H. Walke, Phys. Rev. **51**, 1011 (1937); Walke, Williams, and Evans, Proc. Roy. Soc. **A171**, 360 (1939).

[3] J. D. Kurbatov, J. Phys. Chem. **36**, 1241 (1932).

[4] J. D. Kurbatov, M. L. Pool, and H. B. Law, Phys. Rev. **59**, 919A (1941).

possible minor impurities: carbon, sodium, magnesium, silicon, phosphorus, potassium, titanium, and iron. In addition, active isotopes arising from calcium and oxygen present in the scandium oxide, and from the copper target, were stabilized and removed.

The chemical procedure after the deuteron bombardment of scandium was similar to that used after the proton bombardment except for the elimination of the different radioactive isotopes formed by deuteron bombardment.

The procedure consisted in dissolving the activated scandium oxide in nitric acid. The resulting solution was then successively evaporated with additions of nitric, of hydrochloric, and of hydrofluoric acids to remove any N^{13}, O^{15} and F^{18} present.

This treatment was followed, after the addition of one-hundredth gram-ions of sodium, potassium, magnesium, calcium, copper, and cobalt to stabilize the corresponding radioactive isotopes in solution, by the precipitation of scandium and radioactive titanium with excess ammonia. However, no inactivated titanium was added as a carrier. After filtration, the activity of the solution was measured with the G-M immersion tube. The above precipitation of scandium and titanium with stabilizers was repeated if any perceptible activity due to impurities was observed.

There are two procedures commonly used in the separation of scandium and titanium, namely, precipitation of scandium with hydrofluoric acid and with oxalic acid. Both reactions were employed in the present work. The first one was used primarily for the separation of titanium and scandium, while the second was used only for purification.

After the precipitated hydrous oxides of scandium and radioactive titanium were treated with acid, considerable active titanium still remained on the filter paper, even after the scandium was dissolved. The solution was then treated with hydrofluoric acid to precipitate the scandium. After filtration, most of the active substance was found in the solution and was called titanium fraction *A*.

The scandium precipitate was dissolved and inactive titanium was added for the first time. The scandium was reprecipitated with hydrofluoric acid yielding titanium fraction *B* and scandium fraction 1.

The titanium that remained on the filter paper after the first filtration was dissolved in acid, inactive scandium was added, and the solution was treated with hydrofluoric acid. This procedure gave titanium fraction *C* (filtrate) and the practically inactive scandium fraction 2 (precipitate).

The three fractions of titanium were purified separately by the precipitation of titanium with ammonia after stabilizers for the impurities had been added; and the two scandium fractions were dissolved and reprecipitated as the oxalate in the presence of stabilizers for the possible impurities, Fe^{59}, P^{32}, $Zn^{63, 65}$.

The relative intensities of the activities in the different fractions of titanium and scandium can be seen in Table I. The activities are computed for the same time, a few hours after bombardment.

The activity measured in the three titanium fractions, *A*, *B*, *C*, was found to be the three-hour period. The weak activity of the scandium fractions indicated the efficiency of separation.

To test the efficiency of precipitation of scandium and titanium without the use of a carrier,

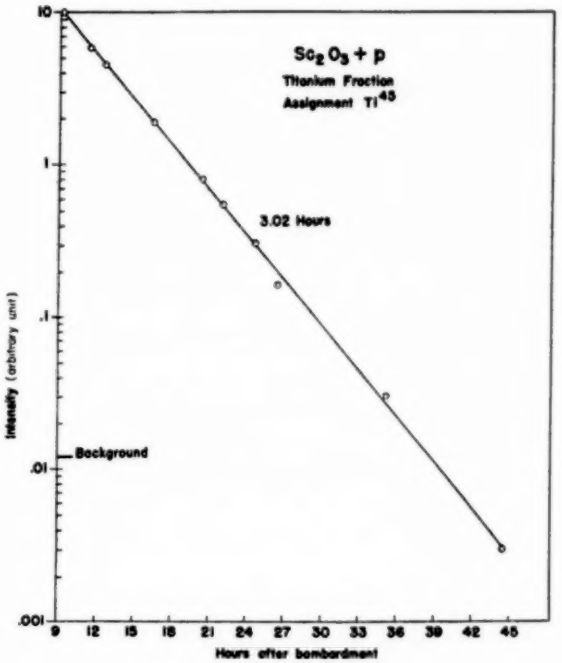

FIG. 2. Decay curve for Ti^{45}.

the following experiment was performed: Activated scandium oxide (bombardment time, 2 hr.) was dissolved in hydrochloric acid and the solution was diluted to one liter. Only three milliliters of this solution were used, from which the scandium and active titanium were precipitated by ammonia without a carrier. The precipitate contained 7.57 units of activity seven hours after bombardment, and the half-life was determined as 3.11 hours, which indicates the presence of Ti^{45}. The filtrate contained 0.5 unit of activity or 6.6 percent. Since the half-life of Ti^{45} is 3.08 hours, the decay constant λ is 6.22×10^{-5}. If one accepts arbitrarily that the unit of activity measured on the electrometer is of the order of magnitude of one microcurie, the total weight of Ti^{45} precipitated without carrier was found to be 4.45×10^{-14} gram.

Activation of Scandium with Deuterons

Scandium oxide was bombarded with 10-Mev deuterons for four hours, and the active titanium was separated chemically. The activity of this titanium fraction was found to have a period of 3.04 hours, and was followed for five half-lives.

The activity produced in scandium with either protons or deuterons is of such an intensity that it can be followed and the half-life obtained even without chemical separation. This strong activity apparently did not disturb the determination by other investigators of the 85-day period of Sc^{46}. Thus, the Ti^{45} must have been completely separated chemically from the scandium, even though no attempt was made to separate titanium but only to establish the scandium period.[5] If the filtrate, after separation of scandium, was not tested for activity, it might easily have been discarded.

Thus these investigators confirmed our contention that pure radioactive titanium can be separated without a carrier.

Also, the same workers did not observe Ti^{45} after bombardment of calcium with α-particles.[6] The loss of Ti^{45} was probably due to the chemical separation of scandium, titanium, and calcium which was performed with the addition of scandium and titanium carriers, according to classical radio-chemistry, and in which the recovered titanium fraction had an activity similar to that of the scandium fraction. This factor indicates the contamination of the titanium fraction by scandium.

Table I. (Sc+p). *Relative activities of titanium and scandium.*

Fraction	Relative Activity
Ti *A*	187
Ti *B*	3.4
Ti *C*	31
Sc 1	1.58
Sc 2	

Activation of Calcium with Alpha-Particles

The calcium oxide used in this bombardment was prepared from chalk by several reprecipitations with ammonium carbonate and final conversion to the oxide. The latter was bombarded with 20-Mev alpha-particles for five hours. The titanium fraction obtained after separations of titanium from scandium displayed a half-life of 3.17 hours. This period was followed for four half-lives, indicating the reaction $Ca^{42}(\alpha,n)Ti^{45}$. One might have expected a very weak activity in titanium because the abundance of Ca^{42} is only 0.64 percent.

Since the predominating activity from this bombardment was the four-hour period in scandium obtained from an α,p reaction of Ca^{40}, the chemical procedure was arranged with the single purpose of separating Ti^{45} in the shortest possible time. Therefore, the usual analytical procedure for separating the elements calcium, scandium, and titanium was disregarded.

The procedure consisted in solution of the bombarded calcium oxides in acid, precipitation of scandium and titanium without carriers, filtration of calcium from scandium and titanium, and purification later from other possible activities as described under the proton and deuteron bombardments.

The filter paper, even with no visible precipitate, had practically all of the scandium and titanium activities. The filtrate, containing calcium, had only a very small percentage of the

[5] H. Walke, Phys. Rev. **52**, 669 (1937).

[6] H. Walke, Phys. Rev. **57**, 169 (1940).

total activity as measured on the Geiger-Müller counter, so it was disregarded.

The scandium and titanium precipitate was dissolved in acid and the solution was treated with hydrofluoric acid, after a scandium carrier had been added. The purification of the scandium and titanium fractions was made as described under the (Sc,p) reaction.

Activation of Titanium with Fast Neutrons and Gamma-Radiation

Titanium oxide was bombarded for six hours with fast neutrons from the Li+d reaction. For this bombardment, commercial TiO_2 was purified by the repeated solution and precipitation of titanium. Analysis of the latter indicated 99.8–99.9 percent TiO_2. After bombardment, the weak 3.0-hour activity of the titanium fraction could be followed for only two half-lives, beginning at seven times the activity of the background. These measurements were used to verify the $Ti^{46}(n,2n)Ti^{45}$ reaction, but were too uncertain to be used in determining the final figure for the half-life of Ti^{45}.

With gamma-radiation from the Li+p reaction, on a TiO_2 target, no three-hour activity was obtained. The following nuclear spin considerations suggest an explanation. The angular momentum of Sc^{45} has been observed[7] to be $7/2$; and since $Ti^{45}\rightarrow Sc^{45}+e^+$ is a permitted transition (as shown below) the angular momentum of the titanium nucleus should also be in the neighborhood of $7/2$. But since the Ti^{46} nucleus probably has 0 or 1 unit of spin, bombardment with gamma-rays could hardly increase this to $7/2$.

Maximum Positron Energy

Pictures were taken of the positron tracks in a cloud chamber containing hydrogen at atmospheric pressure and saturated alcohol vapor. The radii of curvature of 887 tracks were measured in a magnetic field of 256 gauss. From the spectrum shown in Fig. 3, the maximum positron energy by inspection is 1.24 Mev. When this end point, together with the half-life, is plotted on a Sargent diagram, the point falls on the first curve with the permitted transitions. The upper limit of the positron spectrum from a Fermi plot is 1.26 Mev, and from a Konopinski-Uhlenbeck plot, 1.40 Mev.

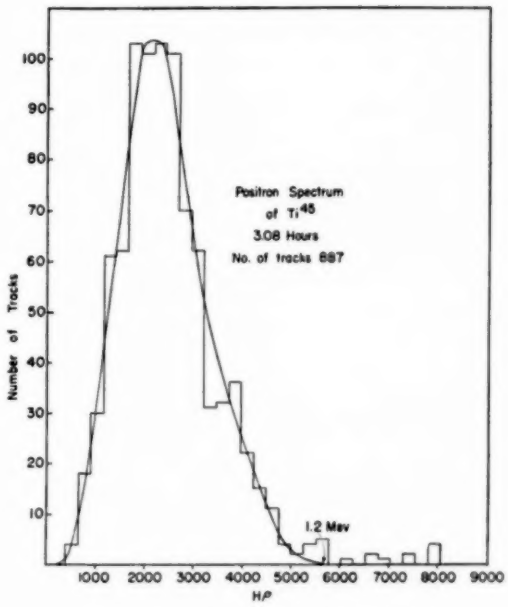

FIG. 3. Positron histogram of Ti^{45}.

If the logarithm of the half-life of Ti^{45} is plotted against its atomic number, the point falls very close to the curve given by Dickson and Konopinski[8] for even atomic nuclei with one excess neutron. The predicted half-life for Ti^{45} was five hours.

Grateful acknowledgment is made for the grants-in-aid by Mr. Julius F. Stone and by The Ohio State University Development Fund. Thanks are also due to W.P.A. project No. 65-1-42-89 for preparation of diagrams and for technical assistance in the operation of the cyclotron.

[7] H. Kopfermann and E. Rasmussen, Zeits. f. Physik **92**, 82 (1934).

[8] G. R. Dickson and E. J. Konopinski, Phys. Rev. **58**, 949 (1940).

Radiations from Radioactive Cobalt

ARTHUR S. JENSEN*
Randal Morgan Laboratory of Physics, University of Pennsylvania,† Philadelphia, Pennsylvania
(Received June 19, 1941)

A cloud chamber has been built and is briefly described. It has been used for measuring the energies of the radiations from the long-lived cobalt isotopes, $Co^{56,58}$, formed by deuteron bombardment of iron. A positron spectrum with a maximum energy of 1.36 ± 0.10 Mev was observed on the histogram. The K-U plot of the data suggests also another spectrum with an energy end point near 0.5 Mev. One internally converted γ-ray near 0.1 Mev was observed in the cloud chamber and resolved into two lines at 117 kev and 130 kev, respectively, by a magnetic spectrograph. Still higher energy γ-rays less intensely internally converted are suggested.

The histogram from a sample of Co^{58} produced by bombarding manganese with α-particles definitely assigns the higher energy positron spectrum to the isotope Co^{58}.

INTRODUCTION

THE activities of the radioactive isotopes of cobalt have been fairly definitely assigned, though the details of the latest investigations have not yet been published. Sampson, Ridenour, and Bleakney[1] were the first to observe long period activity in cobalt when a sample of cobalt was bombarded with slow neutrons. Risser[2] later observed the same activity, and estimated the half-life at 2 years. This value has lately been changed to 5.5 years by Livingood and Seaborg[3] who have followed the activities of chemically separated cobalt samples for some years. Livingood and Seaborg[4] also observed this period in deuteron-activated cobalt. These reactions result in both Co^{58} and Co^{60}, but a half-life of 72 days[3] has been assigned to the isotope Co^{58} by Livingood and Seaborg, who produced this single isotope by bombarding manganese with 16-Mev α-particles;[4] therefore, the long period presumably is to be associated with the isotope Co^{60}. The same shorter period was also observed in their[4] samples of cobalt bombarded with neutrons and deuterons, and later observed by Viktorin[5] in nickel activated by fast neutrons; Livingood and Seaborg[3] confirm the Ni(n, p) reaction.

Perrier *et al.*[6] first observed an activity whose period has been corrected to 270 days[3] in a sample which had a strong iron impurity[4] bombarded with deuterons. In this same sample they also found an indication of what must have been the 72-day Co^{58}. The 270-day activity was produced by Livingood and Seaborg[4] with protons on iron. These two reactions can produce the cobalt isotopes having mass numbers 55, 56, and 58, but since the 72-day activity has already been assigned to Co^{58} by the Mn$+\alpha$ reaction and the 18.2-hour activity of Co^{55} produced by lower energy deuterons has been well known for a long time,[7] the 270-day activity probably belongs to Co^{56}, as it has been assigned.[3] The isotope chart in Fig. 1 summarizes these assignments.

It was pointed out by Perrier *et al.*[6] that most of the particles from their Fe$+d$ sample consisted of electrons, but except for this and the absorption measurements, unpublished except for their results, of Livingood and Seaborg,[3] no attempt has been made to measure the energies of the radiation from the cobalt isotopes 56 and 58. This series of experiments is an attempt to gather more precise information on the radiation energies. A preliminary report of these investigations has already been published.[8]

* George Leib Harrison Fellow, Physics Department, University of Pennsylvania.
† Now at the U. S. Naval Academy, Annapolis, Maryland.
[1] M. B. Sampson, L. N. Ridenour, and W. Bleakney, Phys. Rev. **50**, 382L (1936).
[2] J. R. Risser, Phys. Rev. **52**, 768 (1937).
[3] G. T. Seaborg, Chem. Rev. **27**, 199 (1940).
[4] J. J. Livingood and G. T. Seaborg, Phys. Rev. **53**, 847L (1938).
[5] O. Viktorin, Proc. Camb. Phil. Soc. **34**, 612 (1938).
[6] C. Perrier, M. Santangelo and E. Segrè, Phys. Rev. **53**, 104L (1938).
[7] B. T. Darling, B. R. Curtis and J. M. Cork, Phys. Rev. **51**, 1010A (1937).
[8] A. S. Jensen, Phys. Rev. **59**, 936A (1941).

A sample of iron bombarded in the 60-inch cyclotron at Berkeley with 16-Mev deuterons was received from Professor Alvarez of the University of California. This bombardment may possibly result in the following observed reactions:

$$\mathrm{Fe}(d, n)\mathrm{Co}^{55, 58},$$
$$\mathrm{Fe}(d, 2n)\mathrm{Co}^{56, 58},$$
$$\mathrm{Fe}(d, p)\mathrm{Fe}^{55, 59},$$
$$\mathrm{Fe}(d, \alpha)\mathrm{Mn}^{52, 54, 56}.$$

The stable isotopes $\mathrm{Co}^{57, 59}$, $\mathrm{Fe}^{57, 58}$ and Mn^{55} in either the ground or excited nuclear states are also possible results.

The sample was aged for five months between the time of bombardment and the time of these investigations, thus allowing all but the longer lived activities to decrease to a negligible amount so that, effectively, only $\mathrm{Co}^{56, 58}$, $\mathrm{Fe}^{55, 59}$, and Mn^{54} existed during the experiments. Part of this particular sample had been removed chemically before it was received, so that it consisted mainly of cobalt.

Since the sample contained long periods of iron and manganese as well as the cobalt, a chemical separation was necessary. The iron was removed by the isopropyl ether process (in a ferric solution $8N$ in HCl). In the absence of chlorides, and from a solution of the remainder $1N$ in HNO_3, $KBrO_3$ removed manganese as MnO_2. Cobalt was precipitated as a sulphide from the latter filtrate. The final filtrate contained negligible activity. This sample contained, then, only the 72-day (Co^{58}) and the 270-day (Co^{56}) activities.[3]

A second sample consisting of MnO_2 which was bombarded in the same cyclotron with one microampere-hour of 16-Mev α-particles was also sent to us by Dr. Alvarez. From the isotope chart in Fig. 1, it can be seen that this reaction can produce only stable isotopes and Co^{58}; no chemical separation was thought to be necessary for this sample.

Apparatus

The apparatus which was used for this investigation was an automatic Wilson cloud chamber in a magnetic field, built in this laboratory by Dr. I. C. Cornog and the author. The basic design is quite similar to that of the chambers used by Crane[9] and Delsasso. The sensitive portion of the chamber is 6.5 inches in diameter and 1 inch deep. The piston is cocked by compressed air and the chamber expanded by breaking the circuit of a locking magnet. The clearing field potential of 150 volts is applied between an Aquadag ring on the glass chamber top and the chassis, and grounded out at the instant of expansion. The cycle of events is initiated by a telechron clock, while successive operations are controlled by micro-switches on a camshaft driven by a motor. An electron tube time delay circuit controls the time between the cocking and the expanding of the chamber. The electric control circuit is so designed that the cycle of events, once started, cannot be interrupted except by power failure. Also the switches that put the chamber into operation may be thrown in any order so that the

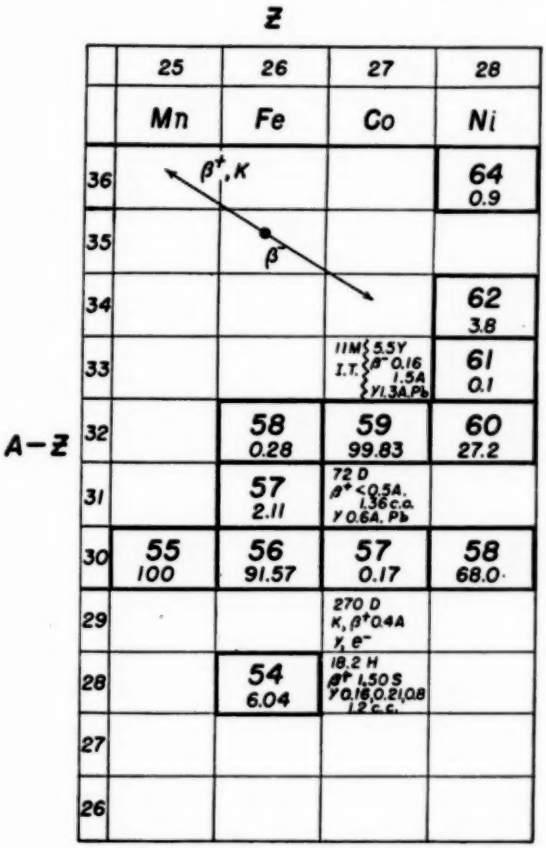

FIG. 1. Isotope chart in the region near cobalt. The data for this chart was taken from G. T. Seaborg, Chem. Rev. 27, 199 (1940). The positron spectrum assigned by this paper is included. A—Absorption; C.C.—cloud chamber; S—spectrograph.

[9] H. R. Crane, Rev. Sci. Inst. 8, 440 (1937).

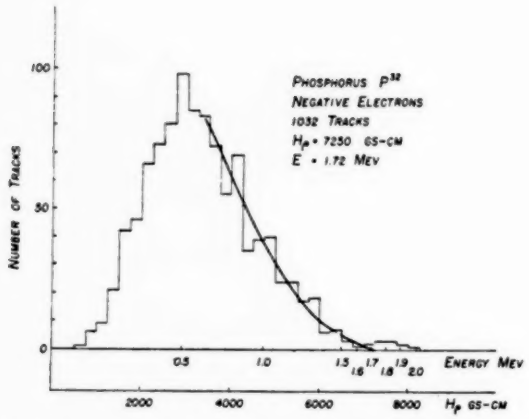

FIG. 2. Histogram of negative electrons from P^{32} showing a single β^--spectrum. Magnetic field strength 540 and 380 gauss.

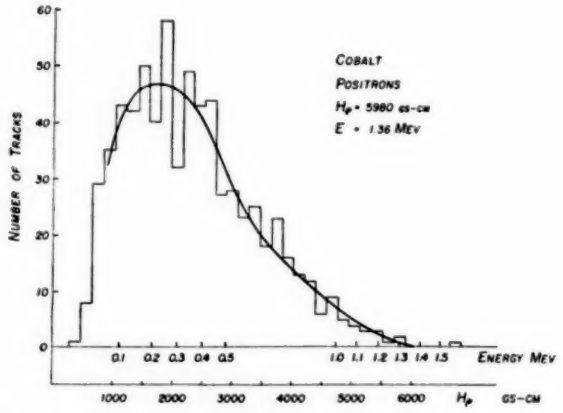

FIG. 3. Histogram of positrons from $Co^{56,58}$. Magnetic field strength 396 gauss.

machine is practically foolproof and can be used as a general laboratory instrument.

The field coils, which were wound with No. 7 square copper wire, are placed approximately in the Helmholtz position. The field was measured by turning it on and off while a search coil was in position. It has a measured constant of 23.3 gauss per ampere which is constant to within 1 percent throughout the sensitive portion of the chamber. The field is turned on about one second before the expansion and off again about three seconds later by means of a "Durakool" mercury switch that makes and breaks a 60-ampere current three times per minute without heating. The ammeter used to measure the current through the coils during the measurement of the field is also used during their operation, and has been checked against a calibrated Weston ammeter.

To reduce scattering, the tracks were photographed in helium, at a pressure slightly above atmospheric. The helium was bubbled through a mixture of *n*-propyl alcohol and water, but to insure saturation of the atmosphere, before the chamber was closed from the air some alcohol was placed on the velvet piston covering that forms the photographic background.

With a Sept motion picture camera, having a 50 mm $f/3.5$ lens, an exposure of 1–10 second at $f/5$ on Eastman Kodak Super XX film was found to be sufficient. The chamber is illuminated through two opposing windows in the walls by four 200-watt G.E. "Covelite" bulbs which are burned at 50 volts normally and at 220 volts during the exposure. There are two bulbs on each side of the chamber. These "Covelite" bulbs are the regular, horizontal U-filament bulbs aluminized on one side to reflect the light. We have found, as have others, that burning the lamps at a lower voltage between flashes substantially lengthens their lives. After approximately 3000 flashes one of the first set of four blew out; the others lasted for about 4000 flashes. The light is brought into a fairly parallel beam by cylindrical condenser lenses, and is further collimated by horizontal slits painted with Aquadag on the chamber wall. Shutters that operate just before and just after the exposure keep the chamber dark at all other times to prevent the heat from the lights from disturbing the temperature equilibrium of the chamber.

EXPERIMENTAL METHOD

The criteria that have been used as guides for the choice of measurable tracks are similar to those which have come to be recognized by other investigators:[10] (1) A track must appear to originate at the source. (2) It must be clear and sharply defined enough to allow measurement to ± 0.5 cm. (3) It must have a constant radius of curvature from the source to the end of the portion considered. (4) Track length: (a) If the radius of curvature is less than 5 cm, the track must make an arc of at least one radian. (b) If $5 < \rho < 15$ cm, the track must be at least 5 cm in

[10] J. R. Richardson and F. N. D. Kurie, Phys. Rev. **50**, 999 (1936).

length. (c) If $\rho > 15$ cm, the track must be long enough (>5 cm) to be unambiguously measurable to ± 0.5 cm when the measurement is repeated at least five times. It is impossible for a track of small radius of curvature to meet a requirement that it be of a given length greater than 5 cm, yet in many cases this track meets all other requirements, and, it seems, should be included in the data.

The pictures were projected through a standard projection system onto a ground glass set in a table top above the projector, and viewed through the glass. The tracks were matched by a set of curves engraved ($\Delta\rho = 0.5$ cm) on a clear celluloid sheet. This set was checked both before and after measuring the tracks to eliminate shrinkage errors. The magnification of the projected tracks was determined by measuring the image of a chromium-plated bar placed in the chamber and photographed simultaneously with the tracks.

TABLE I. P^{32} β^--*spectrum end-point energy (Mev).*

Investigator	$H\rho$ Curve	K–U Plot	Fermi Plot	Method
F. N. D. Kurie *et al.**	1.8	2.15	1.89	cl. ch.
E. M. Lyman†	1.69	2.09	1.69	spect.
J. L. Lawson‡	1.72	2.2	1.72	spect.
A. S. Jensen (this paper)	1.72	2.09	1.77	cl. ch.

* F. N. D. Kurie *et al.*, Phys. Rev. **49**, 368 (1936).
† E. M. Lyman, Phys. Rev. **51**, 1 (1937).
‡ J. L. Lawson, Phys. Rev. **56**, 131 (1939).

The total error in measurement of energies about 1 Mev is estimated for our technique to be less than 10 percent, and, of course, is greater for lower energies. From an investigation of the β^--spectrum of P^{32}, however, the actual error is somewhat smaller since the author agreed with other investigators to within 5 percent (see Fig. 2 and Table I).

The sample produced by the Fe+d reaction was plated from a chloride bath onto a copper strip about 4 mm $\times$22 mm to a density of about 1 mg per cm^2. This strip was cemented with rubber cement to a strip of brass bent in the form of an inverted "L" and waxed with Apiezon "Q" to the glass chamber top.

The second sample, produced by bombarding MnO_2 with α-particles, had a very small specific activity so that only a thick source could be made. All of the activated MnO_2 was bound on a piece of Cellophane tape with water glass, and this tape fastened to another inverted "L" of copper.

Results

A total of 1410 measurable tracks from the Fe+d source were photographed showing both positrons and electrons as well as a γ-ray background. Of these, 693 were of positrons which when plotted as a histogram (Fig. 3) indicate one positron spectrum with a maximum energy at 5980 gauss-cm or 1.36 ± 0.10 Mev. This is in fair agreement with an unpublished measurement made by Livingood and Seaborg which gave 0.45 g/cm^2 range in aluminum for radiation from cobalt made by a Ni(d, α)Co reaction. This range in aluminum indicates by the relationship given by Widdowson and Champion:[11] Energy (Mev) = (range in g/cm^2 + 0.165)/0.536, an energy of 1.2 Mev. A K–U plot of these positrons (Fig. 4), however, shows a change in curvature that indicates a preponderance of low energy particles.

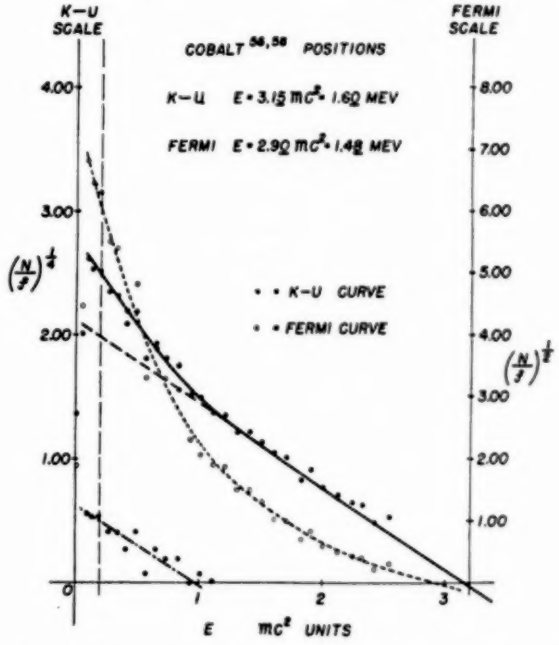

FIG. 4. K-U and Fermi plots of data from $Co^{56,58}$ positrons. Dashed axis indicates estimated lower energy limit of accurate data. Solid line is the K-U curve; dotted, Fermi. Dash-dotted line represents the difference curve obtained graphically from the dashed extrapolated straight line.

[11] Widdowson and Champion, Proc. Phys. Soc. **50**, 192 (1938).

The difference curve suggests a second positron spectrum with an energy end point near 0.5 Mev. This would be in good agreement with the measurement given by Livingood and Seaborg in their table of radioactive isotopes[3] (see Fig. 1).

From the second (Mn+α) sample a total of 143 measurable positron tracks was observed, and a histogram plot (Fig. 5) of these definitely shows an upper energy limit near 1.3 Mev when allowance is made for a thick source and the small number of tracks. This assigns the 1.36-Mev positron spectrum to the 72-day isotope, Co^{58}. On the same series of pictures, 53 measurable tracks of negative electrons were observed. These are too few to show any definite grouping in a histogram, but showed some grouping around 0.1 Mev, while some had energies up to 0.6 Mev. These are very likely Compton recoil electrons produced in the thick source by γ-rays from the Co^{58}.

The other 717 tracks from the Fe+d sample were of negative electrons, whose momentum distribution (Fig. 6) suggests an internally converted γ-ray near 0.1 Mev. This was confirmed by a magnetic spectrograph investigation of the radiation of negative charge made by this author together with E. Plesset of this laboratory,[12] which showed two internally converted γ-rays at 117±2 kev and 130±2 kev respectively. The higher energy tracks in the cloud-chamber distribution curve suggest the existence of higher energy γ-rays that are less frequently internally converted, perhaps the 0.6-Mev γ-ray already reported[3] or one of the difference energy of the two positron spectra. An investigation of these is being made.

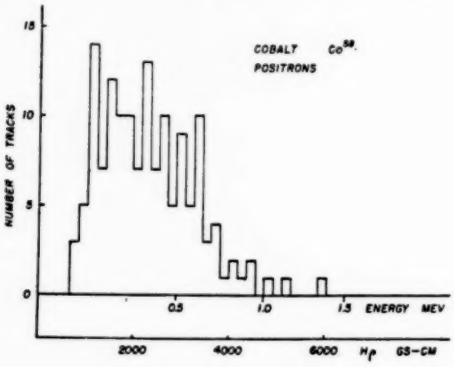

FIG. 5. Positron spectrum from Co^{58}. Magnetic field strength 396 gauss.

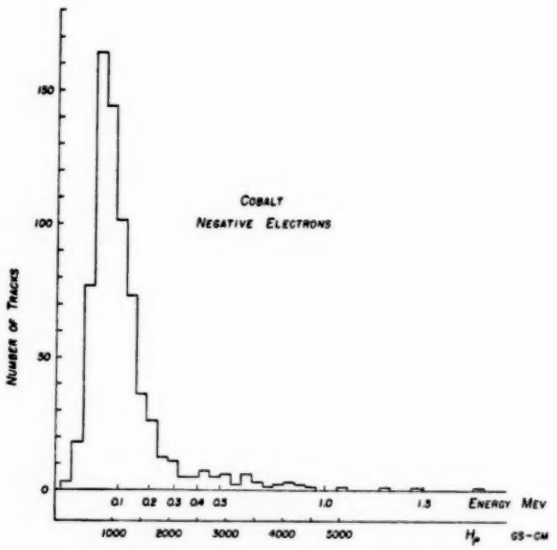

FIG. 6. Negative electrons from $Co^{56,58}$.

ACKNOWLEDGMENTS

The author wishes to express his appreciation to Professor Luis W. Alvarez of the University of California for the samples used in this research, to Professor W. McNabb of the Chemistry Department of the University of Pennsylvania for his patient advice on the separation of the sample, and to Professor Louis N. Ridenour for his competent advice and guidance. It has been a pleasure for the author to work in this laboratory with Dr. I. Clyde Cornog whose efforts and planning alone are responsible for the successful operation of the cloud chamber, and whose advice on problems of experimental technique was so useful. All of this research was done while the author was enjoying the privileges of the Hector Tyndale and the George Leib Harrison Fellowships at this university.

[12] E. H. Plesset, Phys. Rev. **59**, 936A (1941).

The Theory of Cascade Showers in Heavy Elements

H. C. CORBEN*
Palmer Physical Laboratory, Princeton University, Princeton, New Jersey
(Received July 21, 1941)

The one-dimensional equations of the cascade theory of showers are solved, account being taken of the variation with energy of the cross section for pair production, as well, of course, as ionization and bremsstrahlung effects. This modification is necessary for the discussion of cosmic-ray showers and bursts in elements of high atomic number since, for such elements, there is a region of energy (10 Mev–200 Mev for Pb) in which the pair production process is important while the cross section usually assumed for the process is greatly in error. Introducing the usual units t of length and β of energy, both characteristic of the material traversed ($t, \beta = 240$ m, 95 Mev and 0.4 cm, 6.5 Mev for air and lead, respectively), one finds that the maximum number of particles arising in lead from an incident particle of energy $E_0 = \beta\epsilon^t$ varies between $E_0/11\beta$ and $E_0/10\beta$ as E_0 varies between 10^9 ev and 10^{11} ev. For a given ϵ, the maximum number of particles occurs at a distance (in units of t) slightly less for lead than for air, and for large distances the effect of the variation with energy of the pair production cross section is to increase the number of particles and γ-rays to be expected.

I

ALTHOUGH the nature of the penetrating component of cosmic radiation is at present not completely understood, the theory of the multiplication of the soft component in the atmosphere is well established. Indeed, at high altitudes, where the theory is apparently contradicted by experiment, it is, in fact, used as a basis for determining the important part played by protons as primary constituents of cosmic radiation.[1] Treating the process as taking place in one dimension, and making simplifying assumptions for the cross sections for bremsstrahlung by electrons and positrons and pair production by γ-rays, Carlson and Oppenheimer[2] and Bhabha and Heitler[3] have been able to explain the general nature of the variation of the electron-positron intensity with height in the atmosphere, and refinements of this work by Landau and Rumer,[4] Snyder[5] and Serber[6] have given the theoretical multiplication curve quite accurately. It is found that, owing to energy losses of the particles by ionization, the number of particles arising from a single electron incident on a block of material does not increase indefinitely with depth but reaches a maximum value at a depth characteristic of the incident energy and of the nature (atomic number and density) of the material. The important role played by ionization losses is, therefore, apparent. Now the energy below which such losses begin to become greater than the average energy loss of a particle by radiation is approximately $1600mc^2/Z$, where Z is the atomic number of the material traversed. It is, therefore, apparent that, for showers multiplying in elements of high atomic number, loss of energy by ionization ceases to be the dominating process at much lower energies than for showers in the atmosphere. At such energies, however, the approximate expression for the pair production cross section used in all treatments of cascade showers in the atmosphere is quite incorrect, being, in the case of lead, for instance, three or four times the value obtained from the quantum-mechanical formula. The assumed form for the cross section for bremsstrahlung, on the other hand, is in error only by a factor 1.4 at these energies. Thus the direct application to heavy elements of the theory of the multiplication of cascade showers in the atmosphere is inadmissible, for in the case of elements of high atomic number there is a wide region of energy (10 Mev–200 Mev for Pb) in which the pair production

* Commonwealth Fund Fellow, formerly at the University of California.
[1] J. R. Oppenheimer, private communication.
[2] F. Carlson and J. R. Oppenheimer, Phys. Rev. **51**, 220 (1937).
[3] H. J. Bhabha and W. Heitler, Proc. Roy. Soc. **A159**, 432 (1937).
[4] L. Landau and G. Rumer, Proc. Roy. Soc. **A166**, 213 (1938).
[5] H. Snyder, Phys. Rev. **53**, 960 (1938).
[6] R. Serber, Phys. Rev. **54**, 317 (1938).

process is important, while the assumed form for the cross section for the process is greatly in error.

In view of recent experiments[7] in which cascade showers and bursts have been observed in an ionization chamber surrounded with lead, and because of the importance of such an experimental arrangement for the purpose of understanding the behavior of the mesotron,[8] it is of interest to apply the cascade theory to the production of showers in elements of high atomic number. In the following pages the theory of cascade showers is therefore developed, with the assumption of a cross section for the production of pairs by γ-rays which approximates closely to that calculated. As before, the whole problem is regarded as uni-dimensional and fluctuations and the Compton effect are not considered. The calculations are developed in detail for the production of showers in lead.

II

Let us consider an electron of energy E_0, large compared with its rest energy, incident on or formed in a block of material, such as lead, of atomic number Z and nuclear density n. Let $\gamma(E, x)\Delta E$ denote the probable number of γ-ray quanta with energy between E and $E+\Delta E$ at a thickness x, and $N(E, x)$ the probable number of particles (electrons and positrons) at x with energy greater than E. We define $P_\gamma(E, E')\Delta E'\Delta x$ as the probability that a particle of energy E radiates a γ-ray of energy between E' and $E'+\Delta E'$, and $P_p(E', E)\Delta E\Delta x$ as the probability that a γ-ray of energy E' creates a pair of energies between E, $E'-E$ and $E+\Delta E$, $E'-E-\Delta E$, in traversing a thickness Δx. Then

$$P_\gamma(E, E')\Delta E'\Delta x=(K/E^2E')[E^2+(E-E')^2-(\tfrac{2}{3}-\lambda)E(E-E')]f(E)\Delta E'\Delta x$$

and

$$P_p(E', E)\Delta E\Delta x=(K/E'^3)[E^2+(E'-E)^2+(\tfrac{2}{3}-\lambda)E(E'-E)]g(E')\Delta E\Delta x \quad (1)$$

where

$$K=4\alpha Z^2r_0^2n\ln(191/Z^{\frac{1}{3}}), \quad (2)$$

$$\lambda=31/90\ln(191/Z^{\frac{1}{3}})\sim\tfrac{1}{10}\text{ for Pb}, \quad (3)$$

and $f(E)$ and $g(E')$ are practically constant for E, E' greater than $10^3\,mc^2$, and below this energy vary critically with E, E', respectively, and very slowly (a variation we neglect here) with E', E, respectively.

The ionization loss per unit distance may be written

$$(-\partial E/\partial x)\text{ collision}=K\beta$$

where β is an energy characteristic of the material traversed. For lead, $\beta=6.5$ Mev whereas for air $\beta=95$ Mev.

The Compton scattering of the γ-ray quanta by the atomic electrons produces two effects, both of which are relatively unimportant and will be neglected. For high energy quanta most of the energy is transferred to the electron, which continues on in the shower, producing practically the same effects as if the original γ-ray had continued unscattered. Low energy quanta and the electrons with which they collide may be scattered out of the beam, but the loss of energy per unit distance arising from this process is small compared to $K\beta$.

If we write $Kx=t$, the diffusion equations therefore become

$$\frac{\partial\gamma}{\partial t}=-\sigma\gamma g(E)-\frac{1}{E}\int_E^\infty f(E')\frac{\partial N(E')}{\partial E'}[E'^2+(E'-E)^2-(\tfrac{2}{3}-\lambda)E'(E'-E)]\frac{dE'}{E'^2}, \quad (4)$$

$$\frac{\partial N}{\partial t}=\beta\frac{\partial N}{\partial E}+2\int_E^\infty dE'\int_{E'}^\infty\frac{dE''}{E''^3}\gamma(E'')g(E'')[E'^2+(E''-E')^2+(\tfrac{2}{3}-\lambda)E'(E''-E')]$$

$$+\int_E^\infty f(E')\frac{\partial N(E')}{\partial E'}dE'\int_0^E\frac{dE''}{(E'-E'')E'^2}[E'^2+E''^2-(\tfrac{2}{3}-\lambda)E'E'']. \quad (5)[9]$$

[7] M. Schein and P. S. Gill, Rev. Mod. Phys. **11**, 267 (1939).
[8] R. F. Christy and S. Kusaka, Phys. Rev. **59**, 414 (1941).
[9] In recent work by Dresden, Scott and Uhlenbeck [Phys. Rev. **59**, 112A (1941)] these diffusion equations have been solved by means of a Liouville-Neumann series with variable lower limit. As their calculations were es-

The total cross section for energy loss by radiation[10] is

$$\varphi_{\text{rad}}=\frac{1}{E}\int_0^E E'P_\gamma(E, E')dE' \\ =K(1+\lambda/2)f(E) \tag{6}$$

from which it follows that, for $E>20\ mc^2$, $f(E)$ varies slowly between 0.75 and 1. Below $E=20\ mc^2$, as pointed out in the introduction, the energy loss by radiation in heavy elements begins to be smaller than that due to ionization. We shall, therefore, write $f(E)=1$, for it differs appreciably from this value only for energies for which the bremsstrahlung process is unimportant.

The total cross section for pair production is given by

$$\varphi_{\text{pair}}=\int_0^{E'} P_p(E', E)dE \\ =\sigma Kg(E') \text{ where } \sigma=(7/9)-(\lambda/6). \tag{7}$$

For $E'=20\ mc^2$, $g(E')=0.33$ and even for $E'=100\,mc^2$, $g(E')\sim 0.7$. It is just the effect of the variation of $g(E')$ with E' that it is our purpose to investigate. Since ionization losses are the dominating processes for air showers for energies up to 200 mc^2 it is patent that for such showers this variation may be neglected.

We therefore fit the calculated function φ_{pair} as given by Heitler[11] by means of the empirical formula

$$g(E')=\delta_1+\delta_2\ln E'-\delta(\ln E')^2. \tag{8}$$

The coefficients δ_1, δ_2 are given in terms of δ by the condition that, for $E'=E_0>10^3\ mc^2$, $g(E')=1$ and $dg(E')/dE'=0$. Thus we ensure that for $E'\sim E_0$ Eq. (8) yields the correct value and energy dependence for φ_{pair}. We then have

$$g(E')=1-\delta\ln(E_0/E)^2. \tag{9}$$

In the limit $\delta\to 0$ it is clear that $g(E')\to 1$ and the equations go over continuously into those solved by Serber.[6]

The coefficient δ is chosen to give the best fit of (9) to the theoretical curve of reference 11. It is practically independent of the material traversed, but is critically dependent on E_0. In fitting (9) to the calculated curve, it is important to obtain a correct fit for high energies and an approximate fit for low energies, since for most of the shower the average energy of the particles is greater than 100 mc^2. To do this it is necessary to take different forms for the dependence of δ on E_0 for different orders of magnitude of E_0. One finds that

$$\delta=0.30/(\ln E_0-4.50)^2 \text{ for } E_0\sim 10^3\ mc^2, \\ =0.21/(\ln E_0-5.30)^2 \text{ for } E_0\sim 10^4\ mc^2, \\ =0.14/(\ln E_0-6.24)^2 \text{ for } E_0\sim 10^5\ mc^2. \tag{10}$$

This choice of the coefficients makes $g(E')$ a slowly varying function of E_0, the initial energy. While from the point of view of the physical interpretation of $g(E')$ this is meaningless, from the mathematical viewpoint this trick introduces an enormous simplification into the right-hand side of the fundamental Eq. (12). Moreover, the theoretical curve is represented quite accurately by (9), with δ given by (10), for $20\ mc^2<E\leqslant E_0\lesssim 10^5\ mc^2$ and extremely accurately for $E_0/50<E\leqslant E_0$.

As usual, we first solve the equations neglecting the inhomogeneous terms in β arising from the effect of ionization. The advantage of the choice of a form (9) for $g(E')$ involving the energy dependence logarithmically, now becomes apparent, for in a sense these logarithmic terms do not destroy the homogeneity of the equations. This is seen most easily by writing

$$\gamma(E, t)=\frac{e^{-\sigma t}}{E}\frac{1}{2\pi i}\int_{\tau-i\infty}^{\tau+i\infty}\left(\frac{E_0}{E}\right)^y f(y, t)dy, \\ N(E, t)=e^{-\sigma t}\frac{1}{2\pi i}\int_{\tau-i\infty}^{\tau+i\infty}\left(\frac{E_0}{E}\right)^y g(y, t)dy \tag{11}$$

from which it follows that

$$\ln(E/E_0)\gamma(E, t) \\ =\frac{e^{-\sigma t}}{E}\frac{1}{2\pi i}\int_{\tau-i\infty}^{\tau+i\infty}\left(\frac{E_0}{E}\right)^y\frac{\partial f(y, t)}{\partial y}dy, \\ (\ln(E/E_0))^2\gamma(E, t) \\ =\frac{e^{-\sigma t}}{E}\frac{1}{2\pi i}\int_{\tau-i\infty}^{\tau+i\infty}\left(\frac{E_0}{E}\right)^y\frac{\partial^2 f(y, t)}{\partial y^2}dy.$$

sentially for showers in air, the variation with energy of the pair production cross section was not considered, although their method could be extended to include this refinement. I am indebted to Professor G. Uhlenbeck for informing me of this work. I am also indebted to Dr. H. J. Bhabha for informing me that he and Chakrabarthy have recently obtained a solution of the cascade problem for air, correct to within 5 percent. The method adopted by these authors could also be extended to the present problem.

[10] W. Heitler, *The Quantum Theory of Radiation* (Oxford University Press, 1936), p. 172.

[11] W. Heitler, reference 10, p. 201.

Using the relation (9) and omitting, at first, the terms in β, one finds that Eqs. (4) and (5) become

$$\ddot{f}-(\sigma-A(y))\dot{f}-B(y)C(y)f = \rho\left[\dot{f}''-\left(\sigma-A(y)+\frac{B(y)C(y)}{\sigma}\right)f''\right], \quad (12)$$

$$\dot{f}-\rho f''=yC(y)g. \quad (13)$$

in which a dot and a prime denote differentiation with respect to t and y, respectively, $\rho=\delta\sigma$, and

$$\begin{aligned} A(y)&=(4/3+\lambda)(\psi(y)+\gamma)-(5/6+\lambda)\\ &\quad+(1+3\lambda)/3(y+1)+1/(y+2),\\ B(y)&=2/(y+1)-(8+6\lambda)/3(y+2)\\ &\quad+(8+6\lambda)/3(y+3),\\ C(y)&=(4+3\lambda)/3y-(4+3\lambda)/3(y+1)\\ &\quad+1/(y+2). \end{aligned} \quad (14)$$

Since λ is a small slowly varying function of Z, the functions $A(y)$, $B(y)$, $C(y)$ and σ are practically independent of Z. For convenience in comparing the results for lead showers with those already calculated for air, we shall neglect this slight variation, introducing thereby an error of less than 1 percent.

Consider the equation obtained from (12) by neglecting the right-hand side, which depends on the small parameter ρ. The solution of this equation corresponding to the initial condition of one electron of energy E_0 and no γ-rays incident at $t=0$ is

$$f_0(t, y)=[C(y)/\mu_1-\mu_2][\exp(\mu_1 t)-\exp(\mu_2 t)] \quad (15)$$

where μ_1 is the positive root and μ_2 the negative root of the equation

$$\mu^2-(\sigma-A(y))\mu-B(y)C(y)=0. \quad (16)$$

Inserting (15) on the right-hand side of (12), we find that, because of the appearance of terms involving the second derivative of f_0 with respect to y, the exact solution $f_1(t, y)$ of the equation involves terms of order ρt, ρt^2, ρt^3, the ρt^3 terms cancelling because of (16). More precisely,

$$f_1(t, y)=\sum_{r=1,2}(-1)^{r-1}\sum_{n=0}^{3}\alpha_{rn}t^n\exp(\mu_r t) \quad (17)$$

where

$$\begin{aligned} \alpha_{r0}&=(-1)^{r-1}C(y)/D_r,\\ \alpha_{r1}&=\{\rho[\alpha_{r0}''\theta_r+\mu_r''\alpha_{r0}+2\mu_r'\alpha_{r0}']-2\alpha_{r2}\}/D_r,\\ \alpha_{r2}&=\{\rho[\theta_r(u_r''\alpha_{r0}+2\mu_r'\alpha_{r0}')+2\mu_r'^2\alpha_{r0}]-6\alpha_{r3}\}/2D_r,\\ \alpha_{r3}&=\rho\mu_r'^2\alpha_{r0}\theta_r/3D_r,\\ D_r&=2\mu_r-\sigma+A=(-1)^{r-1}(\mu_1-\mu_2),\\ \theta_r&=\mu_r-\sigma+A(y)-B(y)C(y)/\sigma. \end{aligned} \quad (18)$$

Inserting (17) into the right-hand side of (12) we obtain the second approximation

$$f_2(t, y)=\sum_{r=1,2}(-1)^{r-1}\sum_{n=0}^{6}\beta_{rn}t^n\exp(\mu_r t), \quad (19)$$

involving terms of order $(\rho t^3)^2$, and in general the leading term of the nth approximation obtained in this manner is of order $(\rho t^3)^n$. The significance of this will be discussed after we have taken into account the effects of ionization. To do this we follow exactly the calculations of Serber. To obtain an exact solution of the equations, even in the form of a contour integral, is a difficult procedure, but to a first approximation we have

$$N(t, E)=-\frac{e^{-\sigma t}}{4\pi^2}\int_C\frac{dy}{yC(y)}\left(\frac{E}{E_0}\right)^{-y}\int_S ds\frac{\Gamma(-s)\Gamma(y+s)}{\Gamma(y)}\left(\frac{E}{\beta}\right)^{-s}\sum_{r=1,2}K_r(y, s)(-1)^{r-1} \times\sum_{n=0}^{3}\left[\frac{\partial}{\partial t}(\alpha_{rn}t^n\exp[\mu_r t])-\rho\frac{\partial^2}{\partial y^2}\alpha_{r0}\exp(\mu_r t)\right], \quad (20)$$

where

$$\{\mu_r(A(y+s)-A(y))-[B(y+s)C(y+s)-B(y)C(y)]\}K_r(y, s)=s\mu_r K_r(y, s-1). \quad (21)$$

and

$$K_r(y, 0)=1.$$

As before, the main contribution to the shower arises from the terms corresponding to the positive root of Eq. (18), $r=1$. The total number of electrons and positrons at a depth t in the shower, as

estimated from (20) by the method of steepest descents, is, therefore,

$$N(\epsilon, t)=N_0(\epsilon, t)\left[1+\frac{t}{\mu_1\alpha_{10}}(\mu_1\alpha_{11}+2\alpha_{12}-2\mu_1'\alpha_{10}'-\mu''\alpha_{10})+\frac{t^2}{\mu_1\alpha_{10}}(\mu_1\alpha_{12}+3\alpha_{13}-\rho\alpha_{10}\mu_1'^2)+t^3\frac{\alpha_{13}}{\alpha_{10}}\right] \quad (22)$$

where

$$t=(1-\epsilon y)/\mu_1' y, \qquad \epsilon=\ln(E_0/\beta),$$

and $N_0(\epsilon, t)$ is the number of particles at t, calculated by Serber neglecting the variation with energy of the pair production cross section.[12]

Expression (22) has been obtained from the first approximation Eq. (17) involving terms of order ρt^3. In a similar manner an expression for $N(\epsilon, t)$ could be obtained from the nth approximation and it is found to involve terms of order $(\rho t^3)^n$. For large thicknesses t, therefore, the expansion has little meaning. At the point $y=1$, however, which is near the maximum of the shower, θ—and hence α_{13}—vanishes. The leading term in the nth approximation is then of order $(\rho t^2)^n$, a quantity which is small compared to unity and which decreases as ϵ increases. The successive approximations, therefore, form a rapidly convergent series, and for $E_0 \gtrsim 10^4\ mc^2$ the maximum of the shower is given in terms of $(N_0)_{\max}$ to within 5 percent. For $E_0 \sim 10^3\ mc^2$ it is necessary to consider the second approximation, which for this energy differs from the first approximation by 8 percent.

From (22), and estimating the second approximation which is too cumbersome to write down in detail, one finds that

$$N_{\max} \approx (N_0)_{\max}[1-0.57\delta(\epsilon-1)(\epsilon+0.18)+0.1\delta^2(\epsilon-1)^4] \quad (23)$$

with δ given by (10), and

$$(N_0)_{\max}=0.4E_0/\beta(1+1.6(\epsilon-1))^{\frac{1}{4}}.$$

It is clear that the maximum value of N occurs for a value of t and hence of y, slightly less than that which makes N_0 a maximum. The difference is very small, however, and the error involved in taking $N_{\max}=(N)_{y=1}$ is of order 1 percent.

For a given value of ϵ, the value of δ given by (10) is much smaller for air than for lead. The corresponding correction to $N_{\max}$ for air is, therefore, much smaller, being of order 7 percent and decreasing with increasing ϵ. With present calculations of the multiplication of cascade showers in air, which are possibly in error by as much as 20 percent, this refinement is therefore negligible.

For all thicknesses the number of γ-ray quanta predicted from the above calculations will be greater than that given by the application of the usual cascade theory, but for $t<3t_{\max}$ the number of particles predicted is less. Owing to the uncertainty of these and previous calculations, however, we give numerical values only for the maximum of the particle multiplication curve in lead (Table I), calculated from (23) for various values of the initial energy E_0. The maximum number of particles is seen to vary between $E_0/11\beta$ and $E_0/10\beta$ as E_0 varies from 10^9 ev to 10^{11} ev, i.e., between $E_0/8E_c$ and $E_0/7E_c$ where $E_c=\beta/\ln 2$ is the critical energy, at which the average rates of energy loss by ionization and radiation are equal.

TABLE I. *The maximum number of particles arising in lead and in the atmosphere from a single electron of energy E_0 is given for various values of the ratio E_0/β, where β is an energy characteristic of the material traversed.* ($\beta=6.5$ *Mev for* Pb, *95 Mev for air.*)

E_0/β	155	1550	15500
$(E_0)_{Pb}$	10^9 ev	10^{10} ev	10^{11} ev
$(N_{\max})_{Pb}$	13.5	148	1550
$(E_0)_{air}$	1.5×10^{10} ev	1.5×10^{11} ev	1.5×10^{12} ev
$(N_{0\max})_{air}$	21.9	200	1940

The author wishes to thank Professors J. R. Oppenheimer and W. Pauli for advice and encouragement in the preparation of this paper.

[12] Reference 6, Eq. (7).

Multipole Nature of Elementary Sources of Radiation—Wide-Angle Interference

SIMON FREED AND S. I. WEISSMAN
George Herbert Jones Laboratory, University of Chicago, Chicago, Illinois

(Received July 9, 1941)

It has been shown possible in wide-angle interference experiments to analyze radiation with respect to its multipole character. The fluorescence from ions of europium in solution consisted of different kinds of radiation in that they possessed different interference properties. From the behavior of the fringe systems, one group of spectral lines was identified as arising from magnetic dipoles while two other groups had their origin in the forced oscillations of electric dipoles. The multipole character of the radiation of a quantum transition was found modified by a change in the microscopic fields about the emitting ions.

TWO beams issuing from a source of light at a wide angle may be brought to give sharp interference fringes provided the dimensions of the source are very small. The observed fringes being the superposition of the fringes from all the elementary centers depend upon the intensities and polarizations of the two diverging rays from each center and these, in turn, are expressions of the structure of the radiation fields characteristic of emitting electric or magnetic dipoles or of poles of higher order. Hence, without prior knowledge of quantum states, one is in position to ascertain the nature of the radiation from the properties of the interference pattern and draw conclusions concerning the possible quantum transitions. Halpern and Doermann[1] have deduced how the visibility of the fringes for each kind of radiation from isotropic point sources varies with the angle of divergence of the beams, with the orientation of polarizing apparatus the beams traverse, and with the experimental arrangement in general.

To illustrate the method and give a rather perspicuous example of some of the factors at work, we shall discuss the wide-angle interference experiment of Selényi[2] which we have modified to a minor degree in the present investigation.

A fluorescent film of fluid in between the plane of a right half-cylinder C and a thin sheet of mica M constitutes the source of radiation. It is excited to fluorescence by light condensed to form a luminous spot on the axis. To obtain distinct fringes without overlapping, that is, to achieve in the fluorescent spot a sufficiently close approximation to the ideal point source, the thickness of the source should be no more than about one-twentieth a wave-length of light, and its diameter about one-twentieth the expected linear separation of the fringes. The separations are greater the thinner the mica, and with mica 0.008 mm thick, the source may be several tenths of a mm in diameter.

The two beams of Fig. 1 diverge from the source 0 at the angle 2θ and are rendered parallel by the total reflection of one of them at the mica-air interface. The fringes originating in the crossing of the pencils of rays at finite angle become visible only after the colors are resolved and viewed in the spectroscope S, the image of the slit for the different colors may be seen crossed with interference fringes. With a solution of fluorescein as the film, a system of fringes appeared having a sinusoidal distribution of in-

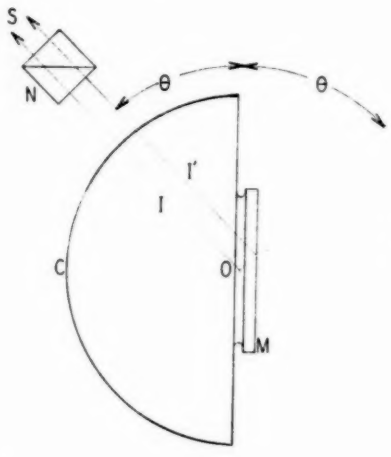

FIG. 1. Schematic representation of apparatus.

[1] O. Halpern and F. W. Doermann, Phys. Rev. **52**, 937 (1937); F. W. Doermann, Phys. Rev. **53**, 420 (1938); F. W. Doermann and O. Halpern, Phys. Rev. **55**, 486 (1939).

[2] P. Selényi, Ann. d. Physik **35**, 444 (1911); Zeits. f. Physik **108**, 401 (1938); Phys. Rev. **56**, 477 (1939).

tensity with black minima when the angle of divergence 2θ was 90° and the Nicol prism N was set to transmit light with electric vector perpendicular to the plane of the two beams I, I'. After the Nicol prism had been turned through ninety degrees, the image of the slit was uniformly illuminated—i.e., the fringes were now absent. This behavior of the light led Selényi to conclude that the fluorescence centers were electric dipoles.

His argument follows: Let it be assumed that the isotropic source of light may be properly represented as the superposition of light from three mutually perpendicular sets of independent oscillating electric dipoles. Consider the radiation from a set of dipoles whose axes are at right angles to the plane of the beams I, I' and have the Nicol prism oriented so that the only radiation transmitted has its electric vector also perpendicular to the plane I, I'. Not only will the direct beam I radiated by this set of dipoles traverse the Nicol prism but also the beam diverging from it at 90° and reflected at the mica-air interface, now the beam I'. The intensities of the two interfering beams will be nearly equal[3] and hence the resulting pattern of fringes may be expected to be completely sinusoidal in its intensity distribution. The two remaining sets of oscillating electric dipoles with axes in the plane I, I' may be imagined so disposed that one set has its axes along the direct beam I and the other at right angles to I. The dipoles along I will not radiate in that direction nor will those at right angles radiate along I' and hence no fringes are to be observed when the Nicol prism is turned to transmit this radiation.

The same result is arrived at by Halpern and Doermann, taking account of the phase relations of the rays from the dipoles in all random orientations. They demonstrate, however, that the identification made by Selényi is not unique. Rays propagated by magnetic quadrupoles at this particular angle of divergence (90°) furnish a fringe system which responds to the orientations of the polarizing prism in the same way as the fringes from electric dipoles. At another angle of divergence, particularly if the choice is 45°, the two kinds of radiation may be distinguished.

[3] The indices of refraction of the glass, mica, and film differ but little and the reflection on the mica surface may be taken as ideal.

FIG. 2. Wide angle interference fluorescence of the salcylaldehyde compound of europium at 6100A. (a) $\theta=22.5°$, $\chi/2=0°$; (b) $\theta=45°$, unpolarized; (c) $\theta=45°$, $\chi/2=90°$. $\chi/2=90°$ when the electric vector of the polarizing prism is perpendicular to the plane I, I'.

The visibility of the fringes from magnetic quadrupoles is now reduced to zero while that from electric dipoles is scarcely altered from the value it had at the divergence 90°.

We confirmed Selényi's results with a film of fluorescein and examined the fringes at an angle of divergence of 45° also but noted little change in the visibility. The radiation emanates, then, from electric dipoles as Selényi had supposed.

Our spectrograph, with its three prisms, strongly polarized any light entering it, and, as a result, there was but little radiation falling on the photographic plate at one of the required orientations of the Nicol prism N. In order to maintain constant the polarization of the light entering the spectrograph, a quarter-wave plate was attached with a drop of glycerin to the Nicol prism (actually a Glan-Thomson prism) so that the beam was rendered circularly polarized. Another quarter-wave plate was fixed before the slit of the spectrograph at such an orientation that the plane polarized beam issuing from this plate was at the angle of maximum transmission of the spectrograph. The direction of this plane was independent of the orientations of the Glan-Thomson prism.

The ions of the rare earths might be expected to afford opportunity for the study of various kinds of multipole radiation. In the optical transitions, all the electrons contributing to the quantum character of the states remain within the same shell ($4f$) and therefore electric dipole radiation is "forbidden" by the Laporte rule, which is valid for ions in the gaseous state, or, in general, when the environment of the ions possesses a center of inversion. Furthermore, the intensity of the fluorescent radiation is very weak compared with the usual electric dipole radiation from gases or from dyestuffs such as fluorescein. Such feeble intensities are to be expected

in radiation from magnetic dipoles, from electric or magnetic quadrupoles, etc.

The absorption and fluorescent spectrum of the ions of europium in crystals and in solution have been analyzed in terms of quantum states and the symmetries of the electric fields about the ions.[4] The effective spectral region for excitation lies between 3500A and 4000A. The fluorescence is unpolarized and may be regarded as emerging from an isotropic source. One group at about 6100A corresponds to a transition from $J=0$ in the upper state to $J=2$ of the basic multiplet $F_{0123456}$. Another group at 5880A originates in the same upper level $J=0$ and ends in the $J=1$ level of the basic multiplet, and a line at 5790A corresponds to the 0→0 transition.

Europium nitrate in about $2M$ solution of glycerin, not entirely free of water, yielded two groups of lines in fluorescence of sufficient intensity when excited by light from a carbon arc carrying fifty to sixty amperes direct current. The lines were rather broad and it was not found possible to resolve the components of the group representing the decomposition of the basic state by the electrical fields of the environment of the ions. When the observations were made at $\theta=45°$ and the Glan-Thomson prism was set to transmit light with its electric vector perpendicular to the plane I, I', the 6100A group, $J=0\rightarrow J=2$, was crossed with sharp fringes, while the 5880A group, $J=0\rightarrow J=1$, was of uniform intensity along the image of the slit. When the polarizing prism was rotated through 90° the situation was reversed, the 6100A group became uniform in its intensity whereas the 5880A group was crossed with fringes. With θ changed to 22.5°, both groups showed distinct fringes at both orientations of the prism. According to theory, the 0→2 transition gave rise to electric dipole radiation and the 0→1 transition to magnetic dipole radiation. The 0→1 transition was about one-fifth as intense as the 0→2 transition from this solution of europium. Unfortunately, the 0→0 transition at 5790A, forbidden completely in a spherically symmetrical environment, was too feeble for these measurements.

However a $0.2M$ solution in benzene of the ammonia-salicylaldehyde compound[5] of europium furnished this line with sufficient intensity (Fig. 2). The other groups also appeared with greater intensity than from the nitrate. The 0→0 line proved to be electric dipole radiation. We also confirmed the nature of both the 0→2 and the 0→1 transitions. However, despite the fact that the fluorescent spectrum from this compound was much sharper and the structure within the groups was resolved, the radiations of the 0→1 and 0→2 groups were not as pure in their multipole character as from the nitrate. Especially was this true in the 0→1 transition where what had appeared as magnetic dipole radiation was now definitely mixed with another species. A change in the environment of the ion had brought about a change in the species of the radiation.

The kinds of radiation revealed in these experiments are in accord with their feeble intensities. The 0→0 and 0→2 transitions are excluded as electric dipole radiation in fields of spherical symmetry and only the presence of fields of low symmetry about the ions in solution[6] can "force" the appearance of such radiation, and then with weak intensities. The spherical rotational symmetry must be reduced to C_3 or less before the 0→0 transition can take place and to tetragonal or less for the 2→0 transition. Both also require the absence of a center of inversion. The 1→0 transition is not excluded as magnetic dipole radiation in spherically symmetrical fields but the transition probability is very low. Fields of low symmetry may increase the feeble intensity but it would still be of an entirely different order of magnitude from the strong radiation emitted in spontaneous electric dipole transitions.

We are much indebted to the Penrose Fund of the American Philosophical Society for the support it has given this investigation. We also wish to acknowledge the assistance of Works Projects Administration Official Project 665-54-3-387.

[4] H. Gobrecht, Ann. d. Physik **28**, 670 (1937); S. Freed and S. I. Weissman, J. Chem. Phys. **8**, 878 (1940).

[5] Prepared in the same way as the acetylacetonate of reference 6(b) but was found on analysis to have some ammonia attached to it.

[6] (a) S. Freed and S. I. Weissman, J. Chem. Phys. **6**, 297 (1938); (b) S. Freed, S. I. Weissman and F. E. Fortess, J. Am. Chem. Soc. **63**, 1079 (1941).

Magnetic Rotatory Power of Crystalline Nickel Sulfate in the Ultraviolet Region

J. J. O'Connor, C. Beck, and N. Underwood
Vanderbilt University, Nashville, Tennessee

(Received July 7, 1941)

Previous measurements of the magnetic rotatory power of crystalline $\alpha-NiSO_4\cdot 6H_2O$ in the visible region of the spectrum and at one point in the ultraviolet have been extended into the ultraviolet as far as the 0.2537μ line of mercury. An unsymmetrical anomaly has been found at the strong 0.3850μ absorption band. The constants in the equation for magnetic rotatory dispersion have been evaluated so that Verdet constants calculated from the equation agree with the experimental values throughout the visible and ultraviolet except within the 0.3850μ absorption band.

Introduction

UNLIKE the majority of substances, crystalline $\alpha-NiSO_4\cdot 6H_2O$ contains, within the optical range of the spectrum, critical wavelengths which markedly affect the natural rotatory power of the crystals. Only one of these critical wave-lengths appears in the region between 0.2537μ and 0.6000μ. This occurs at the center of the 0.3850μ absorption band and noticeably influences the natural rotation over the region between 0.2850μ and 0.4850μ.[1,2]

Interest in the possible effect of this band on the magnetic rotatory power of the crystals led to investigations from 0.6050μ to 0.4358μ in the visible[3] and at one point 0.3470μ in the ultraviolet.[1] The absorption band was found to have no effect on the magnetic rotations at the wavelengths employed. Insufficient light intensity prevented measurements between 0.3470μ and 0.4358μ. Recently, however, an improved method for measuring natural rotation has been devised and successfully applied to the ultraviolet region including the absorption band.[2] By a slight modification of this method, measurements of the magnetic rotation have now been made inside the absorption band and into the ultraviolet as far as 0.2537μ.

Apparatus and Method

Since the method used in these observations is very nearly the same as that described for measuring natural rotation in the ultraviolet,[2] many of the details are omitted here. The essential parts of the apparatus are indicated in Fig. 1. Radiation from a quartz mercury arc A passed through a Bausch and Lomb double prism monochromator B, the Glan-Thompson polarizer C, a removable glass plate D (inserted for orienting the crystal), the pole piece of the magnet coil M_1, the nickel sulfate crystal E, the pole piece of the magnet coil M_2, the Wollaston double-image prism F, and then fell on a photographic film in the holder G. The magnet was a special Leybold-Lange drilled core electromagnet. The current through the coils was controlled by an ammeter-rheostat arrangement which made it possible to hold the current constant within $\frac{1}{2}$ percent. The dimensions of the apparatus were such that the maximum angle between the axis of the magnet and the optical axis was limited to 1°.

With the crystal out, a position of the polarizer may be found for which the two photographic images produced by the Wollaston are of equal density. (There are actually four such positions spaced approximately 90° apart.) If the crystal is inserted, the position of the polarizer must be changed by an angle equal to the natural rotation of the crystal in order to produce again images of equal density. The application of the magnetic field along the light path necessitates a further change corresponding to the magnetic rotation.

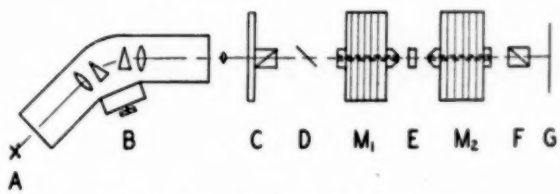

FIG. 1. Schematic diagram of apparatus.

[1] F. G. Slack and P. Rudnick, Phil. Mag. **28**, 241 (1939).
[2] L. R. Ingersoll, P. Rudnick, F. G. Slack, and N. Underwood, Phys. Rev. **57**, 1145 (1940).
[3] F. G. Slack, R. T. Lageman, and N. Underwood, Phys. Rev. **54**, 358 (1938).

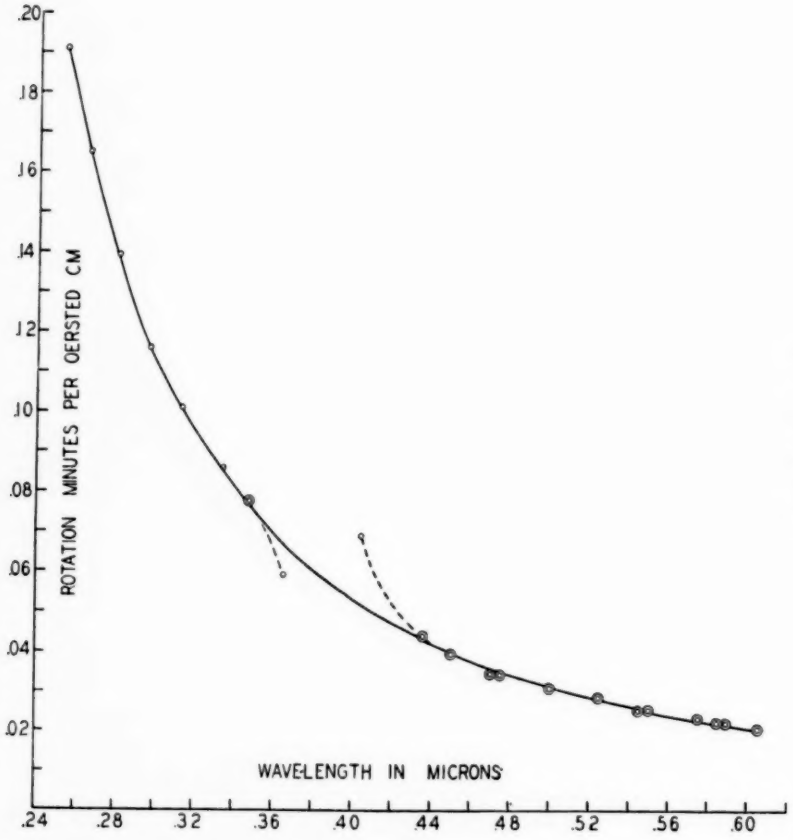

FIG. 2. Magnetic rotatory power of crystalline nickel sulfate $6H_2O$. New data are indicated by circles; the point at 0.3470 micron is from data by Slack and Rudnick; other values are taken from visual data by Slack, Lageman, and Underwood. The smooth curve is a graph of Eq. (5).

In practice, the crystal was inserted and oriented; the magnetic field was applied; and a position of the polarizer was determined such that images of equal density would be produced on the photographic film. The field was then reversed by reversing the direction of the current through the electromagnet, and the new position of the polarizer which corresponded to images of equal density was found. One-half the angular separation of these two positions gave the net magnetic rotation. The field strength was determined by measuring the rotation of the plane of polarization produced by calibrated glass specimens in the field. For a current of six amperes and a pole piece separation of 8.85 mm, the field was found to be 7430 oersteds.

The method outlined above has been found to give rotation measurements reproducible within 0.2° for the particular crystals used. More nearly perfect crystals would lower this figure somewhat. Since the percentage accuracy of the results depends upon the amount of rotation involved in the measurement, the thicker crystals were used except in the region of very low transmission. In this unfavorable region it is thought that the average of several trials taken for each wave-length does not differ greatly from the correct value.

EXPERIMENTAL RESULTS

Magnetic rotation measurements were made at eight different wave-lengths. The results are listed in Table I. Included with these for purposes of comparison are results previously published for the visible and ultraviolet with references to the original articles. The first column lists the wave-lengths in microns at which observations have been made. In the second column are given the experimentally determined Verdet constants in minutes per oersted-cm. In most cases the new values given here are averages obtained from two to four observations. The third column contains the Verdet constants computed from Eq. (5), to be discussed later. The differences between the values in columns two and three are noted in the fourth column. These data are shown graphically

in Fig. 2. A striking paramagnetic anomaly is indicated near 0.3850μ.

Since, for a given wave-length and field strength, left- and right-handed crystals gave no detectable difference in rotation per cm, the results derived from both types are averaged together in Table I. The magnetic rotations were found to be positive in every case. The crystal specimens used in these determinations were laminae cleaved from "Baker's Analyzed" crystals and ranged in thickness from 4.04 mm to 0.56 mm. All measurements were made with the optic axis, which is perpendicular to the cleavage plane,[4] accurately oriented parallel to the transmitted beam of light. Although no special attempt was made to control the temperature, it did not vary greatly from 24°C.

Discussion of Results

It is desirable to fit an equation for magnetic rotatory dispersion to the experimentally determined Verdet constants. The general equation for magnetic rotatory power is[5]

$$\alpha=\frac{e}{2mc^2}\lambda\frac{dn}{d\lambda}, \tag{1}$$

in which α is the Verdet constant. The quantity $dn/d\lambda$ may be evaluated from any of several equations for the index of refraction. The following Lorenz-Lorentz equation is given by W. Schutz:[6]

$$\frac{n^2-1}{n^2+2}=\frac{e^2N}{3\pi mc^2}\sum_{i=1}^{s}\frac{f_i\lambda_i^2\lambda^2}{\lambda^2-\lambda_i^2}, \tag{2}$$

$$\fallingdotseq\frac{e^2N}{3\pi mc^2}\frac{f_r\lambda_r^2\lambda^2}{\lambda^2-\lambda_r^2}\equiv\frac{L\lambda^2}{\lambda^2-\lambda_r^2}, \tag{2'}$$

in which n represents the index of refraction. If a value of $dn/d\lambda$ is obtained from (2) and inserted in (1) one finds

$$\alpha=\frac{e^3N}{2\pi m^2c^4}\frac{(n^2+2)^2}{9n}\sum_{i=1}^{s}\frac{f_i\lambda_i^4\lambda^2}{(\lambda^2-\lambda_i^2)^2}, \tag{3}$$

$$\fallingdotseq\frac{e^3N}{2\pi m^2c^4}\frac{(n^2+2)^2}{9n}\frac{f_m\lambda_m^4\lambda^2}{(\lambda^2-\lambda_m^2)^2}\equiv\frac{(n^2+2)^2A\lambda^2}{9n(\lambda^2-\lambda_m^2)^2}. \tag{3'}$$

[4] C. A. Beevers and H. Lipson, Zeits. f. Krist. **83**, 123 (1932).
[5] T. M. Lowry, *Optical Rotatory Power* (Longmans, Green) p. 463.
[6] W. Schutz, *Handbuch der Experimental Physik*, Vol. 16, p. 85.

Equations (2), (2'), (3), and (3') do not take into account dispersion caused by paramagnetic anomalies. The symbols undefined in the equations above have the following significance: e and m are the charge and mass of the electron; c is the speed of light in a vacuum; N is the number of molecules per cc in the refracting medium; λ is the wave-length of light for which the index of refraction is n. λ_i is the wave-length of one of the s absorption lines in the far ultraviolet which affect the index of refraction. To each of these absorption lines there corresponds a particular oscillator strength f_i. In the case of refractive dispersion, λ_r is an effective mean of the λ_i and f_r is an effective sum of the f_i. In the case of rotatory dispersion, λ_m and f_m again represent effective values.

If the experimental values for the Verdet constants are plotted against wave-lengths as in Fig. 2, it becomes evident that the effect of the band does not extend outside the region lying between 0.3470μ and 4400μ. Therefore Eq. (3') should accurately represent the experimental values for all wave-lengths not falling within this range. Before the constants in Eq. (3') can be evaluated, however, the indices of refraction must be known for the wave-lengths at which Verdet constants have been determined. Unfortunately, indices of refraction are available for

Table I. *Magnetic rotatory power of crystalline nickel sulfate.*

Wave-Length in Microns	Magnetic Rotatory Power in Minutes per Oersted-cm	Magnetic Rotatory Power, Eq. (5)	Difference
0.2537	0.1925	0.1927	−0.0002
.2654	.1650	.1659	−0.0009
.2804	.1380	.1401	− .0021
.2967	.1167	.1178	− .0011
.3131	.1017	.1010	+ .0007
.3341	.0860	.0846	+ .0014
.3470[1]	.0775[1]	.0767	+ .0008
.3650	.0580	.0669	− .0089
.4047	.0685	.0513	+ .0172
.4358[3]	.0438[3]	.0430	+ .0008
.4500[3]	.0392[3]	.0399	− .0007
.4700[3]	.0345[3]	.0362	− .0017
.4750[3]	.0343[3]	.0351	− .0008
.5000[3]	.0312[3]	.0314	− .0002
.5250[3]	.0287[3]	.0280	+ .0007
.5461[3]	.0256[3]	.0256	+ .0000
.5500[3]	.0255[3]	.0252	+ .0003
.5750[3]	.0236[3]	.0229	+ .0007
.5850[3]	.0223[3]	.0220	+ .0003
.5890[3]	.0221[3]	.0217	+ .0004
.6050[3]	.0207[3]	.0204	+ .0003

TABLE II. *Indices of refractions, n.*

λ	n	λ	n
0.6566	1.5078	0.4862	1.5173
0.5893	1.5109	0.4340	1.5228

only four wave-lengths,[7] as given in Table II. It is necessary, therefore, first to evaluate the constants in Eq. (2′) and then calculate the indices of refraction for the other wave-lengths. Evaluation of the constants in (2′) by giving all four values equal weight results in

$$\frac{n^2-1}{n^2+2}=\frac{0.29243\lambda^2}{\lambda^2-(0.0897)^2}. \tag{4}$$

λ in this and the following equation is in microns. The indices of refraction computed from (4) and the experimental Verdet constants listed in Table I are sufficient for the evaluation of A and λ_m in Eq. (3′). If all the experimental values outside the band are given equal weight,

$$\alpha=\frac{(n^2+2)^2}{9n}\,\frac{0.00509\lambda^2}{(\lambda^2-0.123^2)^2}. \tag{5}$$

The full line in Fig. 2 is the graph of Eq. (5). The agreement between computed and experimental Verdet constants, as indicated by Table I and Fig. 2, is satisfactory except within the region of the anomaly.

Since Eq. (3) is theoretically derived from (2), it might seem that the critical wave-lengths (λ_r, λ_m) should agree. Actually, values of 0.0897μ and 0.1230μ have been found for the critical wave-lengths. It will be shown that, in general, $\lambda_m>\lambda_r$ and $f_m<f_r$.

Equating the right members of (2) and (2′) and expanding in power series in $1/\lambda^2$ gives

$$\sum_{i=1}^{s} f_i\lambda_i^2\left(1-\frac{\lambda_i^2}{\lambda^2}\right)^{-1}\leqq f_r\lambda_r^2\left(1-\frac{\lambda_r^2}{\lambda^2}\right)^{-1}$$

or

$$\sum_{i=1}^{s} f_i\lambda_i^2+\frac{1}{\lambda^2}\sum_{i=1}^{s} f_i\lambda_i^4+\cdots\leqq f_r\lambda_r^2+\frac{1}{\lambda^2}f_r\lambda_r^4+\cdots. \tag{6}$$

Expanding the right members of (3) and (3′) similarly results in

$$\sum_{i=1}^{s} f_i\lambda_i^4\left(\frac{1}{\lambda^2}\right)\left(1-\frac{\lambda_i^2}{\lambda^2}\right)^{-2}\leqq f_m\lambda_m^4\left(\frac{1}{\lambda^2}\right)\left(1-\frac{\lambda_m^2}{\lambda^2}\right)^{-2}$$

or

$$\left(\frac{1}{\lambda^2}\right)\sum_{i=1}^{s} f_i\lambda_i^4+\left(\frac{2}{\lambda^4}\right)\sum_{i=1}^{s} f_i\lambda_i^2\leqq\left(\frac{1}{\lambda^2}\right)f_m\lambda_m^4+\frac{2}{\lambda^4}f_m\lambda_m^6+\cdots. \tag{7}$$

From (6) and (7) it is seen that

$$\sum_{i=1}^{s} f_i\lambda_i^4=f_r\lambda_r^4=f_m\lambda_m^4. \tag{8}$$

The ratio of the second to the first coefficient in the right member of (1) may be equated to the corresponding ratio in the left member to give

$$\frac{f_r\lambda_r^4}{f_r\lambda_r^2}=\lambda_r^2=\frac{\sum_{i=1}^{s} f_i\lambda_i^2\cdot\lambda_i^2}{\sum_{i=1}^{s} f_i\lambda_i^2}. \tag{9}$$

Similarly from (2)

$$\frac{f_m\lambda_m^6}{f_m\lambda_m^4}=\lambda_m^2=\frac{\sum_{i=1}^{s} f_i\lambda_i^4\cdot\lambda_i^2}{\sum_{i=1}^{s} f_i\lambda_i^4}. \tag{10}$$

The right members of (9) and (10) show λ_r^2 and λ_m^2 to be weighted means of the λ_i^2 but with weights differing in such a way as to give the longer wave-lengths more prominence in the cases of λ_m^2, i.e.,

$$\lambda_m>\lambda_r. \tag{11}$$

From (8) it is now apparent that

$$f_m<f_r. \tag{12}$$

To represent the anomalous rotation in the region of 0.3850μ, an unsymmetrical term $B\lambda^2/(\lambda^2-\lambda_B^2)$ may be added[6] to the symmetrical term $0.00509\ \lambda^2/(\lambda^2-0.123^2)^2$ in Eq. (5). It is evident that

$$\frac{(n^2+2)^2}{9n}\cdot\frac{B\lambda^2}{\lambda^2-\lambda_B^2}$$

must satisfy two conditions: (1) it must give values inside the band approximately equal to the

[7] J. W. Mellor, *A Comprehensive Treatise on Inorganic and Theoretical Chemistry*, Vol. 15, p. 459.

differences between the Verdet constants determined by experiment and those calculated by use of Eq. (5); and (2) it must become vanishingly small at wave-lengths 0.3470μ and 0.4500μ.

It has been found that if the second condition is fulfilled, this term can account for only about 50 percent of the differences inside the band. Part of the discrepancy can be accounted for by the theory of the extended band. If the band is assumed to have the shape of the probability curve, which the absorption band for the solution seems to have,[8] the theory will account for about 65 percent of the discrepancy instead of 50 percent. This is not considered to be within the experimental error. The broken lines in Fig. 2 have been arbitrarily drawn in to fit the experimental results.

The limited data available on the absorption band prevent any further attempt to devise an equation which will fit over the entire visible and near ultraviolet regions. It is thought that the exact nature of the band may be better known when low temperature measurements have been completed in the absorption region.

ACKNOWLEDGMENTS

We are greatly indebted to Dr. Philip Rudnick for aid in the theoretical interpretation of the data.

[8] R. W. Roberts, Phil. Mag. **28**, 601 (1939).

SEPTEMBER 15, 1941 PHYSICAL REVIEW VOLUME 60

Electron Diffraction Studies of Thin Films

II. Anomalous Powder Patterns Produced by Small Crystals[1]

L. H. GERMER AND ADDISON H. WHITE
Bell Telephone Laboratories, New York, New York

(Received July 21, 1941)

The (200) ring has been observed to be relatively very weak in electron diffraction patterns produced by extremely small crystals of face-centered cubic type. To study this anomaly we have obtained microphotometer curves from copper films in which the mean linear dimensions of the crystals, as estimated from half-breadths of diffraction rings, varied from 20A to 67A. From each curve the ratio of intensities of the (200) and (111) rings has been determined, and this ratio is found to vary from 0.14 for the 20A crystals to 0.42 for the 67A crystals, the latter figure agreeing within experimental error with 0.48 the theoretical value calculated for large crystals of copper. In order to find what to expect from extremely small crystals, we have carried through the usual calculation to determine the scattering from gas molecules, assuming for each molecule N similar atoms with a face-centered cubic arrangement and nearly spherical shape. For $N=55$ no (200) ring can be detected in the scattering pattern, while for $N=379$ the (200) ring is very plain and all of the rings have relative intensities appropriate to large crystals. The previously reported intensity anomaly is thus accounted for on the basis of smallness of the individual crystals. The very smallest crystals which we have produced give ring intensity ratios intermediate between those calculated for crystals of 55 and 379 atoms each. This is a somewhat smaller size than that estimated from half-breadths of diffraction rings produced by these smallest crystals.

SOME thin films produce electron diffraction powder patterns in which the relative intensities of the rings are quite abnormal. In many cases, rings which show unusual intensity ratios are very broad, and it seems certain that the anomalous intensities are associated with extremely small individual crystals. This effect has been pointed out in diffraction patterns from films of nickel hydroxide,[2] gold[3] and the aluminum hydrate known as boehmite.[4] It is especially marked in patterns from very thin films of metals having the face-centered cubic structure, and gold films producing such exceptional patterns

[1] The first section of this work, "I. Structure of very thin films," appeared in Phys. Rev. **56**, 58–71 (1939).

[2] L. H. Germer, Zeits. f. Krist. **100**, 277 (1938).
[3] L. H. Germer, Phys. Rev. **56**, 58 (1939).
[4] L. H. Germer and K. H. Storks, J. Ind. Eng. Chem. Anal. Ed. **11**, 583 (1939).

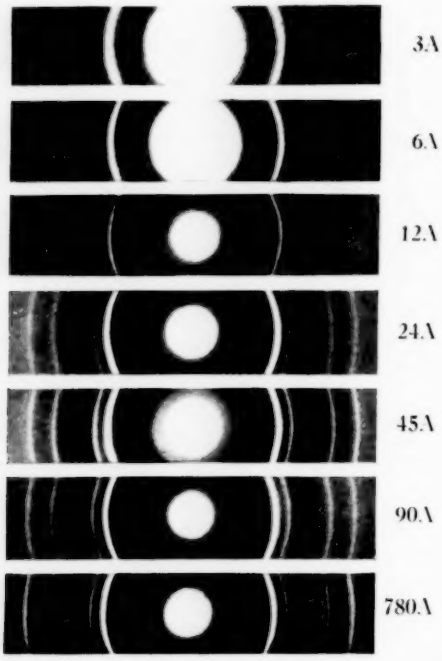

FIG. 1. Electron diffraction patterns from films of copper of various mean thicknesses, approximately 3×2^mÅ where $m=0$, 1, 2, 3, 4, 5 and 8.

have been described as "partly amorphous"[3] without, however, implying by this expression any precise knowledge of the actual structure. This paper is concerned with an interpretation of this phenomenon for the case of face-centered cubic crystals. The explanation probably applies also to intensity anomalies produced by small crystals of less simple structure, but there are, of course, unexplained intensity ratios in patterns produced by relatively large crystals to which the present considerations do not apply.

The set of diffraction rings, which is thought of as peculiar to randomly oriented crystals of face-centered cubic type, is actually characteristic only of aggregates of rather large crystals of this type. That this is true is obvious at once from the fact that four atoms at the corners of a regular tetrahedron form a complete face-centered cubic crystal. These four atoms scatter parallel radiation in phase only for those orientations and in those directions for which the atoms of an extended face-centered cubic crystal built upon these atoms scatter in phase; yet it is well known that the "powder pattern" produced by randomly oriented tetrahedra (approximately the CCl_4 pattern) has no obvious resemblance to that of face-centered cubic crystals. If one imagines a single atom added to each of a number of randomly oriented tetrahedral groups of four atoms, in such a way as to make of each a "face-centered cubic crystal of five atoms," then it is clear that the diffraction pattern produced by the assemblage will be altered; and if one continues to add single atoms in this manner, always maintaining the groups approximately spherical in shape, the pattern will be changed progressively and will approach that of extended face-centered cubic crystals.

With these models in mind, we have calculated diffraction patterns to be expected from randomly oriented "face-centered cubic molecules" containing various numbers of atoms, and have compared the results with densitometer traces of electron diffraction patterns from films made up of extremely small copper and gold crystals.

PATTERNS FROM COPPER FILMS

The diffraction patterns of Fig. 1 were produced by films of copper which had been vaporized upon Formvar supporting foils by the method described in reference 3. The vaporization was carried out in the diffraction camera, and in each case the pattern was obtained without exposing the freshly prepared metal film to air. Copper happens to be the metal used because this investigation developed incidentally to studies of the oxidation of copper, which have not yet been published.

From visual inspection of the patterns of Fig. 1 it is clear that the sharpest rings were formed by the thick films, and that the very thin films produced broad rings. The ring broadening is due to smallness of the individual copper crystals, and the change of ring width with mean film thickness agrees with the previous observation of a relation between film thickness and average crystal size.[3] Patterns taken with films inclined by 45° to the primary beam direction are indistinguishable from those taken at normal incidence, from which we conclude that preferred orientation does not occur and that crystals tend, on the average, to be as thick normal to a film as parallel to it.

The intensity anomaly under consideration is exhibited clearly by the patterns from the films of

mean thickness 3A and 6A. The (111) ring is relatively much too strong; this is particularly noticeable when one compares the adjacent (111) and (200) rings. A similar abnormality is shown by the pattern from a very thin gold film which was reproduced as Fig. 5 of reference 3. In the latter, strong broad rings appear at positions corresponding to (111), (311)/(222) and (331)/(420), but (200) and (220) rings cannot be seen, although they appear weakly on the original plate.

From a microphotometer curve of each of the patterns reproduced in Fig. 1 we have obtained a quantitative estimate of the breadth at half-maximum of the (111) ring, and of the ratio of the intensities of the (200) and (111) rings. The resulting values are written down in Table I, together with mean crystal dimensions C calculated from the half-breadths ΔR by means of the Scherrer formula in the form $C=L\lambda/\Delta R$, where $L\lambda=2.34\times10^{-6}$ mm^2 = the product of the specimen-plate distance and the electron wave-length, and where each directly observed value of half-breadth (column 2) has been decreased by 0.2 mm, which is the observed half-breadth of diffraction rings produced by films made up of fairly large crystals.

The method of determining these quantities is illustrated by the curves of Fig. 2. The continuous curve a represents the photographic density of the pattern obtained from the copper film of 3A mean thickness. The difference between this and the interpolated background, indicated by the broken line b, represents diffraction features produced by the copper film and by its Formvar support. Features from the latter are naturally much more prominent in this pattern than in those from copper films of greater mean thickness and their estimation is of special importance in this case. The first ring from the Formvar foil has its maximum at a radius of about 4.9 mm, and the second at about 10.8 mm, nearly coinciding with the (111) copper ring. The shapes of these two Formvar rings and their relative intensities were determined from a diffraction pattern obtained from this particular Formvar foil immediately before vaporizing copper upon it. With these data on hand, together with the integrated intensity of the 4.9-mm Formvar ring appearing in Fig. 2, one can at once draw in upon the interpolated background b the appropriate curve for the 10.8-mm Formvar ring. In this way the broken curve c was obtained. The (111) and (200) diffraction features from the copper film are represented by the difference between curves a and c.

Separation of the (111) and (200) diffraction rings of copper presents some difficulty because of their breadths. These breadths are so great that the atomic scattering factor for electrons f varies considerably from one side of a ring to the other and, together with an angle factor of $1/R^2$, causes each diffraction ring to be unsymmetrical, falling off from its maximum intensity more rapidly with increasing than with decreasing radius. This distortion we have eliminated by dividing each observed intensity, the difference between points at the same radius on the a and c curves of Fig. 2, by the factor f^2/R^2 and plotting the resulting values on an arbitrary scale as the inset curve d. In this computation we have taken $f=(Z-F)/R^2$, where $Z=29$, the atomic number of copper, and values of F for copper are obtained from the tables of Pauling and Sherman.[5] On the assumption that the (111) feature as thus corrected is symmetrical, its outer half is represented by the curve e passing through the points indicated by crosses. The (200) ring appears then as the area between curves d and e, and this feature is redrawn as curve g. This curve is somewhat

TABLE I. *Data on (111) rings.*

Mean Thickness of Film (10^{-8} cm)	Half-Breadths of (111) Rings: Dir. Meas. (mm)	Half-Breadths of (111) Rings: Corr. for Primary Beam Size* (mm)	Calc. Mean Crystal Dimensions (10^{-8} cm)	Intensity Ratio of (200) to (111) Ring
Data obtained from the diffraction patterns of Fig. 1				
3	1.35	1.15	20	0.14
6	1.04	0.84	28	0.18
12	0.68	0.48	49	0.33
24	0.60	0.40	58	0.36
90	0.55	0.35	67	0.42
45,780 about the same as the 90A film				
Data obtained from a gold film				
1.6	1.10	0.90	26	0.21

* The absolute precision of the values of calculated mean crystal dimensions does not justify a more nearly correct but more elaborate correction for the primary beam size. If, for example, one corrects for a primary beam size of 0.2 mm by the approximate method given by Taylor [Phil. Mag. 31, 339 (1941)], one obtains 18.5A (rather than 20A) for the mean size of crystals in the 3A film, and 55A (rather than 67A) for the mean size in the 90A film.

[5] L. Pauling and J. Sherman, Zeits. f. Krist. **81**, 1 (1932).

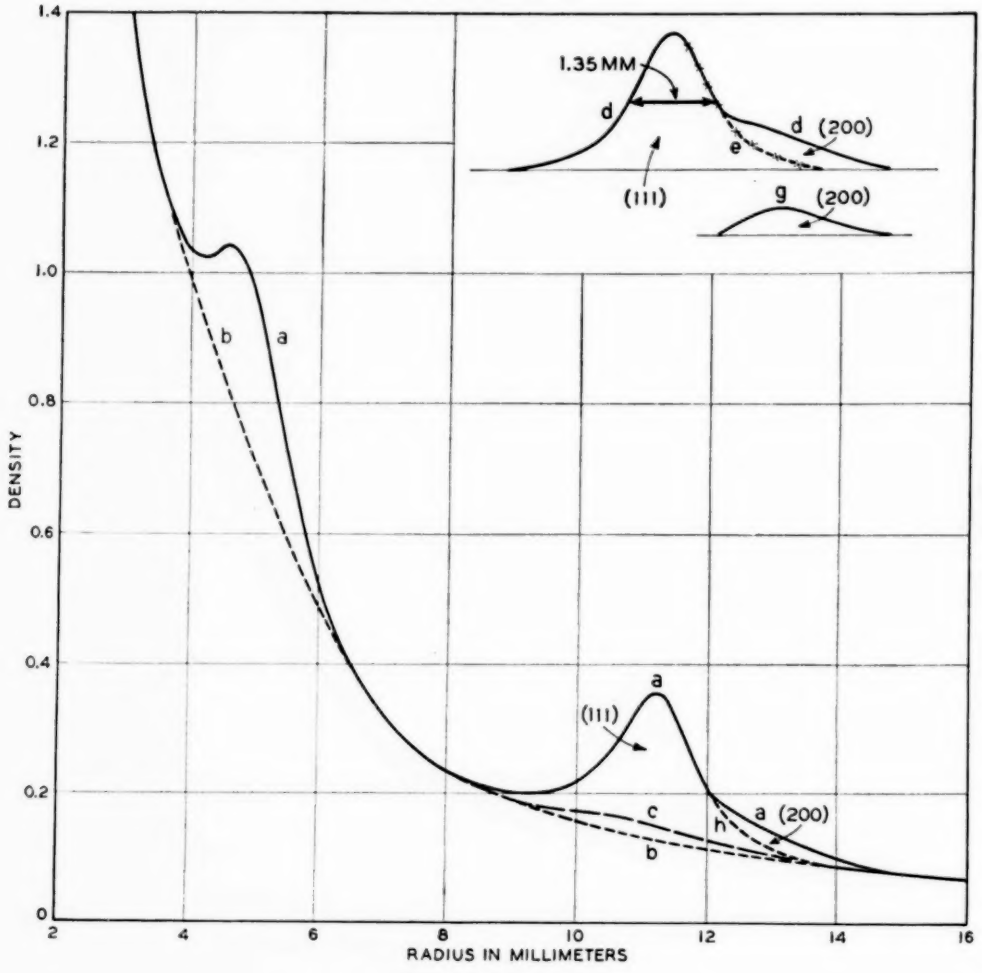

FIG. 2. Microphotometer curve of the diffraction pattern from the 3A copper film. (See Fig. 1).

unsymmetrical presumably because of slight errors. The integrated intensity obtained from curve *g* does not possess high precision, but it is reassuring to find that the positions of the intensity maxima of the (200) and (111) rings as determined in this way, 13.0 and 11.3 mm, respectively, are in the ratio $\sqrt{4}/\sqrt{3}$, and the half-breadth of the (200) ring is not very greatly different from the rather accurate value 1.35 mm found for the (111) ring, curve *d–e*. In order to compare the "observed" intensities the ordinates of the curve *e* have been multiplied by f^2/R^2 and then added to those of curve *c* to produce curve *h*, the outer half of the (111) ring. The (200) ring is then the area between curves *a* and *h*, and the ratio of this area to that of the (111) ring is determined to be 0.13.

Calibration of an Eastman process plate similar to those upon which the diffraction patterns of Fig. 1 were obtained has shown that the photographic density D is related to the intensity I by $D = \text{const.}\ I^{1.2}$ for D in the range 0.05 to 1.3. This relation is so nearly linear that density and intensity have been used interchangeably in all of the above considerations. The final integrated intensities of the (200) and (111) rings have, however, been obtained from the integrated densities by means of this relation, taking the density of each feature to be that of the center of gravity of its area. When this is done the ratio of intensities of the (200) and (111) rings is 0.14, (whereas the ratios of integrated densities is 0.13).

All of this procedure of calculation and correction has been repeated upon microphotometer curves from the copper films of mean thickness 6A, 12A, 24A and 90A, and sufficient observations have been carried out upon the patterns from the 45A and 780A films to convince us that they

would yield data substantially identical with those from the 90A film. All of the results are given in Table I. One observes that the ratio of intensities of the (200) and (111) rings increases with increasing crystal size, and the largest value of this ratio, 0.42 for the 90A film, agrees within the limits of error of the measurements with $(f^2p/R^2)_{200}/(f^2p/R^2)_{111}=9f^2_{200}/16f^2_{111}=0.48$, the theoretical value calculated for large crystals using Pauling and Sherman[5] values of F for copper.

On the last line of Table I are given data from a microphotometer trace of the pattern from a very thin gold film. This was a "sandwich" film made by vaporizing gold to a mean thickness of 1.6A upon each side of a Formvar foil. The ratio 0.21 of the intensities of the (200) and (111) rings found for this film is much less than the theoretical ratio 0.44 calculated for large gold crystals using values of F for gold interpolated from the Pauling and Sherman tables.

From a more extended microphotometer curve from the pattern of the 90A film we have determined the relative intensities of the first five diffraction rings, and have found that all of these intensities agree moderately well with those calculated for large crystals from ratios of values of the function f^2p/R^2, p representing the multiplicity of crystal planes. The numerical values are written down in the second and third columns of Table II. After a correction for the temperature effect[6] has been applied to the calculated ratios of the third column the agreement is still better and within experimental error.

Calculated Powder Diffraction Patterns for Small Crystals

The theoretical expression for the intensity of coherent scattering from gas molecules is proportional to $\sum\sum f_i f_j \sin(sr_{ij})/sr_{ij}$. For the case under consideration, in which the "molecules" are independent face-centered cubic crystals, this has the form $\sum_n B_n f^2 \sin(x\sqrt{n})/x\sqrt{n}$. $x=\pi\sqrt{2}Ra_0/L\lambda$; a_0 = edge of unit cell; B_n = twice the number of atom pairs in the crystal having the separation $a_0(n/2)^{\frac{1}{2}}$, where n is any positive whole number including zero, and $B_0=N$.

We have omitted the factor f^2 and have calculated the function $I'=\sum B_n \sin(x\sqrt{n})/x\sqrt{n}$ for crystals made up of 4 atoms, 13 atoms, and 55 atoms, choosing, for a 13-atom crystal a single atom and its twelve nearest neighbors and, for a 55-atom crystal, a single atom and its neighbors at distances of $a_0(1\frac{1}{2})^{\frac{1}{2}}$, $a_0(2\frac{1}{2})^{\frac{1}{2}}$, $a_0(3\frac{1}{2})^{\frac{1}{2}}$, and $a_0(4\frac{1}{2})^{\frac{1}{2}}$. Values of B_n for these crystals are given in the last column of Table III, and the calculated curves I' are plotted in Fig. 3 against $y=x/\pi\sqrt{2}=Ra_0/L\lambda$. To serve as reference points vertical lines are drawn at the bottom of Fig. 3 at $y=\sqrt{3}$, $\sqrt{4}$, $\sqrt{8}\cdots$ etc., which are the positions of rings corresponding to large face-centered cubic crystals.

It is clear from inspection that these theoretical curves have less sharp features, and are less like patterns from extended face-centered cubic crystals, than the diffraction patterns from even the very smallest copper crystals. Thus we conclude that these smallest crystals contain, on the average, more than 55 atoms, which, of course, they must if the mean dimensions of Table I, as estimated from half-breadths, are at all reliable; and, if one is to obtain agreement between theoretical and observed curves, he must calculate I' for crystals containing a number of atoms N considerably greater than 55.

The calculation is laborious for N large, as is also determination of the coefficients B_n. The latter work can, however, be avoided by an approximation which is accurate for large values of N. We can write $B_n=Nb_n\epsilon_n$, where b_n is the number of atoms at a distance $a_0(n/2)^{\frac{1}{2}}$ from any particular atom in an infinite face-centered cubic crystal and ϵ_n lies in the range $0\leq\epsilon_n\leq1$. The numbers b_n are written down at once with the aid of a table of quadratic forms for the cubic system,[7] and values of ϵ_n are easily calculated on

Table II. *Relative intensities of diffraction rings.*

Ring	Measured on Pattern from 90A Film	Calc. for Large Crystals from Relative Values of f^2p/R^2	From Calc. Curve for 379 Atom Model
(111)	1	1	1
(200)	0.42	0.48	0.45
(220)	0.27	0.30	0.29
(311)	0.20	0.32	0.43
(222)	0.08	0.09	

[6] *International Tables for the Determination of Crystal Structures*, Vol. 2, pp. 574–575.

[7] Reference 6, pp. 474–501.

the simplifying assumption of perfectly spherical crystals of volume $V=\pi D^3/6=Na_0^3/4$. About any point P within such a crystal we imagine a sphere of radius $a_0(n/2)^{\frac{1}{2}}$, and define ϵ_n' at the point P as the fraction of the surface of this sphere which lies within the crystal of diameter D. ϵ_n will then be quite approximately equal to the average value of ϵ_n' inside the spherical crystal. For distances u from the center lying in the range $0\leq u\leq[D/2-a_0(n/2)^{\frac{1}{2}}]$, $\epsilon_n'=1$ and for the range $[D/2-a_0(n/2)^{\frac{1}{2}}]\leq u\leq D/2$ it is easy to show that $\epsilon_n'=[2u-a_0(n/2)^{\frac{1}{2}}+(D^2/4-u^2)/a_0(n/2)^{\frac{1}{2}}]/4u$. By carrying out the integration $\epsilon_n=(1/V)\int\epsilon_n'dv$, one obtains,

$$\epsilon_n=1-[(2n)^{\frac{1}{2}}/4d](3-n/2d^2), \qquad (1)$$

where $d=D/a_0$. ($\epsilon_n=0$ for $n\geq 2d^2$.)

To test the approximation used, we have applied Eq. (1) to crystals of 4 atoms, 13 atoms, and 55 atoms. In these cases, by taking for the volume of each atom $a_0^3/4$, we have $d=(3N/2\pi)^{\frac{1}{3}}$ where $N=4$, 13, and 55, respectively. Values of ϵ_n calculated for these crystals are written down in the second column of Table III, and corresponding values of $Nb_n\epsilon_n$ in the fourth column. The latter agree quite well with the accurate coefficients B_n for crystals having the same number of atoms and the most nearly possible spherical shape; this agreement is justification for the use of Eq. (1) in calculation of the diffraction pattern from crystals having a greater number of atoms.

TABLE III. *Comparison of the accurate values of the coefficients. B_n for nearly spherical crystals with approximate values $Nb_n\epsilon_n$ calculated for exact spheres of the same volumes.*

	Approximate			Accurate
n	ϵ_n	b_n	$Nb_n\epsilon_n$	B_n
	4-atom crystals			
0	1.000	1	4.0	4
1	.238	12	11.4	12
2	.053	6	1.3	—
3	.000	24	0.0	—
	13-atom crystals			
0	1.000	1	13	13
1	.451	12	70	72
2	.264	6	21	24
3	.148	24	46	48
4	.074	12	11	12
5	.028	24	9	—
6	.005	8	1	—
	55-atom crystals			
0	1.000	1	55	55
1	.650	12	429	432
2	.514	6	170	180
3	.417	24	551	528
4	.340	12	224	228
5	.277	24	366	384
6	.225	8	99	96
7	.181	48	478	480
8	.143	6	47	54
9	.111	36	220	216
10	.084	24	111	96
11	.062	24	82	96
12	.044	24	58	72
13	.029	72	115	96
14	.017	0	0	—
15	.009	48	24	—
16	.003	12	2	12
17	.000	48	0	—

We have calculated the scattering pattern from crystals for which $d=4\sqrt{2}$, which corresponds to $N=2\pi d^3/3=379$ atoms. This value of d was chosen because the diameter of corresponding individual crystals of copper, $D=4\sqrt{2}a_0=20.4$A, is close to the linear dimensions of copper crystals in the thinnest films as estimated from the half-breadths of (111) rings given in Table I. It is, thus, of especial interest to compare the calculated curve I' for crystals of 379 atoms with the microphotometer curve of the pattern from the copper film of 3A mean thickness.

For assumed spherical crystals of 379 atoms, $\epsilon_n=1-(n^{\frac{1}{2}}/16)(3-n/64)$. It is obvious that the expression $\sum(Nb_n\epsilon_n)\sin(x\sqrt{n})/x\sqrt{n}$ will have terms up to and including $n=63$. This summation has been carried out at 33 values of x and the result is plotted against $y=Ra_0/L\lambda$ in Fig. 3, with the calculated curves for crystals of 4, 13, and 55 atoms. The degree of detail exhibited by the curve for the 379-atom model is greater than that of patterns from the thinnest copper films; in particular the (200) ring is much less clear on the curve of Fig. 2, although the (311) and (222) rings are not resolved in either case.

The calculated curves of Fig. 3 are for any crystals of face-centered cubic type. We have modified the curve for the 379-atom crystals by multiplying each term in the theoretical expression by $f^2=(Z-F)^2/R^4$ for copper, values of F being taken from Pauling and Sherman. The resulting curve $I=\sum(Nb_n\epsilon_n)f^2\sin(x\sqrt{n})/x\sqrt{n}$, which is plotted against $y=Ra_0/L\lambda$ in Fig. 4, is the complete theoretical expression for the scattering intensity except for omission of the incoherent atomic scattering and the temperature effect, which would not greatly change the curve. Figure 4 exhibits peaks whose areas are not at all proportional to areas of the corre-

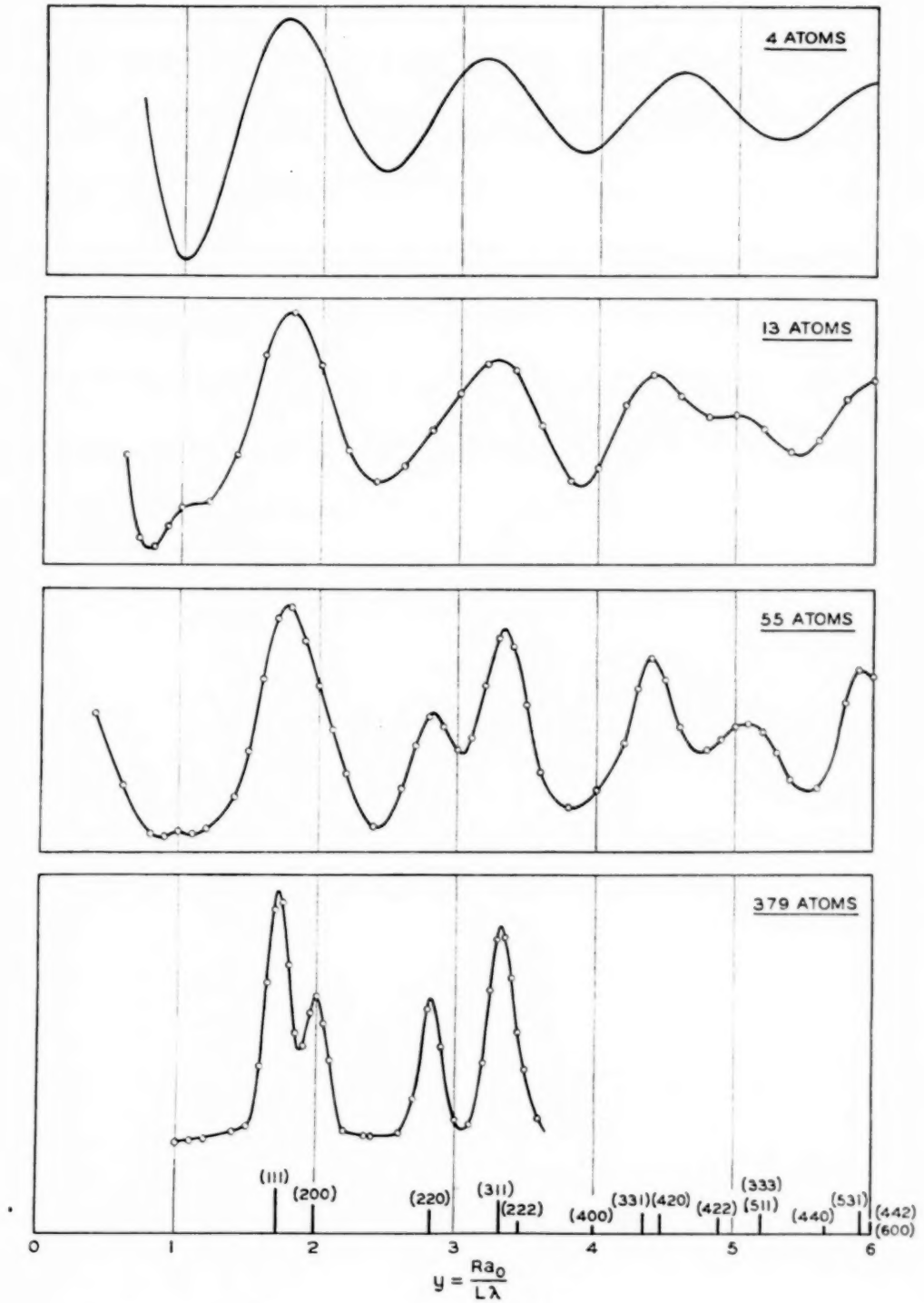

FIG. 3. Theoretical curves, $\Sigma B_n \sin(x\sqrt{n})/x\sqrt{n}$, for nearly spherical face-centered cubic crystals of 4 atoms, 13 atoms, 55 atoms, and 379 atoms.

sponding features of Fig. 2 and its extension, not reproduced here, as far as the (311)/(222) ring; they appear to be more nearly appropriate to large crystals. In fact, the microphotometer curve of the pattern from the 90A film, which is not reproduced here, seems, on casual inspection, to be almost identical with Fig. 4, except for a small amount of background in the former which is not present in the theoretical curve presumably because of failure to include the incoherent scattering, and except for the fact that the (311) and (222) rings can be resolved in the former curve and not in the latter. To obtain a quantitative comparison we have estimated the areas of the (111), (200), (220) and unresolved (311)/(222) peaks in Fig. 4 and have written them down in the last column of Table II. It is obvious that they agree well with ratios of f^2p/R^2 given in the second column and moderately well with relative intensities of rings from the 90A film. After correcting the theoretical values for the temperature effect, the latter agreement is within experimental error.

We would like to have calculated the scattering curve for a spherical model containing about 200 atoms ($d=4.3$) and to compare the relative intensities of the (200) and (111) rings obtained from it with the value 0.14 from the curve of Fig. 2. Observation of the expected agreement seemed, however, not to justify the labor which would be involved. We have actually found only that the relative intensities of rings produced by

TABLE IV. *Comparison of diameters of the crystal models d with dimensions C/a_0 computed from breadths at half-maximum of peaks of the calculated scattering curves.*

	Δy Breadth at Half-Max. of Theor. Peaks Fig. 3	C/a_0 Corresp. Mean Crystal Sizes per A Edge of Unit Cell	d Diam. of Near-Spherical Models per A Edge of Unit Cell
	13-atom crystals		
(111)/(200)	0.57	1.8	1.84
(220)/(311)/(222)	0.73	1.4	
	55-atom crystals		
(111)/(200)	0.52	1.9	2.97
(220)	0.44	2.3	
(311)/(222)	0.35	2.9	
	379-atom crystals		
(111)	0.19	5.3	5.66
(200)	0.24	4.2	$(4\sqrt{2})$
(220)	0.18	5.6	
(311)/(222)	0.22	4.5	

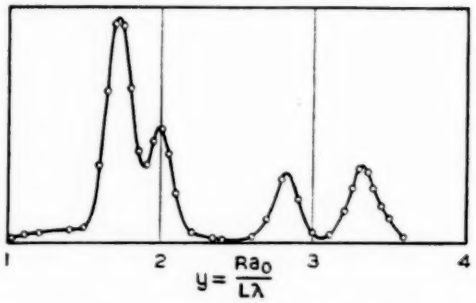

FIG. 4. Theoretical scattering curve for spherical copper crystals of 379 atoms.

crystals in the 3A film correspond to a model intermediate in size between 55 and 379 atoms, although such a model would give rings having a greater half-breadth than those from the actual film.

It is evident that normal powder diffraction patterns characteristic of face-centered cubic crystals cannot be expected unless the individual crystals contain several hundred atoms. The abnormal patterns produced by crystals of two or three hundred atoms each are adequately accounted for.

It is of interest to compare the diameters of the near-spherical and spherical crystal models, containing 13, 55, and 379 atoms, with linear dimensions calculated for these models from half-breadths of peaks of the computed scattering curves. Breadths at half-maximum Δy of peaks of the curves of Fig. 3 have been estimated and are written down in Table IV. From these we have calculated the ratio of the linear dimensions of the individual crystals C to the edge of the unit cell from the equation $C/a_0=1/\Delta y$ which is equivalent to the Scherrer formula in the form $C=L\lambda/\Delta R$. These calculated ratios C/a_0 tend to be smaller than values of d for the corresponding models, whereas in the case of the experimental films we have concluded that the estimates of crystal size from half-breadths are larger than estimates obtained from relative intensities.[8]

[8] In a recent paper [J. Chem. Phys. 9, 492 (1941)] we calculated mean dimensions of black carbon crystallites of the order of 20A. It was found that different diffraction features from a specimen of carbon gave dimensions which varied by more than the estimated experimental error, and this we were unable to account for. We note now that exactly this phenomenon is exhibited in Table IV by data for the 379-atom model (which also has dimensions of about 20A), and it seems altogether probable that a calculation carried out for the appropriate carbon model would yield results in agreement with the observations.

Theory of Internal Friction Introduced by Cold Working

CLARENCE ZENER
Washington State College, Pullman, Washington

(Received July 9, 1941)

Experiments indicate that those changes in a cold worked metal which give rise to internal friction are distinct from those changes which give rise to hardening and to the broadening of x-ray lines. It is suggested that this internal friction is due to the inability of certain areas on slip planes to maintain shearing stresses. The theoretical consequences of this suggestion are carried out, and are found to be in agreement with present experimental data.

IT is well known that internal friction is introduced into metals by cold working. The changes in the metal which give rise to this internal friction are apparently not related to the changes which give rise to an increase in hardness, and to a broadening of x-ray lines. For this internal friction is removed by annealing at temperatures so low that neither the hardness[1,2] nor the breadth of the x-ray lines[3,4] is affected. Such low temperature annealing does, however, remove to a large extent the residual macroscopic stresses introduced by cold work.[5] Perhaps for this reason, the opinion has frequently been expressed that the internal friction introduced by cold work is caused by these residual stresses.[2,3,6] No mechanism has been suggested, however, whereby residual stresses would give rise to internal friction measured at small strain amplitudes. An alternative explanation has been advanced by the author.[7] In this theory the internal friction is due to the thermal currents flowing between the microscopic stress inhomogeneities introduced by cold work. If this were the case, the internal friction should vary in a characteristic manner with frequency. However, recent measurements[8] have shown this internal friction to be independent of the frequency of measurement over a wide frequency range.

The view has been advanced[9–11] that the elastic after-effect may be explained in terms of a two-phase system, a continuous elastic phase and a discontinuous plastic phase. If the proper assumptions are made so that the observed elastic after-effect is reproduced, the associated internal friction automatically becomes independent of the frequency of measurement.[10] This theoretical result, combined with the observed invariance of cold work internal friction with frequency, leads us to suspect that the same physical changes in a cold worked metal are responsible for both the elastic after-effect and internal friction, and that these changes may be described, at least phenomenologically, in terms of a disperse plastic phase.

The essential characteristic of a disperse plastic phase is that it cannot permanently sustain shearing stress. If a constant load is applied, the initial shear energy in the plastic phase is gradually relaxed, resulting in a further elongation of specimen. The theory of the influence of such relaxation centers upon internal friction is developed in §1. In §2 we apply this theory to cold worked metals.

The same problem may, in principle, be attacked from the viewpoint of the dislocations introduced by cold working.[12] However, until we know the laws which govern the movements of the dislocations, and in particular, until we can calculate the consequences of their interaction with each other, more insight is to be gained from the phenomenological viewpoint here adopted.

[1] R. Wegel and H. Walther, Physics **6**, 141 (1935).
[2] W. Köster and K. Rosenthal, Zeits. f. Metallkunde **30**, 245 (1938).
[3] J. Norton, Trans. A.I.M.E. **137**, 49 (1940).
[4] S. T. Stephenson and F. Niemann (personal communication).
[5] For aluminum, see L. W. Kempf and K. R. Vanhorn, A.I.M.E. Tech. P. No. 1334 (1941).
[6] W. Köster, Zeits. f. Metallkunde **32**, 282 (1940).
[7] C. Zener, Phys. Rev. **53**, 582 (1938).
[8] C. Zener, C. Clarke, C. S. Smith, A.I.M.E. in press.
[9] v. Wartenberg, Verh. d. D. Phys. Ges. **20**, 113 (1918).
[10] R. Becker, Zeits. f. Physik **33**, 185 (1925).
[11] M. F. Sayre, J. Rheology **3**, 206 (1932).
[12] For review, see F. Seitz and T. A. Read, J. App. Phys. **12**, 100, 170 (1941).

§1. Theory of Relaxation Centers

A detailed discussion of the relation between relaxation centers and creep phenomena has been given by Becker.[10] His approach was not, however, well suited for the calculation of internal friction. This calculation was carried out only for one particular type of distribution of relaxation centers. It is thus necessary to give a more general discussion of the relation of relaxation centers to internal friction.

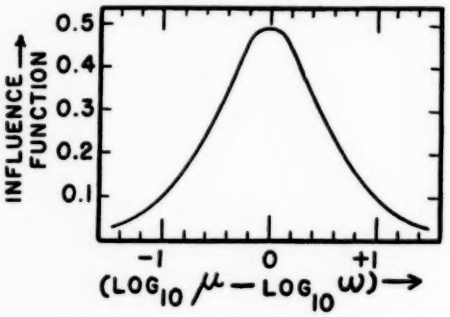

Fig. 1. Influence function $\frac{1}{2}\,\mathrm{sech}(\ln\mu-\ln\omega)$.

The method here adopted will be to calculate first the internal friction due to a single relaxation center. We then assume the centers to be sufficiently far apart so that their contributions to the internal friction are additive.

We consider an isolated unit volume containing a single relaxation center. We denote the macroscopic strain and the corresponding macroscopic stress by e and S, respectively. There are two elastic constants corresponding to the ratio e/S. One, C_∞, is the constant measured so rapidly that no appreciable relaxation takes place. This is the constant measured by very high frequency vibrations. The other, C_0, is the constant measured by a quasi-static method. It is necessarily larger than C_∞.

If there were no relaxation, the time rate of change of e would be $C_\infty dS/dt$. The relaxation contributes an additional term $\mu(C_0S-e)$, where μ is called the relaxation constant. The general relation between stress and strain is thus given by

$$(d/dt+\mu)e=(C_\infty d/dt+C_0\mu)S. \qquad (1)$$

In order to calculate the internal friction associated with a definite angular frequency ω, we substitute into Eq. (1)

$$e=\mathfrak{e}e^{i\omega t}, \quad S=\mathfrak{S}e^{i\omega t},$$

where $\mathfrak{e}$ and $\mathfrak{S}$ are complex constants. The ratio $\mathfrak{S}/\mathfrak{e}$ is called the complex modulus. We write it in the form $M+iN$. The ratio $Q^{-1}=N/M$ is a common measure of internal friction.[13] We find

$$Q^{-1}=(C_0-C_\infty)\mu\omega/(C_0\mu^2+C_\infty\omega^2). \qquad (2)$$

We now assume, as is usually the case, that C_0 is only slightly larger than C_∞, and so shall replace C_0 by C_∞ in the denominator.

When we add the effects of all the relaxation centers, it will be convenient to have the contribution of each center in the form of a strength factor times an influence function. This is possible if we regard $\ln\mu$ and $\ln\omega$ as variables in place of μ and ω. Thus we may write

$$\mu\omega/(\mu^2+\omega^2)=\tfrac{1}{2}\,\mathrm{sech}(\ln\mu-\ln\omega).$$

Equation (2) may thus be written as

$$Q^{-1}=\tfrac{1}{4}(C_0-C_\infty)/C_\infty\cdot\tfrac{1}{2}\,\mathrm{sech}(\ln\mu-\ln\omega).$$

This is the desired form. A plot of the influence function is given in Fig. 1.

We now define a weighting factor $W(\ln\mu)$ as the contribution to $(C_0-C_\infty)/C_\infty$ of all the relaxation centers lying within a unit logarithmic range at $\ln\mu$. The total internal friction is then given by

$$Q^{-1}=\int_{-\infty}^{\infty}W(\ln\mu)\cdot\tfrac{1}{2}\,\mathrm{sech}(\ln\mu-\ln\omega)d\,\ln\mu. \qquad (3)$$

If W is only a slowly varying function of its argument, a useful formula is obtained by expanding W about $\ln\mu=\ln\omega$. This expansion gives the series

$$Q^{-1}=(\pi/2)W(\ln\omega)+(\pi^3/16)d^2W/d\,\ln\mu^2|_{\mu=\omega}+\cdots. \qquad (4)$$

§2. Relaxation Centers in Cold Worked Metals

It is commonly accepted that, in plastic deformation, the individual grains do not deform homogeneously, but that a finite slip occurs

[13] C. Zener, Phys. Rev. **52**, 230 (1937).

across certain planes. After slipping the two sides of a plane do not join together perfectly. The crystal structure may be broken down to a depth of several atomic distances. At best there are regions of misfits along the plane. Whatever the imperfections, it is reasonable to suppose that they render it impossible for certain areas permanently to maintain a shearing stress. But the relaxation of shearing stress across an area must also be accompanied by a partial relaxation of stress on either side of the area, and hence throughout a finite volume. Each area which cannot permanently maintain a shearing stress therefore constitutes a relaxation center.

The theory developed in §1 may be applied to these relaxation centers as long as the applied stresses are so small that the linear relation of Eq. (1) between stress and strain is valid. This is the case in those measurements of internal friction which are independent of the amplitude of vibration.

Cold working has a greater effect upon the internal friction of a metal the greater its purity. Thus, for a given elongation, 99.99 percent pure aluminum has an internal friction nearly twice as large as 99.5 percent pure aluminum.[6] The internal friction of the most drastically cold worked 70–30 alpha-brass[8] is, after recovery at room temperature for several days, not more than 10^{-4}. Values for pure copper of more than 10 times this have been reported.[1,2] It is to be expected that, as the homogeneity of a metal increases with increasing purity, the larger will be the areas of the weak places along the slip planes, and hence the larger the effective volume of the centers of relaxation.

In many cases the internal friction has been found to increase rapidly with increasing temperature. This is not the case, however, for that part of the internal friction introduced by cold working.[8] In the case of 70–30 alpha-brass, cold worked and then annealed at 100°C, it even decreased slightly in the range from room temperature to 80°C. According to the theory of relaxation centers, this independence with temperature is correlated with the independence with frequency. If the relaxation centers have the same heat of activation, an increase of temperature will increase the log of all the relaxation constants by the same amount, $\Delta \ln\mu$. By Eq. (3), this has the same effect as a decrease of log angular frequency by the same amount $\Delta \ln\mu$. Hence, if a change of frequency has no effect upon the internal friction, it is to be expected that a change in temperature will have only a slight effect.

Without further information, we cannot predict the frequency dependence of the internal friction. It depends upon the variation of the weighting function $W(\ln\mu)$ in the vicinity of $\ln\mu = \ln\omega$. If, as in alpha-brass, the internal friction is independent of frequency in a certain range, we conclude that the weighting factor is independent of μ for the same range of $\mu/2\pi$.

A decrease of the elastic modulus always accompanies cold working,[6] provided it is not carried so far as to introduce fiber structure. Conversely, low temperature annealing raises the elastic modulus. These effects are, of course, required by the theory of relaxation centers. For the introduction of such centers, as by cold working, must lower the elastic modulus; removal of the centers, as by annealing, must raise the modulus.

Formation of a Gas Layer on a Silver Surface

A. G. EMSLIE*
Williams College, Williamstown, Massachusetts
(Received July 21, 1941)

The results of Farnsworth and Winch on the change with time of the photoelectric work function of a freshly deposited silver surface are interpreted in terms of the adsorption of a gas layer. The relatively small over-all change in the work function and the slow rate at which it approaches its final value lead to the conclusion that the adsorbed particles form a mobile molecular film. The variation in the adsorption rate, deduced from the experimental data, agrees with Langmuir's theory of odd and even phases of the adsorbed particles. The theory permits an estimate to be made of the surface mobility of the molecules, the result being that the average time spent by a molecule before moving to an adjacent adsorption site is about 30 minutes. Comparison of the initial adsorption rate with the rate of arrival of the molecules at the surface indicates that a large fraction of the incident molecules is reflected. The experimental technique of Farnsworth and Winch seems to be well suited for further study of the kinetics of adsorption on clean metal surfaces at room temperature.

INTRODUCTION

ALTHOUGH adsorbed layers of gas on metals have been studied extensively, it appears that no definite conclusion has yet been reached concerning the nature of such layers when formed at room temperature. The large heats of adsorption of oxygen and hydrogen films on tungsten[1] suggest that the adsorption is atomic at room temperature. On the other hand, Blodgett and Langmuir[2] found that the accommodation coefficient of hydrogen with tungsten, measured at 357°K, changed after heating the tungsten. They inferred that a hydrogen film formed at low temperatures is molecular, while at high temperatures it is atomic. A similar conclusion was drawn for oxygen on tungsten by Johnson and Henson,[3] who found that an activation energy was required to form an atomic film. Some more evidence in favor of molecular films is given by Roberts.[4]

The purpose of this paper is to show that additional information on this question can be obtained from the recent results of Farnsworth and Winch[5] on the photoelectric work function of silver.

EXPERIMENTAL DATA

The results of Farnsworth and Winch include measurements of the photoelectric work function φ for a freshly deposited silver surface. It was found, after depositing the silver film, that φ increased rapidly at first, then more slowly, and finally settled down to a steady value after about 24 hours. The total change in φ was of the order of 0.1 ev.

An empirical equation of the form

$$\varphi=\varphi_A-(\varphi_A-\varphi_0)(1+at)^{-\frac{1}{2}} \qquad (1)$$

represents the experimental values satisfactorily, where φ_0 and φ_A are the initial and final values of φ, a is a constant, and t is the time. Figure 1 shows how the equation fits the experimental points.

CONDENSATION RATE

The change in φ is assumed to be due to condensation on the silver surface of the residual gas in the apparatus, which was at a pressure of about 10^{-8} mm Hg. Other possible explanations are recrystallization of the silver deposit or diffusion of trapped gas to the surface. Recrystallization is unlikely since the surface was at room temperature. Diffusion is improbable since the

* Recipient of a Research Grant from the Class of 1900 Fund of Williams College.

[1] J. K. Roberts, Proc. Roy. Soc. **A152**, 445 (1935); **152**, 473 (1935).

[2] K. B. Blodgett and I. Langmuir, Phys. Rev. **40**, 78 (1932).

[3] M. C. Johnson and A. F. Henson, Proc. Roy. Soc. **A165**, 148 (1938).

[4] J. K. Roberts, "Some problems in adsorption" (Cambridge Physical Tracts), pp. 89 and 113.

[5] H. E. Farnsworth and R. P. Winch, Phys. Rev. **58**, 812 (1940).

silver deposit exceeded 500 atomic layers in thickness.

Bosworth[6] has shown that the contact potential difference between clean tungsten and hydrogen-covered tungsten is proportional to the fraction θ of the surface covered, which is equivalent to saying that φ depends linearly on θ. If we assume the same law to apply here, we find Eq. (1) becomes

$$1-\theta=(1+at)^{-1}. \qquad (2)$$

Hence

$$d\theta/dt=\tfrac{1}{2}a(1+at)^{-\frac{1}{2}}=\tfrac{1}{2}a(1-\theta)^{3}. \qquad (3)$$

Thus the *net* rate of condensation is proportional to $(1-\theta)^3$.

It will appear later that Eq. (3) is consistent with the formation of a gas layer containing one molecule for every two silver atoms on the surface, or 6.3×10^{14} gas molecules per cm^2. This figure multiplied by the initial value of $d\theta/dt$, i.e., 2.1×10^{-3} sec.$^{-1}$ for the data in Fig. 1, gives an initial condensation rate of 1.3×10^{12} molecules per cm^2 per sec. Now, with a pressure of 10^{-8} mm Hg in the apparatus, the number of molecules striking 1 cm^2 per sec. is 5.6×10^{12}. We have assumed their mean velocity to be 5×10^{4} cm/sec. The fact that the two rates are comparable confirms the hypothesis of adsorption of residual gas molecules. Since the incident rate is about four times the initial condensation rate, the clean silver surface must reflect a large fraction of the molecules.

Interpretation

As stated in the introduction, there is considerable evidence that adsorbed layers at room temperature are molecular, in spite of the large heats of adsorption. The results of Farnsworth and Winch support this point of view because of the very small change in φ caused by the adsorbed film, contrasted with the changes of more than 1 ev in the *thermionic* work function due to adsorbed *atomic* films. We therefore infer that the adsorbed particles are molecules and not atoms.

The next point to be decided is whether the molecular layer is mobile or immobile. If the molecules remain indefinitely at the points where they condense, the number of sites available for adsorption, when the film is nearly complete, will be proportional to $1-\theta$. Thus the condensation rate for an immobile film should be proportional to $1-\theta$, which is quite contrary to Eq. (3). It must, therefore, be concluded that the film is mobile.

The properties of mobile films have been discussed by Langmuir[7] in terms of odd and even phases of the adsorbed particles. A particle is in an even phase if the sum of its surface coordinates, in units of the spacing of the underlying metal atoms, is an even integer; otherwise, it is in an odd phase. When the adsorbed molecules are large enough to prevent occupation of neighboring sites, the adsorption takes place in two stages, the first rapid, the second slow. The rapid adsorption builds up a patchy film containing a closely interwoven pattern of the two surface phases. The slow adsorption is due to surface mobility and evaporation which produce a gradual decrease in the total length of the phase boundaries. This makes new sites available for adsorption and therefore causes the net condensation rate to change quite slowly when θ tends to unity. Langmuir finds that the rate should finally be proportional to $(1-\theta)^3$, in agreement with Eq. (3).

Now, the energy required for evaporation must, in general, be more than that required to take a molecule over the potential hill between two adsorption sites. Thus surface mobility will take place at a lower temperature than evapora-

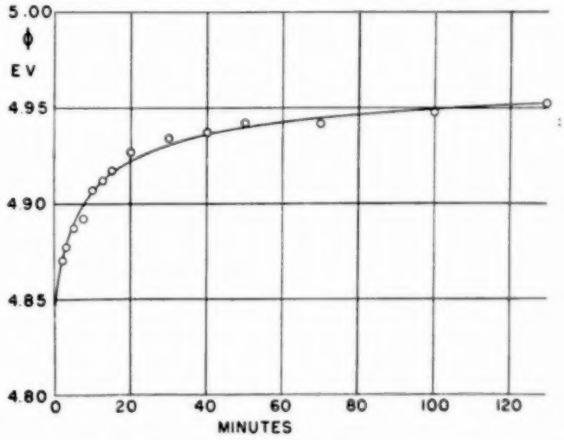

FIG. 1. Plotted points are experimental values. The curve represents empirical equation (1) with $a=0.25$ min.$^{-1}$.

[6] R. C. L. Bosworth, Proc. Camb. Phil. Soc. **33**, 394 (1937).

[7] I. Langmuir, J. Chem. Soc., p. 511, April, 1940.

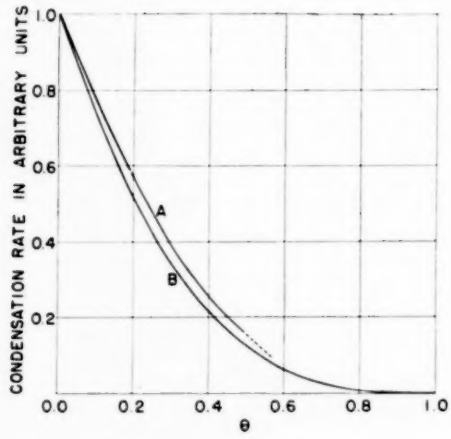

FIG. 2. Condensation rate as a function of fraction of surface covered. Curve B is experimental, curve A theoretical.

tion. This has been pointed out by Roberts.[8] It appears, therefore, that mobility should be the important factor governing the motion of the phase boundaries. In that case, Langmuir's calculations show[9] that, for large values of θ,

$$2t/\tau_K = 0.26/(1-\theta)^2, \tag{4}$$

where τ_K is the average time that elapses before an adsorbed molecule, located at an external corner of one phase, hops into an available site in the other phase. From Eq. (4) we obtain

$$d\theta/dt = (1-\theta)^3/0.26\tau_K. \tag{5}$$

Comparing this with Eq. (3), and using the value of 0.25 min.$^{-1}$ for a (Fig. 1), we find that $\tau_K = 31$ minutes.

For smaller values of θ, the condensation rate will be approximately the same as for an immobile film. Curve A (Fig. 2), showing how the rate varies with θ, was obtained by using a model described by Roberts[10] and by assuming that each adsorbed molecule prevents adsorption on the four neighboring sites. The curve is to be compared with the experimental curve B, representing the expression $(1-\theta)^3$. The fact that curve B lies below curve A may be due indirectly to the mobility of the adsorbed molecules. Since τ_K is fairly small, the potential hills between sites must be of the order of kT in height. Thus the molecules will describe quite large oscillations about their mean positions. This could cause partial screening of the four *next* nearest sites and therefore produce a lowering of the condensation rate.

[8] Reference 4, p. 23, footnote.
[9] Reference 7, Eqs. (65) and (66).
[10] Reference 4, p. 35.

SEPTEMBER 15, 1941 PHYSICAL REVIEW VOLUME 60

Non-Laue Maxima in the Diffraction of X-Rays from Rocksalt—Temperature Effect

O. J. BALTZER
Wayman Crow Hall of Physics, Washington University, St. Louis, Missouri
(Received July 3, 1941)

No previous quantitative measurements have been made of the temperature dependence of the non-Laue diffraction maxima at lowered temperatures, although it has been known that the non-Laue diffraction pattern of many crystals nearly disappears at liquid-air temperature. In the present experiment, an ionization chamber and electrometer tube circuit have been used in determining the intensity of the non-Laue maxima observed when copper $K\alpha$ x-rays are diffracted from a rocksalt crystal. Measurements have been made at room temperature and at liquid-air temperature for the 200, 400, and 600 regions of scattering. It is found that the experimental decrease in intensity at liquid-air temperature is in fair agreement with an expression of the form $(1-e^{-2M})$, where e^{-2M} is the well-known Debye-Waller temperature factor.

1. INTRODUCTION

IT has been established that the intensity of the non-Laue diffraction maxima is dependent upon the temperature of the crystal specimen. Preston[1] showed that the intensity of these dif-

[1] G. D. Preston, Proc. Roy. Soc. **A172**, 116 (1939).

fuse spots was greatly enhanced at elevated temperatures for crystals of sodium chloride, aluminum, and magnesium, but that the temperature effect was less with diamond. Laval,[2] using an ionization chamber method, measured the scattered intensity at room temperature and at 500°C for potassium chloride and found a marked increase at the higher temperature. Raman and Nilakantan[3] have reported a definite increase with temperature for sodium nitrate. Lonsdale and collaborators[4] have observed that for many crystals, including KCl and $NaNO_3$, the diffuse spots almost completely disappear at liquid-air temperatures, and that this temperature effect is completely reversible.

Although there is sufficient qualitative evidence that the intensity increases with temperature, there have been no published quantitative data, with the exception of Laval's work in 1939, regarding the temperature dependence of the non-Laue diffraction maxima. If, as the Faxen-Waller-Zachariasen theory[5–7] supposes, the non-Laue diffraction maxima are a result of a thermal diffuse scattering, then we would expect to find a large decrease in intensity at liquid-air temperature. According to the theory proposed by Raman and his associates,[8] however, the phenomenon is not primarily thermal in origin so that the temperature effect would be less pronounced in this theory. It is, therefore, worth while to attempt a quantitative measurement of the intensity at lowered temperatures and to obtain the numerical ratio of the diffracted intensity at room temperature to the intensity at liquid-air temperature. The present research has been restricted to a study of the effect of low temperature upon the intensity of the non-Laue maxima observed when Cu $K\alpha$ x-rays are diffracted from rocksalt.

[2] J. Laval, Bull. Soc. Franc. de Mineralogie **62**, 137 (1939).
[3] C. V. Raman and P. Nilakantan, Proc. Ind. Acad. Sci. **11**, 398 (1940).
[4] K. Lonsdale, Nature **146**, 806 (1940); K. Lonsdale, I. Knaggs, and H. Smith, Nature **146**, 332 (1940).
[5] H. Faxen, Zeits. f. Physik **17**, 266, 277 (1923).
[6] I. Waller, Zeits. f. Physik **17**, 398 (1923).
[7] W. H. Zachariasen, Phys. Rev. **57**, 597 (1940); W. H. Zachariasen, Phys. Rev. **59**, 207 (1941).
[8] C. V. Raman and P. Nilakantan, Proc. Inc. Acad. Sci. **11**, 379, 389 (1940).

2. Apparatus and Experiment

A demountable, copper target x-ray tube was operated at a potential of approximately 25 kilovolts peak and at a current of 20 milliamperes. A constant voltage double motor-generator set in parallel with a bank of storage batteries was used to decrease fluctuations in line voltage. A gradual deposition of evaporated tungsten and of decomposed carbon from the diffusion pump oil was found to cause a detectable decrease in the intensity of the Cu $K\alpha$ radiation. The target was, therefore, cleaned at frequent intervals, and, as a further precaution, a liquid-air trap was used to secure improved vacuum conditions. A nickel filter, 0.0082 gram/cm², gave an intense beam of Cu $K\alpha$ x-rays together with a weak background of continuous radiation that did not interfere in the scattering measurements. The primary beam was defined by fixed collimating slits of lead. The dimensions of the slit closer to the x-ray tube were 0.030 cm wide by 0.100 cm high, and of the further slit were 0.024 cm wide by 0.088 cm high, with a separation of 5.0 cm between the slits. The rocksalt crystal was separated by a distance of 2.0 cm from the second slit. All measurements were made with the crystal displaced by more than 2° from a Bragg angle of strong reflection. Under this condition, no Bragg reflection can possibly occur, so that the relatively large divergence of the primary beam is not only permissible but also serves to minimize the statistical fluctuations in the measurements.

In order that the crystal be cooled down to

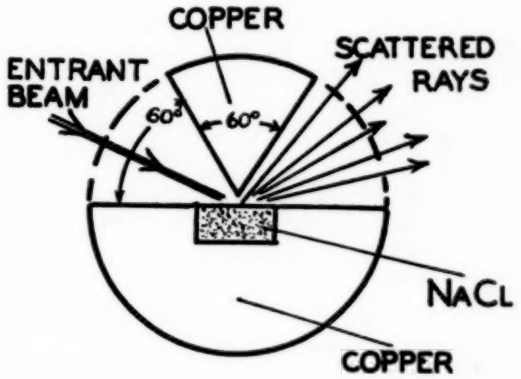

Fig. 1. Horizontal section through copper crystal holder for use at low temperature. Vertical dimension of slot for entrant beam was 3 mm. Opening for scattered rays had a vertical angular width of 15°.

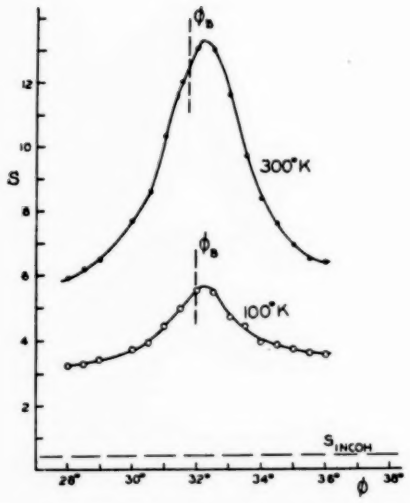

FIG. 2. Intensity of non-Laue diffraction maximum of Cu $K\alpha$ x-rays from rocksalt. Crystal displaced by 3° from 200 Bragg position of selective reflection.

liquid-air temperature without condensation of water vapor on the face of the crystal, it is necessary that the crystal be kept within a leak-free, evacuated spectrometer chamber. A vacuum chamber of radius $2\frac{3}{4}''$, mounted on a goniometer head, was constructed for this reason and also to prevent spurious intensity measurements resulting from scattering from air, and to lessen any decrease in x-ray intensity due to absorption in air. The exit for x-rays diffracted from the rocksalt was through a slot in the vacuum chamber extending from the primary beam position of $\phi=0°$ to a scattering angle of $\phi=115°$, so that all reflections of Cu $K\alpha$ rays from rocksalt out to the 600 reflection could be studied. The slot was covered by Cellophane, 0.008 cm thick, which withstood the atmospheric pressure outside the evacuated chamber.

The crystal and crystal holder could be rotated within the vacuum chamber by means of a vacuum-tight shaft, and the angular position of the crystal could be read with a precision of 1′. The ionization chamber could also be rotated about the axis of the goniometer, and its angular position could be determined with a similar accuracy. The crystal holder was constructed from a solid cylindrical copper block with slots cut in the block for the entrant beam upon the crystal and for the scattered x-rays, as indicated in Fig. 1. The front, cleavage face of the rocksalt crystal rested upon a vertical plane passing through the axis of rotation of the spectrometer. Because of the geometrical design of the holder which shielded and almost completely surrounded the crystal, it was assumed that the temperature of the crystal face was within a few degrees of the temperature of the crystal holder. On top of the copper block containing the crystal was a sylphon bellows which served as a liquid-air reservoir. Liquid air could be poured into the reservoir from outside the spectrometer by means of a vacuum-tight connecting shaft.

Measurements of the scattered x-ray intensity and of the intense primary beam were made with an argon-filled ionization chamber coupled to a Western Electric D-96475 low grid current tube in the Barth type of balanced amplifier circuit.[9] The ionization chamber had an effective length of 7.5 cm and a diameter of 3 cm and contained argon at a pressure of 1.5 atmospheres. The ionization chamber window measured 2.46 mm wide by 15.0 mm high and was at a distance of 8.25 cm from the axis of rotation of the crystal.

The rocksalt specimen was cleaved from an artificially grown parent crystal. A series of photographs taken at increasing distances from the specimen indicated that the divergence of the 200 Bragg reflection line from the cleavage face was less than 2′. This indicates that the rocksalt was reasonably perfect and that there was little warping or distortion of the surface layer.

Measurements of the scattered intensity were made using both the steady deflection and the more sensitive rate-of-drift methods. It is desirable that the observed galvanometer deflec-

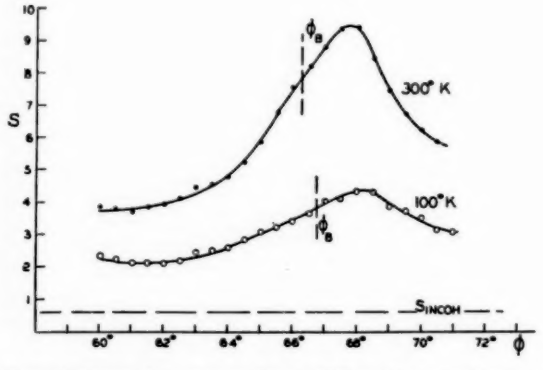

FIG. 3. Intensity of non-Laue diffraction maximum of Cu $K\alpha$ x-rays from rocksalt. Crystal displaced by 3° from 400 Bragg position of selective reflection.

[9] D. B. Penick, Rev. Sci. Inst. **6**, 115 (1935).

tions be reduced to some form giving an absolute intensity of scattering which is independent of any particular experimental arrangement. This was done by transforming all readings to S values, where S is the ratio of the observed scattering per electron to the scattering from one electron as given by the J. J. Thomson theory.[10] Experimentally, we have

$$S=\frac{4\mu}{\rho}\frac{W}{NZ}\frac{m^2c^4}{e^4}\frac{R^2}{A(1+\cos^2\phi)u(\phi,i)}\cdot\frac{D_{\phi,i}}{D_0}, \quad (1)$$

where $D_{\phi,i}$ and D_0 are the observed deflections due to the scattered rays and to the primary x-ray beam, respectively; R is the crystal-ionization chamber distance; A is the area of the ionization chamber window;

$$u(\phi,i)=\frac{2\sin(\phi-i)}{\sin(\phi-i)+\sin i} \quad (2)$$

is a geometrical factor to correct for the absorption effects within the crystal at a glancing angle of incidence i upon the crystal face;[11] W and Z are the average atomic weight and the average atomic number of (Na+Cl); N is Avogadro's number; and $\mu/\rho=74.8$ is the mass absorption coefficient of Cu $K\alpha$ x-rays in (Na+Cl).

The intensity of scattering of the non-Laue diffraction maxima associated with the 200, 400, and 600 reflections of Cu $K\alpha$ x-rays was determined for various scattering angles and for various values of $\Delta\equiv j-\theta$, where j is the glancing angle of incidence on the reflecting planes, and θ is the Bragg angle for reflection. For $\Delta>7°$, especially at a temperature of 100°K, the non-Laue diffraction maxima are extremely broad and barely distinguishable above the background of weak diffuse scattering; for $\Delta<1°$, the divergent primary beam permitted some ordinary Bragg reflection to occur. Measurements were, therefore, restricted to the region $2°<\Delta<7°$ in this investigation.

It is important that allowance be made for the contraction of the grating space as the temperature of the crystal is reduced. Due to this contraction, it was experimentally observed that the Bragg angle for the 600 reflection of Cu $K\alpha$ x-rays at 100°K was 35′ greater than the corresponding Bragg angle at 300°K. This agrees, within the limits of the experimental error, with the value 37′ calculated from the temperature coefficient of linear expansion, $\alpha=3.8\times10^{-5}$, for rocksalt.[12]

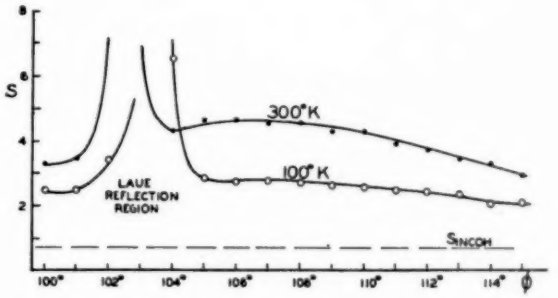

FIG. 4. Intensity of non-Laue diffraction maximum of Cu $K\alpha$ x-rays from rocksalt. Crystal displaced by −4° from 600 Bragg position of selective reflection.

The temperature contraction was always taken into account by making all measurements with respect to the Bragg angles of reflection at each particular temperature. Thus, a value of $\Delta=3°$ at liquid-air temperature implies that the crystal was displaced by 3° with respect to a Bragg angle at liquid-air temperature and not with respect to the corresponding Bragg angle at room temperature.

3. EXPERIMENTAL RESULTS

Figure 2 is a typical result illustrating the diminution in scattered intensity at 100°K for the non-Laue diffraction maximum associated with the 200 region of reflection. The experimental points represent the scattered intensity in S units as the ionization chamber is moved, at small angular intervals, across the region of strong diffuse reflection. For this particular example, the crystal was displaced by 3° with respect to the 200 Bragg angle. Other distribution curves for $2°<\Delta<7°$ showed a similar relative decrease in intensity as the temperature is reduced, and it is concluded that there is no large change in the temperature effect for these different values of Δ.

The observed scattering is made up of two parts—one due to coherent scattering, the other

[10] G. E. M. Jauncey and W. D. Claus, Phys. Rev. **46**, 941 (1934).
[11] G. E. M. Jauncey and W. A. Bruce, Phys. Rev. **50**, 414 (1936).
[12] *International Critical Tables* (McGraw-Hill, 1928) **3**, p. 43.

TABLE I. *Comparison of the experimental ratio of intensity scattered at a temperature of 300°K to that scattered at 100°K with the ratio calculated from the expression* $(1-e^{-2M})$. *The values of the crystal setting in each reflection are those shown in Figs. 2–4.*

Region of Reflection	Temperature Effect	
	Experimental	Calculated
200	2.25	2.43
400	2.18	2.18
600	1.91	1.89

due to incoherent scattering. The incoherent scattering does not depend upon the temperature or upon the orientation of the crystal and is not connected with the non-Laue diffraction maxima. The incoherent scattering must, therefore, be subtracted from all observed S values if we wish to know the resultant S_{coh}. The magnitude of the incoherent scattering, which is indicated on the graphs by the horizontal dashed line, S_{incoh}, may be calculated from the relation,[13]

$$S_{incoh}=\frac{1-\dfrac{(\sum E_r^2)_{Na^+}+(\sum E_r^2)_{Cl^-}}{Z_{Na}+Z_{Cl}}}{\left(1+\dfrac{h}{mc\lambda}\,\mathrm{vers}\phi\right)^3}, \qquad (3)$$

where (ΣE_r^2) is the incoherent scattering function tabulated by Compton and Allison.[14]

After subtracting the incoherent scattering from all observed measurements, it is found that the intensity of the non-Laue diffraction maximum associated with the 200 reflection from rocksalt is, at 300°K, approximately 2.25 times greater than the intensity at 100°K. This ratio is obtained by averaging over the entire diffuse reflection region contained within the scattering angles $\phi=29°$ to $\phi=36°$; if we consider the peak intensity alone, the ratio of the relative scattering at 300°K to that at 100°K becomes more nearly 2.5. Possibly this indicates that the peak intensity may fall off somewhat more rapidly than the intensity diffracted at neighboring scattering angles.

From the large decrease in scattered intensity at 100°K, it is apparent that photographs taken at liquid-air temperature would reveal almost complete disappearance of the diffuse reflection pattern as has already been noted by Lonsdale.[4] The exposure time at 100°K must be more than doubled in order that the same photographic blackening be obtained.

In Fig. 3, the crystal was displaced by 3° from the 400 Bragg angle. The coherent scattering within the strong scattering region $\phi=62°$ to $\phi=71°$, is 2.18 times more intense at room temperature than at liquid-air temperature. The peak intensity is reduced by a factor of 2.35 at liquid-air temperature.

The position of maximum intensity of the diffuse reflection is clearly displaced from the position (marked by the vertical lines ϕ_B), at which the Bragg spectrum line may be observed. The divergence of the primary beam limits the accuracy of the measured value of $90'\pm15'$, although this is in reasonably good agreement with the displacement observed in the photographic method.[15]

The non-Laue diffraction maxima become more diffuse at larger scattering angles. Figure 4 gives the scattering intensity distribution in the region of the 600 reflection for $\Delta=-4°$. The shift in the position of the intense Laue spots is due to the temperature contraction of the crystal. The non-Laue diffraction pattern is shifted by a similar amount. If we take into account this shift and also correct for the incoherent scattering, we find that the non-Laue diffraction intensity is reduced by a factor of 1.91 at liquid-air temperature.

4. Conclusion

According to the Debye-Jauncey-Harvey-Woo[16–18] theory of diffuse scattering from crystals, the intensity of the coherent portion of the scattering is proportional to the factor $(1-e^{-2M})$ where e^{-2M}, the well-known Debye-Waller[6] temperature factor, is a function of the scattering angle and of the absolute temperature. If, for the characteristic temperature of rocksalt, the

[13] G. G. Harvey, P. S. Williams, and G. E. M. Jauncey, Phys. Rev. **46**, 365 (1934).
[14] A. H. Compton and S. K. Allison, *X-Rays in Theory and Experiment* (D. Van Nostrand, 1935), p. 782.
[15] G. E. M. Jauncey and O. J. Baltzer, Phys. Rev. **59**, 699 (1941).
[16] P. Debye, Ann. d. Physik **43**, 49 (1914).
[17] G. E. M. Jauncey and G. G. Harvey, Phys. Rev. **37**, 1203 (1931); G. E. M. Jauncey, Phys. Rev. **42**, 453 (1932).
[18] Y. H. Woo, Phys. Rev. **38**, 1 (1931); Y. H. Woo, Phys. Rev. **41**, 21 (1932).

value $\Theta = 281°C$ is chosen and if NaCl is treated as a simple cubic crystal, the calculated ratio for the temperature effect according to the factor $(1-e^{-2M})$ is found as shown in the last column of Table I. The experimental value for the decrease in scattered intensity at 100°K relative to the intensity at 300°K for the non-Laue diffraction maxima associated with the 200, 400, and 600 orders of reflection is given in the second column. It is seen that the agreement between the second and third columns is fairly good. No quantitative comparison of the experimental results with the predictions of the Faxen-Waller-Zachariasen theory have been made because an exact evaluation of the theoretically scattered intensity is rather difficult. However, a temperature dependence of the form $(1-e^{-2M})$ will be approximately valid so that it can be stated that the present experimental evidence does not disagree radically with conclusions based upon the Faxen-Waller-Zachariasen theory.

The author is greatly indebted to Dr. G. E. M. Jauncey for his interesting and helpful discussions concerning this investigation.

SEPTEMBER 15, 1941 PHYSICAL REVIEW VOLUME 60

Positive and Negative Thermionic Emission from Molybdenum

R. W. WRIGHT
University of Wisconsin, Madison, Wisconsin
(Received July 31, 1941)

The positive and negative thermionic emission from molybdenum has been studied. The electron work function was found to be 4.20 volts and the positive ion work function was 8.6 volts. The positive ion constant term was in good agreement with Smith's equation.

THE positive ion emission from molybdenum has been studied by several investigators with discordant results. These studies have been attempts to determine the positive ion work function and the constant term in Smith's[1] equation which, for molybdenum, has the following form:

$$\ln I + 0.453 \ln T + 6.22\times10^{-4}T = -(\varphi_{0+}e/kT) + 28.39. \quad (1)$$

Smith also considered the energy cycle:

$$\varphi_{0-} + \varphi_{0+} = H_0 + V, \quad (2)$$

where φ_{0-} is the electron work function, φ_{0+} the positive ion work function, H_0 is the heat of evaporation of a neutral atom and V is the ionization potential of the atom.

Moon[2] has obtained from the Langmuir-Kingdom-Saha theory of positive ion emission, the following relation:

$$\frac{n_p}{n_a} = \frac{\sigma_p}{\sigma_a} \exp\left[-\frac{11{,}600(V-\varphi_{0-})}{T}\right], \quad (3)$$

where n_p and n_a are the rates of evaporation of positive ions and neutral atoms, σ_p and σ_a the statistical weights of the two, V is the ionization potential and φ_{0-} is the electron work function.

Smith[1] found that his data fit Eq. (1) with $\varphi_{0+}=6.1$ volts and a constant term of 15.9. Barnes[3] obtained $\varphi_{0+}=8.2$ volts and a constant term equal to 26.5; values which are in better agreement with the theory. Barnes also noted that his data failed to give a straight line, the low temperature points falling above the line drawn through the high temperature points. Wahlin and Reynolds[4] found $\varphi_{0+}=8.3$ volts for well outgassed molybdenum. They used the value of H_0 equal to 5.75 volts taken from the unpublished work of Dr. E. R. Piore. Grover,[5] using a modified Dempster mass spectrograph, to be certain that the ions measured were from the molybdenum and not from some alkali impurity, found $\varphi_{0+}=8.9$ volts and a constant term of 25.3. He

[1] L. P. Smith, Phys. Rev. **35**, 381 (1930).
[2] P. B. Moon, Proc. Camb. Phil. Soc. **28**, 490 (1932).
[3] L. L. Barnes, Phys. Rev. **42**, 491 (1932).
[4] H. B. Wahlin and J. A. Reynolds, Phys. Rev. **48**, 751 (1935).
[5] Horace Grover, Phys. Rev. **52**, 982 (1937).

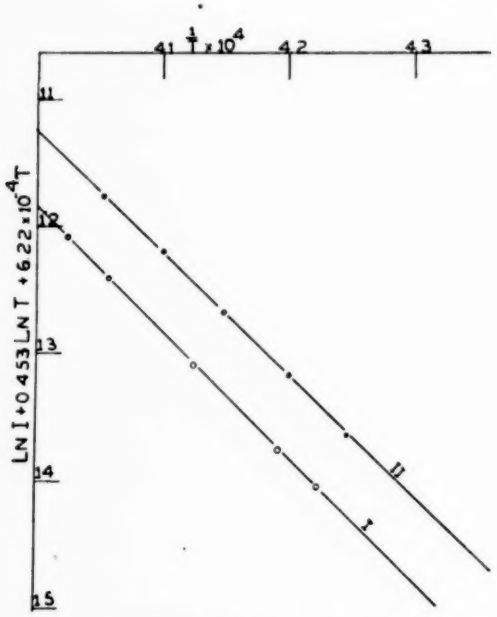

FIG. 1. Thermionic emission from molybdenum.

found that it was impossible, or at least not profitable, to free the molybdenum samples of potassium impurities. The present investigation gives a constant term in better agreement with Eq. (1).

In the following discussion, data are presented on the work function φ_{0+} and Smith's constant for filaments where special care has been taken to free the experimental tube, which was of the usual single guard ring type with the filaments in the form of a U, of alkali impurities. It is important to free the experimental tube of such impurities since it is possible for them to be volatilized during the high temperature heating necessary for obtaining positive ion data. Since these impurities might be freed from cold portions of the tube and become positively ionized by hitting the hot filament, these ions would then be included in the current measured as positive ions from the filament. By alternate periods of baking and flaming the experimental tube, and outgassing of the cylinders by use of an induction furnace, it was possible to free the tube effectively of alkalis. This process of alternate baking and induction heating was carried on for a period of 500 hours, while the oven temperature was reduced from 450°C to 300°C. During this time the filament was heated up to 2000°K. Temperatures were measured with an optical pyrometer that had been calibrated by sectoring up and down from the gold point.

The molybdenum used in this work was obtained from the Fansteel Metallurgical Corporation. The strip filaments were cut from a sheet of specially purified molybdenum, while the round filaments were taken from commercial Fansteel wire.

ELECTRON WORK FUNCTION

Wahlin and Reynolds[4] reported an increase in the work function φ_{0-} for one of their filaments that had been cold rolled before heating. Since this change could not be reproduced here, the effect they reported was probably due to impurities.

The values for the Richardson constants obtained by averaging the data from six of the strip filaments of pure molybdenum were $\varphi_{0-}=4.20\pm0.02$ volts and $A=55$ amp./cm^2/deg.^{2}. The values obtained from averaging the data for five of the round filaments of commercial molybdenum were $\varphi_{0-}=4.37\pm0.02$ volts and $A=115$.

POSITIVE ION EMISSION

Positive ion data were taken after a filament had reached a steady state, which was indicated by consistent values of φ_{0-} and Richardson's A over a period of 100 to 200 hours. Figure 1, curve I, shows data for one of the strip filaments of pure molybdenum, while curve II is for one of the round filaments of commerical molybdenum. The points shown in these curves were obtained as follows: the filament heating current was increased until a given space current was obtained as measured by a sensitive Leeds and Northrup galvonometer. The temperature was then measured while the space current was held constant by varying the heating current. As the left side of the positive ion emission equation is insensitive to small changes of T, it is easy to average successive runs on a given filament by always measuring the filament temperatures for all the runs at specified space currents. The points of curve I are the average of two runs and those of curve II the average of three runs taken in this manner. For the pure molybdenum the value of $\varphi_{0+}=8.6\pm0.1$ volts with the constant

term of 27.8, while for the commerical molybdenum $\varphi_{0+}=8.3\pm0.1$ volts with the constant term of 27.3. Both of these constant terms are in good agreement with Smith's values in Eq. (1). The values of the currents used in Fig. 1 were calculated for an emitting area of 1 cm².

Neither line in Fig. 1 shows curvature such as that noted by Barnes. This may be taken as a fair indication that the tube and filament were free from alkalis.

Figure 1 shows that the positive ion current from the high electron work function filament is larger than from the low. This is in agreement with Eq. (3). Now if n_a is regarded as constant for small changes of φ_{0-}, and the ratio of Eq. (3) for two different values of φ_{0-} is taken, one obtains:

$$\frac{n_p}{n_p'}=\exp\left[-\frac{11{,}600(\Delta\varphi_{0-})}{T}\right]. \qquad (4)$$

If we use this equation for a temperature of 2500°K and $\Delta\varphi_{0-}=0.17$ volts we find the ratio $n_p/n_p'=2.20$. From Fig. 1, the ratio of the currents at 2500°K is 1.82. Errors due to roughness in calculating the emitting areas of the filaments might account for this difference.

If the values of φ_{0+} and φ_{0-} are substituted in the energy equation [Eq. (2)], one finds, on taking Piore's value of 5.75 volts for H_0 and Catalan and Madariaga's[6] value of 7.15 volts for V, that the equation fails to balance by only 0.1 volt for the pure molybdenum and by 0.23 volt for the commercial material. This is within the limit of experimental error in both cases.

The author wishes to acknowledge his appreciation to Professor H. B. Wahlin who directed this research and to the Wisconsin Alumni Research Foundation for partial support.

[6] M. A. Catalan and P. Madariaga, Anales soc. espan. fis. y. quim. **31**, 707 (1933).

Letters to the Editor

PROMPT publication of brief reports of important discoveries in physics may be secured by addressing them to this department. Closing dates for this department are, for the first issue of the month, the eighteenth of the preceding month, for the second issue, the third of the month. Because of the late closing dates for the section no proof can be shown to authors. The Board of Editors does not hold itself responsible for the opinions expressed by the correspondents.

Communications should not in general exceed 600 words in length.

On the Theory of Integer Spin Mesons

MARIO SCHOENBERG
University of São Paulo, Brazil, South America*
August 25, 1941

HERETOFORE it has been assumed that there are two different possibilities for a field whose quanta have spin 0: scalar or pseudo-scalar wave function. For a spin one field an analogous possibility exists; the potentials may either be the components of a four vector or of a pseudo-four vector. We shall show that there is really only one possible kind of particle for each of the considered values of the spin; the difference in the nature of the nuclear forces is not due to the symmetry behavior of the meson field but is due to the fact that the interactions between the nuclear particles and the meson field heretofore used are not the most general ones. By considering more general forms of interaction both forms of the theory for each of the considered values of the spin give the same forces between heavy particles.

The equations of motion of the system nuclear particles —meson field can be obtained from the variational principle:

$$\delta\int L dxdydzdt=\delta\int(L_{\rm Pr}+L_{\rm Neu}+L_{\rm Mes}+L')dxdydzdt.$$

L' is the Lagrangian of the interaction between proton-neutrons and mesons:

$$L'_{0,a}=-c\kappa[g_{0,a}w\phi^*+f_{0,a}v_\alpha\chi^{*\alpha}]+\text{conj. complex}\quad\kappa\chi_\alpha=\partial\phi/\partial x^\alpha \qquad \left.\begin{matrix}\text{Spin 0}\\ \text{Scal. wave}\\ \text{function}\end{matrix}\right\}$$

$$L'_{0,b}=-c\kappa[\tfrac{1}{6}g_{0,b}l_{\alpha\beta\gamma}\phi^{*\alpha\beta\gamma}+\tfrac{1}{24}f_{0,b}s_{\alpha\beta\gamma\delta}\chi^{*\alpha\beta\gamma\delta}]+\text{conj. complex}\quad\kappa\phi^{\alpha\beta\gamma\delta}=\partial\chi^{\alpha\beta\gamma\delta}/\partial x^\alpha \qquad \left.\begin{matrix}\text{Spin 0}\\ \text{Ps. scal.}\\ \text{w.f.}\end{matrix}\right\}$$

$$L'_{1,a}=-c\kappa[g_{1,a}v_\alpha\phi^{*\alpha}+\tfrac{1}{2}f_{1,a}u_{\alpha\beta}\chi^{*\alpha\beta}]+\text{conj. complex}\quad\kappa\chi_{\alpha\beta}=\partial\phi_\beta/\partial x^\alpha-\partial\phi_\alpha/\partial x^\beta \qquad \left.\begin{matrix}\text{Spin 1}\\ \text{Vector potential}\end{matrix}\right\}$$

$$L'_{1,b}=-c\kappa[\tfrac{1}{2}g_{1,b}u_{\alpha\beta}\phi^{*\alpha\beta}+\tfrac{1}{6}f_{1,b}l_{\alpha\beta\gamma}\chi^{*\alpha\beta\gamma}]+\text{conj. complex}\quad\kappa\phi^{\beta\gamma}=\partial\chi^{\alpha\beta\gamma}/\partial x^\alpha \qquad \left.\begin{matrix}\text{Spin 1}\\ \text{Ps. vector}\\ \text{potential}\end{matrix}\right\}$$

$$w=\psi^+{}_{\rm N}\psi_{\rm P}\quad v_\alpha=\psi^+\gamma_\alpha\psi\quad u_{\alpha\beta}=\psi^+{}_{\rm N}\gamma_\alpha\gamma_\beta\psi_{\rm P}$$
$$l_{\alpha\beta\gamma}=\psi^+{}_{\rm N}\gamma_\alpha\gamma_\beta\gamma_\gamma\psi\quad s_{\alpha\beta\gamma\delta}=\psi^+{}_{\rm N}\gamma_\alpha\gamma_\beta\gamma_\gamma\gamma_\delta\psi_{\rm P}$$
$$\kappa=\mu c/\hbar\quad(\mu\text{—meson mass}).$$

These forms of L' are not the most general ones. In order to get more general interactions let us consider the pseudo-scalar $\eta^{\alpha\beta\gamma\delta}$:

$$\eta^{\alpha\beta\gamma\delta}=(-g)^{\frac{1}{2}}\epsilon^{\alpha\beta\gamma\delta}\quad g=|g_{\alpha\beta}|.$$

$\epsilon^{\alpha\beta\gamma\delta}$ is the well-known tensor density, antisymmetric in the four indices and equal to ±1, according to the parity of the permutation $\alpha\beta\gamma\delta$ of the numbers 0, 1, 2, 3. The most general interactions between proton-neutron and mesons are:

$$L'_{0,a}=L'_{0,a}-c\kappa[\tfrac{1}{24}s_{\alpha\beta\gamma\delta}\eta^{\alpha\beta\gamma\delta}\phi^*+\tfrac{1}{6}f_{0,a}l'_{\alpha\beta\gamma}\eta^{\alpha\beta\gamma\delta}\chi^*{}_\delta]+\text{conj. comp.}$$

$$L'_{0,b}=L'_{0,b}-c\kappa[\tfrac{1}{24}g'_{0,b}w\eta^{\alpha\beta\gamma\delta}\chi^*_{\alpha\beta\gamma\delta}+\tfrac{1}{6}f'_{0,b}v_\alpha\eta^{\alpha\beta\gamma\delta}\phi^*_{\beta\gamma\delta}]+\text{conj. comp.}$$

$$L'_{1,a}=L'_{1,a}-c\kappa[\tfrac{1}{4}g'_{1,a}u_{\alpha\beta}\eta^{\alpha\beta\gamma\delta}\chi^*_{\gamma\delta}+\tfrac{1}{6}f'_{1,a}l'_{\alpha\beta\gamma}\eta^{\alpha\beta\gamma\delta}\phi^*{}_\delta]+\text{conj. comp.}$$

$$L'_{1,b}=L'_{1,b}-c\kappa[\tfrac{1}{2}g'_{1,b}v_\alpha\eta^{\alpha\beta\gamma\delta}\chi^*_{\beta\gamma\delta}+\tfrac{1}{4}f'_{1,b}u_{\alpha\beta}\eta^{\alpha\beta\gamma\delta}\phi^*_{\gamma\delta}]+\text{conj. comp.}$$

We see that $L'_{i,a}$ and $L'_{i,b}$ have the same structure; therefore the two forms of the meson theory, for each of the values 0 and 1 of the spin, are perfectly equivalent, since we can describe the same field either by ϕ or by $\eta^{\alpha\beta\gamma\delta}\phi$ and by ϕ_α or $\eta^{\alpha\beta\gamma\delta}\phi_\delta$.

Taking the interactions $L_{i,a}$ we get for the potentials of the nuclear forces:

$$V^0_{\rm PN}=-\frac{c\kappa}{4\pi}[(g\kappa)^2-f'^2(\boldsymbol{\sigma}_{\rm N}\,\text{grad})(\boldsymbol{\sigma}_{\rm P}\,\text{grad})]\frac{e^{-\kappa r}}{r}$$

$$V^1_{\rm PN}=\frac{c\kappa}{4\pi}[(g\kappa)^2+\kappa^2(f^2-f'^2)(\boldsymbol{\sigma}_{\rm P}\cdot\boldsymbol{\sigma}_{\rm N})+(f'^2-f^2-g'^2)(\boldsymbol{\sigma}_{\rm N}\,\text{grad})(\boldsymbol{\sigma}_{\rm P}\,\text{grad})]\frac{e^{-\kappa r}}{r}.$$

* Now at George Washington University with a fellowship of the John Simon Guggenheim Memorial Foundation.

Transport Cross Sections of Monatomic Gas Mixtures

GLENN M. ROE
Department of Physics, University of Minnesota, Minneapolis, Minnesota
September 2, 1941

THE coefficients of viscosity, thermal conduction, diffusion and thermal diffusion as given independently by Enskog and Chapman[1] involve the integrals

$$\Omega(i,s)=\pi^{\frac{1}{2}}\int_0^\infty e^{-y^2}y^{2s+2}\phi(i)dy,$$

$$\phi(i)=(2m_0kT/m_1m_2)^{\frac{1}{2}}y\int_0^\infty(1-\cos^i\chi)bdb,$$

$$\chi=\pi-2\int_{r_{00}}^\infty[r^4/b^2-r^2-r^4V(r)/(kTb^2y^2)]^{-\frac{1}{2}}dr.$$

$i=1,2$; $s=1,2,3$. $V(r)$ is the mutual potential energy of molecules of mass m_1 and m_2, $m_0=m_1+m_2$. r_{00} is the least positive root of the function in brackets.

Previously χ has been integrable only for the rigid

TABLE I. *The functions $h_i(\nu)$.*

ν	$h_1(\nu)$	$h_2(\nu)$	ν	$h_1(\nu)$	$h_2(\nu)$
4	0.38824	0.86761	8	0.27799	0.64567
5	0.33736	0.76777	9	0.26804	0.62385
6	0.30934	0.71143	10	0.26016	0.60609
7	0.29107	0.67360	11	0.25372	0.59123

sphere model and, to the first degree in E/kT, for the Sutherland model; other models required numerical integration. The results have been summarized in reference 1 and by Jones.[2]

Assume that $V(r)$ has a single minimum $-E=V(r_0)<0$, is negative for $r>r_0$, approaches zero more rapidly than r^{-2} for large r, and becomes positively infinite for small r. The ϕ integral will be broken up into the ranges $b\leqq b_0$, and $b\geqq b_0$, where $b_0=r_0(1+R)^{\frac{1}{2}}$, $R=E/kTy^2$, corresponding to $r_{00}\leqq r_0$ and $r_{00}\geqq r_0$, respectively. In the first range put $r=b/v$ and add and subtract R in the denominator.

$$\chi=\pi-2\int_0^{v_{00}}[1+R-v^2-R\{1+V(v)/E\}]^{-\frac{1}{2}}dv.$$

Since $V(v)\geqq -E$ and $[\ ]\geqq 0$, it follows that $\{1+R-v^2\}\geqq R\{1+V(v)/E\}$ and the radical may be expanded. In the second range add and subtract $S=-V(r_{00})/kTy^2$ and expand the radical. This procedure gives χ in powers of $R/(1+R)$ or $S/(1+S)$, and $\cos\chi$ may then be put in similar series form. After integrating over the proper range of b, and over y, the final result is:

$$\Omega(i,s)=(2\pi m_0kT/m_1m_2)^{\frac{1}{2}}[W_0(i,s)-W_1(i,s)+U_2(i,s)-W_2(i,s)+\tfrac{3}{2}U_3(i,s)-W_3(i,s)+\cdots];$$

where

$$W_n(i,s)=\int_0^\infty \exp(-y^2)y^{2s+3}H_n(i,R)dy,$$

$$H_n(i,R)=R^n/(1+R)^n\int_0^1 G_n(i,z)\{d(b^2)/d(z^2)\}zdz,$$

$$G_0(1,z)=2(1-z^2),\quad G_0(2,z)=4z^2(1-z^2),$$
$$G_1(1,z)=2z(1-z^2)^{\frac{1}{2}}F_1(z),\quad G_1(2,z)=2(2z^2-1)G_1(1,z),$$
$$G_2(1,z)=\tfrac{3}{2}z(1-z^2)^{\frac{1}{2}}F_2(z)-\tfrac{1}{2}(2z^2-1)F_1^2(z),$$
$$G_2(2,z)=2(2z^2-1)G_2(1,z)+G_1^2(1,z),$$
$$G_3(1,z)=z(1-z^2)^{\frac{1}{2}}[\tfrac{5}{4}F_3(z)-\tfrac{1}{8}F_1^3(z)]-\tfrac{3}{4}(2z^2-1)F_1(z)F_2(z),$$
$$G_3(2,z)=2(2z^2-1)G_3(1,z)+2G_1(1,z)G_2(1,z),$$

$$F_n(z)=\int_0^z[1+V_1(x)/E]^n(1-x^2)^{-n-\frac{1}{2}}dx,$$

$$V_1(x)=V(r)\quad\text{with}\quad 1/r=x(1+R)^{\frac{1}{2}}/b,$$

$$U_n(i,s)=\tfrac{1}{2}i\int_0^\infty \exp(-y^2)y^{2s+3}I_n(y)dy,$$

$$I_2(y)=\int_{b_0}^\infty[S/(1+S)]^2J_1^2(b)bdb,$$

$$I_3(y)=\int_{b_1}^\infty[S/(1+S)]^3J_1(b)J_2(b)bdb,$$

$$J_n(b)=\int_0^1[1-V_2(x)/V_2(x_{00})]^n(1-x^2)^{-n-\frac{1}{2}}dx,$$

$$V_2(x)=V(r)\quad\text{with}\quad 1/r=x(1+S)^{\frac{1}{2}}/b.$$

The functions W_n and U_n will be in general of order not greater than $(E/kT)^n$, so that for high temperatures only the first few terms are of importance. Although Ω is not given in closed form, the choice of integrable functions $V(r)$ is considerably greater.

Applied to the Sutherland model, with molecular diameter σ, and attractive force varying as $1/r^2$, this method gives:

$$\Omega(i,s)=(\pi m_0kT/2m_1m_2)^{\frac{1}{2}}\sigma^2[(s+1)!f_i+s!g_i(\nu)E/kT+(s-1)!h_i(\nu)(E/kT)^2+\cdots].$$

$f_1=\frac{1}{2}$ and $f_2=\frac{1}{3}$. The functions g_1 and g_2 have already been calculated by James[3] by another method, and are tabulated by Jones[2] with the notation i, and i_2. h_1 and h_2 have been evaluated in terms of the digamma function and are given in Table I. Further approximations to Ω require tabular values of the logarithmic integral. As predicted by James,[3] the functions h_2 are positive, whereas the viscosity data of the rare gases demand that these coefficients be negative. It is evident that the Sutherland model cannot yield accurate results for viscosity or thermal diffusion unless $(E/kT)^2$ is negligible.

Calculations are now in progress for a molecular model possessing both an attractive and a repulsive field.

[1] S. Chapman and T. G. Cowling, *The Mathematical Theory of Non-Uniform Gases* (Cambridge, 1939).
[2] R. C. Jones, Phys. Rev. **58**, 111 (1940).
[3] C. G. F. James, Proc. Camb. Phil. Soc. **20**, 447 (1921).

Radioactive Argon A^{37}

PAUL K. WEIMER, J. D. KURBATOV, AND M. L. POOL
Department of Physics, The Ohio State University, Columbus, Ohio
August 30, 1941

AN artificially radioactive gas has been produced by bombarding solid samples containing potassium, chlorine, calcium, or sulfur with appropriate nuclear particles. The radioactivity has been observed for three months and is found to have a single decay period of 34 days.

Two radioactive isotopes of argon are already known. They are A^{41} which has a half-life of 110 minutes,[1] and A^{35} which has a half-life of two seconds.[2]

In view of the method by which the present activity has been produced, we assign it to A^{37}. To substantiate this assignment the following reactions have been carried out and in each case found to yield a radioactive gas of 34-day half-life.

$$\begin{aligned}
Cl^{37}+H^2 &\rightarrow A^{37}+2n\\
Cl^{37}+H^1 &\rightarrow A^{37}+n\\
K^{39}+H^2 &\rightarrow A^{37}+He^4\\
Ca^{40}+n &\rightarrow A^{37}+He^4\\
S^{34}+He^4 &\rightarrow A^{37}+n
\end{aligned}$$

After chemical treatment of the bombarded sample, the gas liberated was passed through a sodium hydroxide solution and calcium chloride drying tubes, and then admitted into an ionization chamber which was connected to a Wulf bifilar electrometer. Experiments on the type of radiation emitted are in progress.

It is a pleasure to acknowledge the help given by Mr. Julius F. Stone and the Ohio State University Development Fund.

[1] Arthur H. Snell, Phys. Rev. **49**, 555 (1936).
[2] L. D. P. King and D. R. Elliott, Phys. Rev. **59**, 108A (1941), M. G. White, E. C. Creutz, L. A. Delsasso, and R. R. Wilson, Phys. Rev. **59**, 63 (1941).

Disintegration Scheme of the Yttrium Activity of 100-Day Half-Period

J. R. DOWNING, M. DEUTSCH, AND A. ROBERTS
Massachusetts Institute of Technology, Cambridge, Massachusetts
September 2, 1941

THE gamma-radiation from the 100-day activity of yttrium,[1] produced by deuteron bombardment of strontium,[2] has recently been investigated by means of recoil electrons in a cloud chamber[3] and by the photodisintegration of beryllium.[4]

We have investigated these gamma-rays in a magnetic lens spectrometer, by a method previously described.[5] The yttrium source, kindly loaned to the authors by Dr. Francis Moore of Huntington Memorial Hospital, had a gamma-ray intensity equivalent to about 10 micrograms of radium (both radiations filtered by 1 mm of lead). Photoelectrons from lead and tin radiators and Compton recoil electrons from a thick aluminum radiator were investigated (Fig. 1). The observed gamma-ray energies of 0.908 ± 0.02 Mev and 1.89 ± 0.05 Mev are in good agreement with those reported by other workers. Considering the variation of the photoelectric cross section with energy, it is estimated that any gamma-rays between 0.2 and 0.5 Mev which may have escaped detection could not be more than about 1/20 as abundant as the 0.9-Mev gamma-ray, (about 1/10 for gamma-rays outside this energy range, down to about 0.12 Mev).

We have further investigated the disintegration scheme of this activity by observing coincidences between gamma-rays recorded in G-M counters of known efficiency. (Details of the calibration for various energies will be published shortly.) The source used in these measurements was prepared in the M.I.T. cyclotron. The observed number of coincidences was $(1.91\pm0.10)\times10^{-3}$ per recorded gamma-ray. The number to be expected if the two gamma-rays follow each other in cascade, (Fig. 1, insert) is $(1.97\pm0.10)\times10^{-3}$. If the successive emission of two gamma-rays of about 0.95 Mev were alternative to the emission of a single gamma-ray of 1.9 Mev, the intensities about equal as observed by Richardson,[3] the expected coincidence rate would be only 0.54×10^{-3}. Absorption measurements on the coincident gamma-rays also gave results consistent with the disintegration scheme shown in Fig. 1.

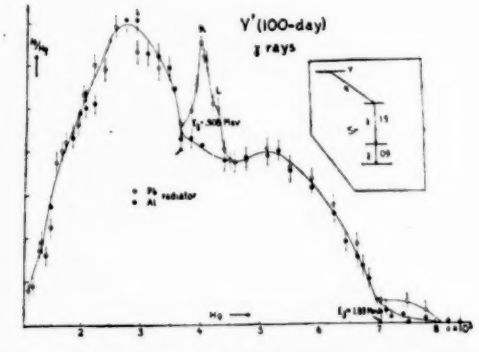

FIG. 1. Energies given are weighted averages of photoelectron and Compton end-point determinations.

These data, together with Richardson's[3] estimate of the relative intensities of the two gamma-rays, also indicate that no more than about one fifth of the disintegrations lead directly to the intermediate level in the Sr nucleus (the neutrino carrying away the excess energy).

Each electron capture process in Y is followed by the emission of a Sr x-ray (or Auger electron). We have measured the number of coincidences between these x-rays and the gamma-rays and found $(3.3\pm0.5)\times10^{-3}$ coincidence per recorded x-ray (measured with a less efficient gamma-ray counter than the gamma-gamma coincidences reported above). The number predicted if each disintegration follows the scheme shown in Fig. 1 is $(3.3\pm0.2)\times10^{-3}$. It appears from this that no more than about one fifth of the disintegrations can lead directly to the ground state of the product nucleus.

It may therefore be concluded that most of the disintegrations of the 100-day yttrium isotope follow the scheme shown in Fig. 1 (except for the unknown *order* of emission of the gamma-rays). The small number (or absence) of direct transitions to the ground state or intermediate level and the absence of positron emission probably indicate a large spin change between initial and final nuclei.

It is a pleasure to acknowledge the friendly interest of Professor Robley D. Evans in this investigation.

[1] L. A. DuBridge and J. Marshall, Phys. Rev. **58**, 7 (1940).
[2] C. Pecher, Phys. Rev. **58**, 843 (1940).
[3] J. R. Richardson, Phys. Rev. **60**, 188 (1941).
[4] G. Scharff-Goldhaber, Phys. Rev. **59**, 937A (1941).
[5] M. Deutsch and A. Roberts, Phys. Rev. **60**, 362 (1941).

The Cosmic-Ray Latitude Effect and the Single Primary Component Hypothesis*

W. F. G. SWANN
Bartol Research Foundation of the Franklin Institute, Swarthmore, Pennsylvania
August 23, 1941

ON the assumption that a single primary component produces mesotrons at a definite altitude in the stratosphere, the writer finds that, if $F(E)dE$ represents the energy distribution of the vertically directed mesotrons at the point of production, then the number of mesotrons at a distance x below this point, and remaining from the group $F(E)dE$ at $x=0$ is Δn_x, where

$$\Delta n_x=[(1+A/(\gamma+1))e^{-\lambda x}-A/(\gamma+1)]^{[\lambda c\tau_0(\gamma+1)+A]^{-1}} F(E)dE, \quad (1)$$

with $A\equiv\alpha\rho_0/\lambda m_0c^2$, and $\gamma\equiv E/m_0c^2$; m_0, τ_0, ρ_0, α being, respectively, the rest mass of the mesotron, its mean life at rest, the atmospheric density at $x=0$, the ionization energy loss per unit of mass (per unit area) traversed, and where λ is the constant in the expression $\rho=\rho_0\exp[\lambda x]$ for the atmospheric density at the depth x.

If we regard the mesotron intensity as responsible for the sea-level latitude effect, we must suppose that the minimum energy of the mesotrons at magnetic latitude

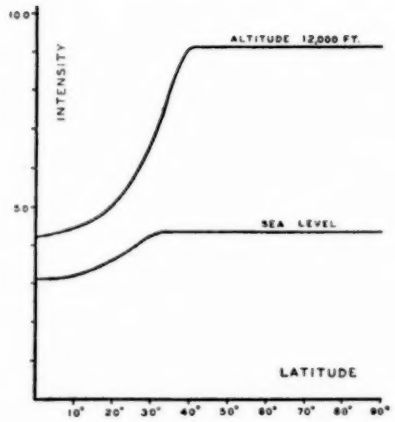

FIG. 1. Latitude effect calculated with formula (1), and the values $\tau_0 = 2\times10^{-6}$ sec., and $m_0 = 160\times$mass of electron.

35°, where the increase of intensity with latitude ceases, must be about 10^9 ev, since that is the energy necessary to penetrate the atmosphere. If the primaries are protons, the energy necessary to penetrate the earth's magnetic field at 35° latitude is 5×10^9 ev, so that for equal distribution of energy among the mesotrons, each proton would give rise to five mesotrons. If the energy distribution law of the protons followed the inverse cube form, the numbers contained above the lower magnetic limit E_m for vertical entry would be proportional to $1/E_m^2$, so that since E_m is 10^{10} ev for the equator, the ratio of the proton intensity at latitude 35° to that at 0° (equator) would be 4 : 1. This would also be the ratio for the corresponding mesotron intensities at latitudes 35° and 0°, for all altitudes, if mean-life considerations were neglected.

However, mesotrons of 2×10^9 ev corresponding to the lower limit for mesotrons at the equator would have a mean life of less than 4×10^{-5} sec., averaged over the path concerned, and, if produced at an altitude of 20 kilometers, only about 0.2 of them would reach sea level. The corresponding mean life for the lower limit at latitude 35° would be smaller, and would result in a smaller fraction of the mesotrons to reach sea level there.

Equation (1) serves as a basis for submitting the above considerations to more exact calculation, and properly integrating over the total energy spectrum. Figure 1 shows the result of the assumption above cited to the effect that a proton splits into five mesotrons at an altitude of 20 kilometers. The figure shows a 30 percent variation of the intensity from the minimum to the upper limit for the sea-level latitude effect, and shows an increase of latitude effect with altitude in accord with experimental findings. A slight modification of the constants, such as ionization energy loss, would bring the calculations into numerical agreement with experiment, while the intention here is merely to demonstrate the general picture.

Also, the details of the assumptions made, and in particular that of the splitting of the proton into five mesotrons of equal energy, are susceptible to wide variations; and, indeed, such variations are demanded if we are to secure a proportion of mesotrons of practically zero kinetic energy at $x=0$, and such as is necessary to account for the flatness of the intensity-zenith angle curve for high altitudes.

*A portion of a paper presented at the Providence, Rhode Island meeting of the American Physical Society, June 20–21, 1941, under the title, "Consequences of the assumption of a single primary component in the cosmic radiation."

Absence of Electronic Raman Effect

L. SIBAIYA
Department of Physics, Central College, Bangalore, India
May 1, 1941

IN a study of the Raman effect in samarium nitrate solutions at different concentrations,[1] it was reported that, in addition to the nitrate frequency at 1047 cm^{-1}, concentrated solutions revealed three new bands in the scattered radiation. These bands had been *tentatively* ascribed to an electronic Raman effect in the Sm^{+++} ion, which, with a close group of levels in the ground state ^6H, could be expected to exhibit this effect. But later experiments in this laboratory and elsewhere[2] have definitely shown that the new bands arise from a selective absorption by the samarium ions from the continuous background of the mercury arc, which is scattered strongly by more concentrated solutions. This explanation of the bands is supported by the fact that they do not make their appearance when the solution is irradiated through a filter allowing only λ4358A. It must therefore be admitted that neither the thallium atoms[1] nor the samarium ions give any evidence of the existence of the electronic Raman effect. The failure to establish this effect in atoms or ions both in the optical and in the x-ray regions argues against the possibility of the existence of such an effect.

[1] L. Sibaiya and H. S. Venkataramiah, Phys. Rev. **56**, 381 (1939).
[2] E. Gross, A. Raskin and A. Seidel, Acta Physicochim. U.S.S.R. **13**, 591 (1940).